Instituto de Neurociencias
Consejo Superior de Investigaciones Científicas
Universidad Miguel Hernández

D. Juan Lerma Gómez, Director del Instituto de Neurociencias, centro mixto de la Agencia Estatal Consejo Superior de Investigaciones Científicas y la Universidad Miguel Hernández,

CERTIFICA:

Que la Tesis Doctoral titulada ***"Developmental regulation of cortical expansion: radial glia cell lineage and neuronal migration"*** ha sido realizada Isabel por Dª Maria Ángeles Martínez Martínez, Licenciada en Biología, bajo la dirección del Dr. Víctor Borrell Franco y da su conformidad para que sea presentada a la Comisión de Doctorado de la Universidad Miguel Hernández.

Para que así conste y surta los efectos oportunos, se firma el presente certificado en San Juan de Alicante a ventinueve de abril de dos mil quince.

Fdo: D. Juan Lerma Gómez

www.in.umh.es
Tel: +34 965 23 37 00
Fax: +34 965 91 95 61
Av Ramón y Cajal s/n
CAMPUS DE SANT JOAN
03550 SANT JOAN D'ALACANT– ESPAÑA

UNIVERSITAS
Miguel
Hernández

Instituto de Neurociencias
Consejo Superior de Investigaciones Científicas
Universidad Miguel Hernández

D. Víctor Borrell Franco, Científico Titular de la Agencia Estatal Consejo Superior de investigaciones Científicas, con destino en el Instituto de Neurociencias, centro mixto de la Agencia Estatal Consejo Superior de Investigaciones Científicas y la Universidad Miguel Hernández,

CERTIFICA:

Que Dª Maria Ángeles Martínez Martínez, Licenciada en Biología, ha realizado bajo su dirección el trabajo experimental que recoge su Tesis Doctoral titulada ***"Developmental regulation of cortical expansion: radial glia cell lineage and neuronal migration"*** y que ha revisado los contenidos científicos y los aspectos formales del trabajo dando su conformidad para que la misma sea presentada a la Comisión de Doctorado de la Universidad Miguel Hernández.

Para que así conste y surta los efectos oportunos, se firma el presente certificado en San Juan de Alicante a veintinueve de abril de dos mil quince.

Fdo: D. Víctor Borrell Franco

www.in.umh.es
Tel: +34 965 23 37 00
Fax: +34 965 91 95 61
Av Ramón y Cajal s/n
CAMPUS DE SANT JOAN
03550 SANT JOAN D'ALACANT– ESPAÑA

UNIVERSITAS
Miguel
Hernández

Developmental regulation of cortical expansion: radial glia cell lineage and neuronal migration

Maria Ángeles Martínez Martínez

2015

Thesis Supervisor: Dr. Víctor Borrell Franco

CSIC
UNIVERSITAS Miguel Hernández
INSTITUTO DE NEUROCIENCIAS

UNIVERSITAS
Miguel
Hernández

AGRADECIMIENTOS

Primero, me gustaría agradecer a mi director de Tesis, Víctor Borrell por todo lo que me ha enseñado y ayudado a lo largo de este camino; por las discusiones y debates que me han permitido crecer científicamente y por haber formado parte de su equipo.

También debo agradecer a todos aquellas personas vinculadas con la ciencia que antes de comenzar la tesis y durante la misma me inculcaron el interés y amor por la ciencia. Entre ellos quiero destacar al Dr. Pedro Robles (primera persona que se atrevió a dejarme entrar en un laboratorio), Dr. Jose Martín Nieto (responsable de mi inclinación hacia la Neurociencia), Dr. Hervé Acloque (amigo y primer mentor en el Instituto de Neurociencias) y muchos otros científicos e investigadores que me han ayudado a llegar hasta aquí.

Me gustaría agradecer a todos los compañeros de diferentes laboratorios, por los momentos que hemos compartido. Desde la gente del laboratorio de la Dra. Eloísa Herrera (especial agradecimiento a mi antigua compañera de laboratorio Celia y a Augusto), también al laboratorio de la Dra. Ángela Nieto (del que me llevo grandes recuerdos y una gran amiga Diana), al laboratorio de la Dra. Beatriz Rico y el Dr. Óscar Marín (con lo que hemos colaborado y trabajado codo con codo, y en los que su gente siempre ha mostrado elevada disponibilidad). Mención especial del último laboratorio a mi compañero y amigo Gabriele Ciceri por todas la horas, experimentos, aprendizaje conjunto y risas que hemos compartido estos años. También, agradecer a la gente del animalario (especialmente a Mari Carmen, Raúl, Gonzalo, Sandra, Vicky y Yolanda), a Giovanna del servicio de imagen y a Begoña, amiga y loca consejera, que con sus ocurrencias e ideas siempre me da energía para avanzar.

Por supuesto, quiero dar las gracias a todos mis compañeros del laboratorio; Bea, Cris, Hugo y Virginia ha sido un placer trabajar con vosotros y os deseo lo mejor en vuestro camino. En especial a Adrián, Camino, Isabel y Esther, con los llevo más tiempo riendo, compartiendo, aprendiendo y casi viviendo. Camino, nuestra postdoc, gracias por enseñarme y ayudarme cada día; Isabel, compañera desde los inicios de esta andadura con la que he pasado horas y horas operando, gracias por todos tus consejos; Adrián, mi friki favorito, mi compañero sin protocolos espero que no cambies nunca y sigas siendo tan buena persona; y Esther, por su actitud positiva, su ayuda y consejos acerca de lo que verdaderamente importa en la vida. Gracias a todos de corazón.

Pero si durante estos años he compartido con mucha gente mi estancia en el INA, sin duda con las dos personas que más lazos he creado ha sido con mis amigos Anna y Geraud. Gracias Geraud por nuestros ratos de cotilleos, interminables noches del vino y confesiones a cualquier hora. Anna ha sido a lo largo del doctorado mi compañera de piso, amiga, confidente y apoyo, muchas gracias por todo; os auguro a los dos un camino de éxito y una felicidad enorme. Y ya sabéis "*Lo mejor está por llegar*".

No puedo olvidarme de mis "hermanos mayores" Sandra y Miguel, dos grandes personas a las que por casualidad la vida puso en mi camino y de las que no quiero perder el vínculo. Gracias por compartir vuestro tiempo conmigo.

Una mención especial de gratitud a los amigos de fuera del mundo científico. A mis amigas de la universidad, Esperanza y Rosiña, con las que probablemente haya vivido una de las mejores etapas de mi vida, gracias por vuestra fuerza y capacidad de superación. A mis amigos de la Marina Alta, Javier y Mayte; Javier gracias por apoyarme siempre y mostrarme que "*la vida es un viaje no un destino*"; a Mayte agradezco todos esos momentos en que nuestra imaginación vuela y soñamos despiertas. Especial agradecimiento a mis amigas de Bonete, (Bea, Mª José G., Maite, Fran, Mari, Mª José P., Marisa, Manoli, y Beatriz), amigas desde el colegio, formamos un grupo que da energía para seguir avanzando; gracias por vuestro apoyo y amistad. Y destacar mi agradecimiento a mi gran amiga Mª José Pérez, seguramente la persona que mejor me conoce y que siempre me saca una sonrisa. Gracias a todos por ser así, no cambiéis nunca.

El pasado verano realicé un viaje a Ruanda que cambió mi concepción del mundo y me permitió concluir esta tesis. Quiero agradecer a mis compañeros de viaje y en especial a los habitantes de Nemba (una pequeña región al norte del país). Sus gentes (principalmente los niños) nos mostraron que con muy poco se puede ser feliz. Partimos con la idea de mejorar un poco las cosas allí pero he de reconocer que si algo cambió en este viaje, fuimos nosotros. Gracias por cambiarme.

Finalmente quiero agradecer a mi familia su apoyo y confianza durante toda mi vida. Son mi pilar fundamental, orgullo y satisfacción. Gracias a mi abuelas, Ángeles y Juana por transmitirme vuestra sabiduría adquirida con la experiencia; pero también a mis abuelos Juan y Francisco que allá donde estén me dan fuerzas para seguir creciendo; a mis tíos/as y primos/as con los que cada reunión es una fiesta inigualable; a mis hermanas, Mª José y Ana, con las que disfruto, me divierto y comparto momentos únicos; y por último y con especial énfasis a mis padres, por todo el esfuerzo para hacerme ser quien soy y gracias a los cuáles existe esta tesis. A mi madre por su fuerza, dedicación, consejos, entereza, amor y confianza en mí. Y a mi padre, tal vez la persona más culta e inteligente que conoceré, gracias por ser cómo eres, transmitirme tus valores y apoyarme incondicionalmente, siempre.

GRACIAS A TODOS

A mis padres, Jose Mª y Mª Ángeles

“Los que aseguran que es imposible no deberían interrumpir a los que estamos intentándolo”. Thomas A. Edison

"Piensa, utiliza tu cerebro hasta que tengas agujetas, pero escucha siempre a tu corazón". Mª Ángeles Martínez

"He aquí mi secreto, que no puede ser más simple: solo con el corazón se puede ver bien; lo esencial es invisible a los ojos". El principito *(*Antoine de Saint-Exupéry)

"Si no tardas mucho, te espero toda la vida". Oscar Wilde

UNIVERSITAS
Miguel
Hernández

TABLE OF CONTENTS

TABLE OF CONTENTS

RESUMEN

La corteza cerebral es la región más extensa del cerebro de mamíferos. Durante su desarrollo tienen lugar diversos procesos como la neurogénesis y la migración neuronal. Las células progenitoras se dividen para generar neuronas, que migran antes de diferenciarse y formar circuitos. Las neuronas piramidales migran guiadas y en íntima relación con fibras de glía radial, que mientras en especies lisencefálicas presentan trayectorias paralelas, en girencefálicas las trayectorias son divergentes. Esta divergencia contribuye a una mayor dispersión de las neuronas en la corteza cerebral y a su expansión tangencial. Nosotros hemos estudiado los procesos que tienen lugar en las neuronas piramidales para promover su dispersión durante la migración radial. Postulamos que la formación de ramas en el proceso de guía podría contribuir a esa dispersión, permitiendo a las neuronas moverse entre diferentes fibras radiales. Hemos observado que la formación de ramas es un mecanismo común durante la migración radial, con especial relevancia en especies girencefálicas, y que estas células con ramas son perfectamente motiles, siendo la formación de ramas un proceso transitorio y dinámico. Otro aspecto de gran relevancia en la formación de grandes cerebros es el incremento en la neurogénesis, que en parte ocurre gracias a la expansión de la población de progenitores basales en zonas germinativas. Entre todos los tipos de progenitores descritos en mamíferos, las Células de Glia Radial basales (bRGCs) juegan un papel importante en la expansión cortical, siendo necesarias aunque no suficientes para la formación de giros. En especies girencefálicas, con gran expansión cortical durante la embriogénesis, las bRGCs residen mayoritariamente en la zona subventricular externa (OSVZ). Utilizando el hurón como modelo de mamífero girencefálico, hemos observado que las RGCs actúan como los principales progenitores neuronales. Además, nuestro estudio demuestra que la formación de la OSVZ depende de un periodo crítico de generación masiva de bRGCs desde la zona ventricular (VZ). Hemos demostrado que las células de Glia Radial apicales (aRGCs) en la VZ se dividen para generar bRGCs, y que lo hacen manera continua para la zona subventricular interna (ISVZ) pero sólo durante un corto periodo embrionario para la OSVZ. Posteriormente, las bRGCs de la OSVZ son capaces de auto-amplificarse, formando un linaje independiente de VZ e ISVZ. Se trata de mecanismo sin precedentes implicado en la expansión y girificación de la corteza cerebral, en el que la expresión de los genes *Cdh1* y *Trnp1* son necesarios y suficientes para controlar el balance de producción de bRGCs y aRGCs durante el desarrollo cortical.

INTRODUCTION

INTRODUCTION

1. OVERVIEW OF THE NERVOUS SYSTEM

The nervous system is composed by the central (CNS) and the peripheral nervous system (PNS). The PNS is formed by neural clusters called peripheral ganglia and afferent and efferent nerves, and it communicates peripheral structures with central nervous system structures. The CNS is composed by the encephalon or brain (located in the cranial cavity), the spinal cord (inside the backbone), and also the eyes and optical fascicles.

The brain is formed by diverse types of cells and the majority of its functions emerge from the activity of specialized cells, the neurons, which communicate with each other and with the rest of the organism (Ramon y Cajal, 1909-1911; Ramón y Cajal, 1911). The brain is implicated in phenomena which happen in everyday life such as being asleep, waking up, feeling cold or pain, holding balance, abstract thinking and retrieving memories. Understanding the form, structure and function of the nervous system inform us about functions and possibilities of this complex structure.

2. BRAIN STRUCTURES

The brain derives during development from a closed tube (neural tube) with an internal cavity filled with liquid, and whose walls are progressively thickened and deformed as it develops. The neural tube is subdivided in three vesicles: prosencephalon (most anterior), mesencephalon and rombencephalon (subdivided into metencephalon and myelencephalon) (Fig. 1, A and B) (Marin and Rubenstein, 2003).

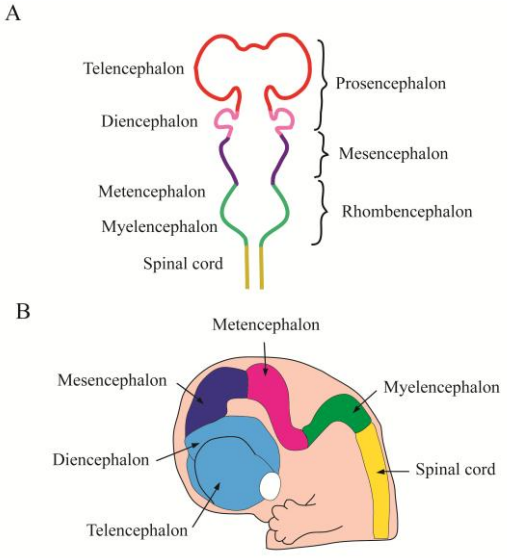

Figure 1. Development of CNS. The CNS is formed by the brain and the spinal cord. Since early development, the neural tube is divided in three major vesicles, which are each subdivided: prosencephalon (telencephalon and diencephalon), mesencephalon and rombencephalon (metencephalon and myelencephalon). [Adapted from Atlas Historia Vegetal y Animal, Universidad de Vigo and (Epstein, 2012)].

The prosencephalon includes the diencephalon and the telencephalon. The telencephalon is subdivided in two major regions: the pallium (roof) and the subpallium (base) (Fig. 2B). The pallium gives rise to the cerebral cortex and hippocampus, whereas the subpallium is subdivided in three main domains: the striatal, pallidal and telencephalic stalk domains, all of which extend medially into the septum. Finally, the olfactory bulbs develop as bilateral evaginations of the rostral pallium (Bulfone et al., 1998; Cobos, 2001). The most voluminous brain structure is, by far, the telencephalon (Fig. 2A). It is composed by two vesicles or hemispheres bound by the preoptic area. Three different poles can be distinguished: frontal, temporal and occipital.

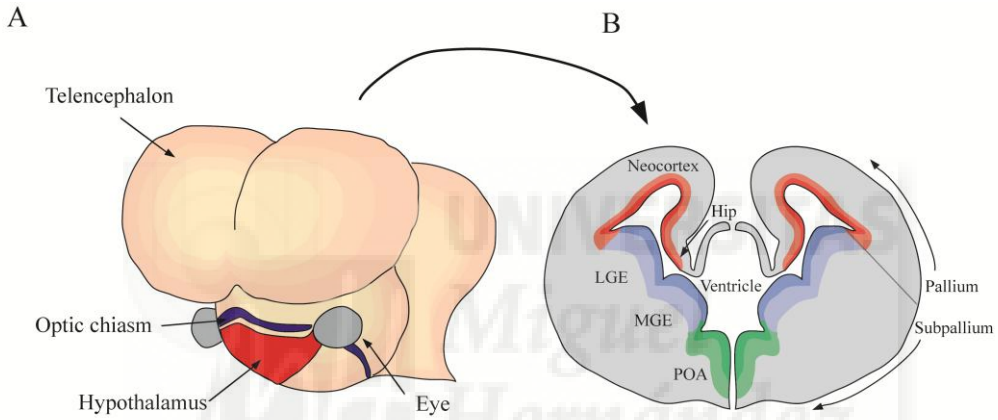

Figure 2. Telencephalic regions. The telencephalon is subdivided in two regions: pallium and subpallium. The pallium develops into the cerebral cortex and hippocampus, while the subpallium is formed by the medial and lateral ganglionic eminences (MGE, LGE) and the preoptic area (POA). [Adapted from (Marin and Rubenstein, 2001; Rowitch and Kriegstein, 2010)].

The cerebral cortex is the outer most part of the forebrain, which in mammals is subdivided into Allocortex, including Archicortex and Paleocortex, and Neocortex, also named Isocortex:

Archicortex is the most evolutionarily ancient part of the cerebral cortex and corresponds to the hippocampal formation. It belongs to the limbic system and is primarily involved in memory formation and retrieval (Insausti, 1993).

Paleocortex includes the olfactory nucleus, piriform cortex and, for some authors, also the olfactory bulb (Humphrey, 1939; Haberly, 1978).

Neocortex is a dorsal telencephalic structure unique to mammals, not present in reptiles or birds. It is the largest region of the mammalian cerebral cortex and the one that exhibits the most substantial phylogenetic expansion and specialization.

3. NEOCORTEX

3.1 Cytoarchitecture

The neocortex is formed by a thin mantle of grey matter enclosing the underlying white matter. The grey matter is composed by a network of projection neurons and local interneurons, as well as glial cells and blood vessels. Interneurons represent about 20-30% of neurons in the grey matter (depending on the species), in contrast to projection neurons which are much more abundant (70-80%). In the radial dimension, neurons are organized in six layers, I through VI (Fig. 3). In general, neurons in deep-layers (V-VI) connect with subcortical structures, while upper layer neurons (II-IV) establish contralateral or ipsilateral cortico-cortical connections (Douglas, 2004). Each layer contains projection neurons with similar cell-type identities and connectivity patterns. In addition, neurons from different layers are stereotypically interconnected in columns, which are the functional microunits of the cerebral cortex (Bystron et al., 2008).

In the neocortex we also can distinguish functional areas, each representing a functionally specialized cortical field and composed by distinct neuron subtypes, density and connectivity. The unique architecture of each area determines its particular functional specialization in the mature brain. In the adult, the transition from one area to another is abrupt with sharp borders (Brodmann, 1909; O'Leary, 2002; Garey, 2006). Each neocortical area has a specific complement of neurons establishing a specific set of connections with other cortical areas and brain structures which, together, comprise the neocortical network that ultimately generates the full repertoire of behaviors and a mature functional cerebral cortex.

3.2 Laminar organization of the Neocortex

As mentioned above, the cerebral cortex is organized in six cellular layers (Fig. 3). In some species, especially primates, some layers are further subdivided, increasing the complexity of cortical anatomy and circuits (Brodmann, 1909; Callaway, 1998b; Garey, 2006; Puelles et al., 2008). Each cortical layer displays some defining characteristics:

- Layer I, or Molecular layer: the outermost layer with a typically low cell density.

- Layer II, or Supragranular layer: a cell-dense layer formed by small-sized cells with pyramidal morphology.
- Layer III, or External Pyramidal layer: mostly composed by small pyramidal cells.
- Layer IV, or Internal Granular layer: composed by cells with a small cell body and stellate or pyramidal in morphology. Stellate and pyramidal neurons project mainly locally within the same cortical column, to Supragranular layer.
- Layer V, or Internal Pyramidal layer: formed by pyramidal cells with a large soma and very large and elaborate apical dendrite. These neurons typically project subcortically, to basal ganglia or spinal cord.
- Layer VI, or Multiform layer: composed by a variety of cells with different forms and sizes, most being pyramidal with a short dendrite. Neurons from this layer project to dorsal thalamic structures (Brodmann, 1909; Puelles et al., 2008).

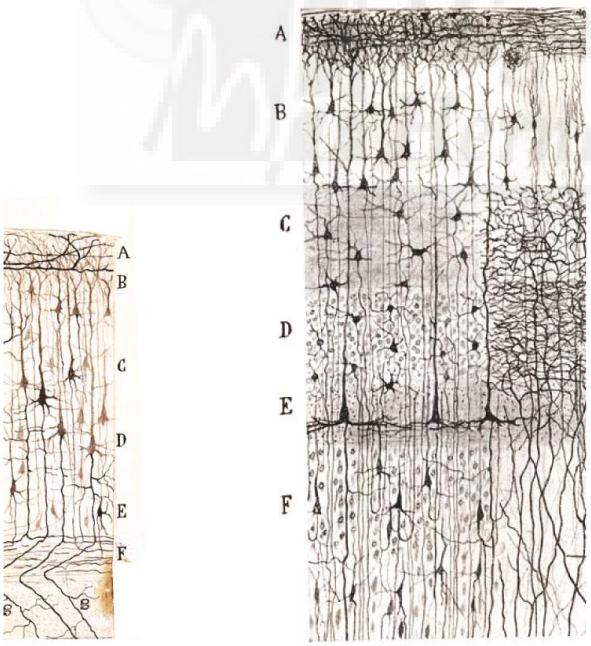

Figure 3. Laminar and cellular organization of the cerebral cortex. Cajal's schemas showing the main zones of the cerebral cortex. On the left, it represents a section of mouse cerebral cortex. On the right, schema of the human visual cortex. **A**, Molecular layer; **B**, Supragranular layer; **C**, External Pyramidal layer; **D**, Granular layer; **E**, Internal Pyramidal layer; **F**, Multiform layer. [Adapted from Cajal drawing in 1890,1891].

3.3 Cellular organization of the Neocortex

The neocortex is a complex and highly organized structure that contains hundreds of different neuronal cell types and a wide range of glial cell types.

3.3.1 Glial cells

Glial cells comprise more than 50% of brain cells, and are active elements in all forms of response, recovery and regeneration to injury and disease. They are much more numerous than neurons. Glial responses to injury and disease serve two main purposes: first, they repair the injured site and preserve the existing cell populations; second, they regenerate lost populations, including both neurons and glia.

The CNS contains three main classes of glial cells: astrocytes, oligodendrocytes and microglia.

3.3.1.1 Astrocytes

These cells present a star-like morphology with multiple arborized processes and end-feet contacting blood vessels. Astrocytes play diverse and crucial roles in normal CNS physiology, regulating synaptogenesis, neurotransmission, metabolic support, and blood-brain-barrier formation and/or maintenance. It has also been described that sites of CNS trauma or disease are populated by reactive astrocytes with three general properties: expression of GFAP, cellular hypertrophy and cellular proliferation (Gallo and Deneen, 2014).

3.3.1.2 Oligodendrocytes

In the CNS, oligodendrocytes are responsible for axon myelination. Myelin is a specialized membraneous structure, where compacted spirals of cytoplasmic membrane from oligodendrocytes extend around the axons of neurons. Oligodendrocytes are very numerous, especially in the white matter, and the position and relation of their cytoplasmic expansions into myelin sheaths is similar to the arrangement of the sheaths of Schwann cells (Río-Hortega, 1921; Penfield, 1924). The importance of myelin for CNS functioning has long been obvious from human diseases such as multiple sclerosis and inherited leukodystrophies, in which the integrity of the myelin sheath is lost, and

also from the severe phenotype of mutant mouse and rat strains in which the myelination process is disrupted (Emery, 2010; Gallo and Deneen, 2014).

3.3.1.3 Microglia

Microglia constitute over 10% of the total cells in the adult CNS and present a considerable heterogeneity (Tremblay et al., 2011; Aguzzi et al., 2013; Kettenmann et al., 2013). Microglia keep vigilant for disruptions to the status quo in the CNS, responding to specific threats in highly programmed ways and calling in reinforcements as needed. The response repertoire of microglia includes cytoskeletal rearrangements leading to morphological changes, stereotypic transcriptional alterations, and proliferation. Recently, several studies have pointed out that microglia processes are highly active, continuously scanning the environment (Davalos et al., 2005; Nimmerjahn et al., 2005), revealing unexpected roles for microglia in normal development, connectivity, and plasticity in the CNS. Thus, microglia are not restricted to responding when things go wrong but are active players in shaping activity in the healthy CNS (Tremblay et al., 2011; Schafer et al.; Wake et al., 2013).

3.3.2 Neurons

There are two broad classes of cortical neurons: inhibitory interneurons which make local connections within the cerebral cortex, and excitatory projection neurons, which extend axons to distant intracortical, subcortical and subcerebral targets (Fig. 4).

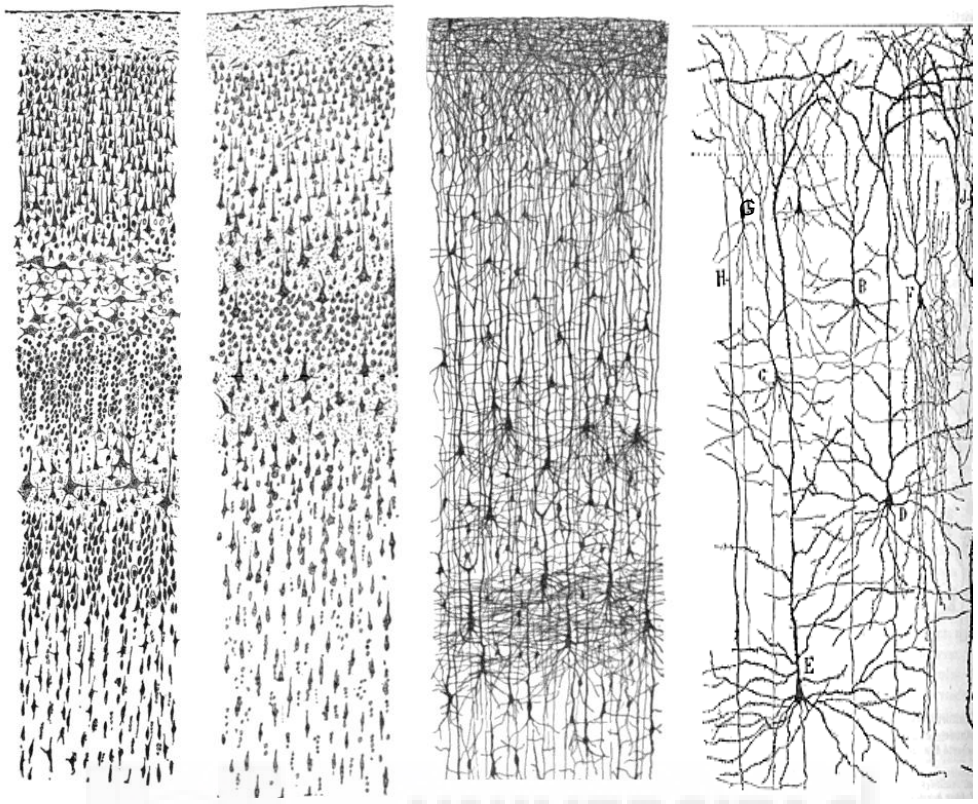

Figure 4. Cellular organization of the cortex. Vertical cross-section with the surface of the cortex at the top. On first section: Nissl-stained visual cortex of a human adult. On the second section: Nissl-stained motor cortex of a human adult. On the third section: Golgi-stained cortex of a one and a half month old infant. On the last section: Golgi stained superficial layers of the human frontal cortex showing small and large pyramidal neurons (**A,B,C,D,E**) and interneurons (**F,G**). The Nissl stain shows the cell bodies of neurons; the Golgi stain shows the dendrites and axons of a subset of neurons. [Adapted from four drawings by Santiago Ramón y Cajal (Ramón y Cajal, 1911)].

3.3.2.1 Excitatory Projections neurons

Projection neurons are excitatory and glutamatergic, characterized by a typical pyramidal morphology: one main apical dendrite extended toward the pial surface with some arborizations, and a main descending axon that may also arborize within the cortex before extending into the white matter (Fig. 4, A to E). Pyramidal neurons transmit information between different regions of the neocortex and to other regions of the brain. During development they are generated by progenitors of the neocortical germinal zone, located in the dorsolateral wall of the pallium.

As mentioned above, within the mature neocortex distinct populations of projection neurons are located in different cortical layers and areas, have unique morphological features, express different complements of transcription factors and serve

different functions within the neural network. Based on the characteristics of their axonal projections, excitatory neurons can be subdivided in:

Associative projection neurons: they extend axonal projections within the same cerebral hemisphere where they reside.

Commissural projection neurons: neurons that extend axonal projections to the opposite cortical hemisphere, via the corpus callosum or the anterior commissure.

Corticofugal projection neurons: neurons that extend axonal projections outside of the cortex. These include cortico-thalamic and subcerebral (cortico-spinal) projection neurons.

Spiny stellate neurons: these are one exception among excitatory neurons, which don't have a pyramidal morphology and don't project away from their immediate vicinity. Spiny stellate neurons have a descending axon but no apical dendrite; instead they have multiple basal dendrites extended in all directions from the cell soma, conferring them with a starry appearance. Spiny stellate neurons are located in layer IV and project only locally within their cortical column, mainly to layers II and III (Callaway, 1998a; Molyneaux et al., 2007).

3.3.2.2 Inhibitory local circuit neurons or Interneurons

Interneurons are inhibitory neurons expressing the neurotransmitter γ-Aminobutic Acid (GABA) that only project their axon locally, within their cortical column (Fig. 4, F and G). They are the most diverse group of neurons within the forebrain in terms of morphology, connectivity and physiological properties. Interneurons comprise only 15-30% of neurons in the cerebral cortex and are central regulators of neocortical function by locally shaping the activity of excitatory circuits. In addition to expressing GABA, they are characterized by having a small and oval cell body and no dendritic spines (Parnavelas, 1977). Interneuron cell types are currently defined using a combination of criteria based on morphology, connectivity pattern, synaptic properties, marker expression and intrinsic firing properties (Kepecs and Fishell, 2014). Traditionally, interneurons were classified only based on marker expression such as: Parvalbumin,

Somatostatin, Neuropeptide Y, Calretinin, Reelin, or following morphological criteria (Ascoli et al., 2008). Accordingly, they are identified as:

Basket cells: multipolar with an extensive branching of the dendrites similar to the structure of a basket. The dendrites contain smooth spines and extend from 12 to 30 mm. Basket cells have shown to form axo-somatic synapses. They are subclassified in small, large and nest basket cells (Marin-Padilla, 1969).

Chandelier cells: represent a small proportion of GABAergic neurons and are characterized by a specific shape of their axon terminals, which form vertically-oriented rows of buttons, or "cartridges". Chandelier neurons synapse exclusively to the axon initial segment of pyramidal neurons, near the site where the action potential is generated (Szentágothai and Arbib, 1974).

Martinotti cells: small multipolar neurons with short branching dendrites. They send their axons specifically to layer I, where they form axonal arborizations. They can receive inputs form different layers but within a single column. Martinotti cells express somatostatin (Ramón y Cajal, 1911; Bacon, 1996).

More types of inhibitory interneurons have been described based on their morphology, including Double-bouquet cells, Neurogliaform cells, Bipolar cells, and others (Ascoli et al., 2008).

3.4 Evolution of the Neocortex

The six layered structure of the neocortex is conserved in all mammalian species (Mountcastle, 1957). But the overall size, length, surface area and shape of the neocortex are different between species (Fig. 5). The variety of brain sizes among vertebrates spans five orders of magnitude, and the size of the neocortex, as the volume of the brain increases, enlarges disproportionately compared to most other parts of the brain, hence becoming its largest portion, a process known as neocorticalization (Finlay and Darlington, 1995; Jarvis et al., 2005). More specifically, differences in neocortical size between species are particularly due to the surface area rather than the thickness: the human neocortex has about 1000 times more surface area than in mouse, but less than 10 times in thickness (Haydar et al., 2000b; Rakic, 2009). Brain shapes are also

found in a remarkably varied repertoire, from spheroidal (manatee, human) to spindle-shaped (rabbit, giant ant-eater) (Welker, 1990).

Along mammalian phylogeny, folding of the neocortex may have emerged as a solution to the problem of increasing cortical surface area without massively increasing head size (Kelava et al., 2013). Indeed, the human neocortex is highly convoluted (gyrencephalic), presenting a complex pattern of fissures (sulci) and ridges (gyri), in contrast to the mouse neocortex which is smooth (lissencephalic). In order to fold, the neocortex needs to be pliable (DeFelipe et al., 2002; Kriegstein et al., 2006).

In general, a large neocortex contains more neurons than a small one; however, the number of neurons relative to neocortical volume varies considerably across mammalian orders. In rodents and insectivores, as neocortical size increases, neuron density tends to decrease, due to a corresponding increase in cell size (DeFelipe et al., 2002; Herculano-Houzel et al., 2006; Herculano-Houzel, 2012). In primates, on the other hand, neuron density remains relatively constant as neocortical size increases (Charvet et al., 2013) with no correlative increase in cell size (Herculano-Houzel et al., 2006; Herculano-Houzel, 2009).

Figure 5. Neocortex evolution. Differences in size, length, shape and surface of the neocortex between mammalian species are obvious. Scale bar: 5 cm.

4. DEVELOPMENT: GERMINAL LAYERS

During the very early development of the vertebrate embryo, neural fate is induced by the organizer (Hensen Node in amniotes) in a stage called gastrulation, and then maintained in the neural ectoderm by the underlying notochord Subsequently, the neural plate undergoes patterning of the future distinctive CNS regions, as well as neurulation to form the closed neural tube (Puelles et al., 2008). The wall of the early neural tube consists of a pseudostratified epithelium composed by NeuroEpithelial cells (NECs). NECs continuously move their nuclei from the apical to the basal sides of the neural tube depending on their phase of the cell cycle, in a process called interkinetic nuclear migration (INM). At the onset of neurogenesis, NECs change their identity and turn into Radial Glia Cells (RGCs), which will generate, directly or indirectly, all excitatory neurons and glial cells of the cerebral cortex (Paridaen and Huttner, 2014). As the first cortical neurons are formed, two distinct cellular layers become distinguishable: preplate, containing the earliest population of neurons; and ventricular zone (VZ), containing the cell bodies of RGCs. As development progresses, cortical thickness increases in size, and new types of progenitor cells and germinal layers emerge.

4.1 Ventricular Zone

The Ventricular Zone (VZ) is a pseudo-stratified epithelium characterized by a high density of cells with an elongated soma, radially orientated nuclei, columnar arrangement and limiting with the telencephalic lateral ventricle. In the VZ, the great majority of epithelial cells are Radial Glial Cells (RGCs) that make apical-basal contacts (Smart et al., 2002). Like NECs, RGCs undergo INM and mitosis at the apical surface of the cortical primordium (Dehay et al., 1993; Smart et al., 2002).

4.2 Subventricular Zone

At mid stages of cortical development the VZ is overlaid by a secondary germinal layer called subventricular zone (SVZ). This is characteristically formed by a high density of small progenitor cells without polarity nor particular orientation or arrangement, known as basal progenitors. Whereas in rodents the SVZ is relatively small, in primates this is remarkably larger. In fact, the primate SVZ is distinguished by its subdivision into an inner (ISVZ) and outer region (OSVZ) (Smart et al., 2002; Lukaszewicz et al., 2005; Zecevic et al., 2005; Fish et al., 2008). The ISVZ is similar to the SVZ of mouse, and

the SVZ of earlier stages in the primate embryo, characterized by containing a high density of small rounded cells, whereas the OSVZ displays a much lower density of cells. The striking similarity between the ISVZ and the SVZ seems to suggest that the ISVZ may emerge first in development and the OSVZ later, as a further specialization of the former. The OSVZ was initially identified in primates and thus thought to be unique to them (Smart et al., 2002), but recently it has been identified and described in many other mammalian species, both gyrated and lissencephalic, including rat, ferret and marmoset (Rakic, 2003; Reillo et al., 2011). The OSVZ is a very complex layer containing a highly heterogeneous mixture of cortical progenitor populations expressing different combinations of the transcription factors Pax6, Tbr2, Olig2, Sox2, and also containing radially and tangentially migrating neurons, radial glia fibers and axons (Sidman and Rakic, 1973; Letinic et al., 2002; deAzevedo et al., 2003; Zecevic, 2004; Zecevic et al., 2005; Bystron et al., 2006; Howard et al., 2006; Mo et al., 2007; Bayatti et al., 2008; Mo and Zecevic, 2008; Mo and Zecevic, 2009; Hansen et al., 2010; Reillo et al., 2011). Additional characterizations suggest that the emergence of the OSVZ at mid-stages of development may occur as a specialization from the ISVZ, as it may have also occurred during mammalian evolution (Reillo et al., 2011; Reillo and Borrell, 2012). Very importantly, variations in the size and thickness of the OSVZ across mammals are strongly correlated with the size and degree of folding of their cerebral cortex, supporting a central role for the OSVZ in neocortical expansion.

5. DEVELOPMENT: NEURAL PROGENITORS

As already mentioned, the neocortex is the largest brain region in mammals. Such selective expansion from the initial neural tube results from the combined effect of three parameters: (1) a greater initial pool of NECs prior to the onset of neurogenesis; (2) increased neuronal production through increased self-renewal of RGCs and the formation of “intermediate” transient-amplifying neurogenic basal progenitor cells (IPCs), forming the SVZ; and (3) a longer neurogenetic period. Indeed, all of these parameters seem to be related to expansion of the neocortex, especially in primates (Florio and Huttner, 2014; Taverna et al., 2014).

5.1 Types of Neural Progenitors

From a cell biological perspective, the developing mammalian neocortex contains three principal classes of neural progenitor cells (NPCs): apical progenitors, confined to the apical most germinal layer, the VZ; basal progenitors, which cluster forming a second germinal layer basal to the VZ, the SVZ; and subapical progenitors (Fig. 6). The relative abundance of each type of neural progenitor varies between different neocortical regions, developmental stages and species (Fietz and Huttner, 2011; Lui et al., 2011; Borrell and Reillo, 2012; LaMonica et al., 2013).

5.1.1 Apical progenitors

Apical progenitors undergo mitosis at the luminal surface of the VZ, while being integrated into the apical adherens junction belt and exposing part of their plasma membrane to the ventricular lumen (Gotz and Huttner, 2005).

5.1.1.1 Subtypes of Apical Progenitors

There are three different types of apical progenitors: Neuroepithelial Cells, apical Radial Glia Cells and Short Neural Progenitors (Fig. 6) (Borrell and Calegari, 2014).

5.1.1.1.1 Neuroepithelial cells

NECs are cells polarized along their apical-basal axis that span the entire width of the neocortical neuroepithelium, resting on the basal lamina with their basal plasma membrane, and facing the lumen of the neural tube with their apical plasma membrane (Huttner and Brand, 1997; Gotz and Huttner, 2005). NECs form adherens junctions with each other at apical-most domain of their lateral membrane. Neuroepithelial cells (NECs) are the only type of progenitor cell in the early cortical primordium, forming a monolayer epithelium known as the neural plate. However, because NECs undergo INM along their cell cycle, this neuroepithelium acquires the false appearance of containing multiple cell layers, and hence it is referred to as a pseudostratified neuroepithelium. Because NECs are the founders of the cortical primordium, their lineage gives rise to all excitatory neurons of the neocortex. But immediately prior to the onset of neurogenesis, NECs acquire novel features, such as downregulation of epithelial markers and de novo expression of glial cell markers (GLAST, GFAP or Vimentin) (Choi and Lapham, 1978; Levitt and Rakic, 1980; Engel and Muller, 1989), and thus they become aRGCs (Gotz and Huttner, 2005).

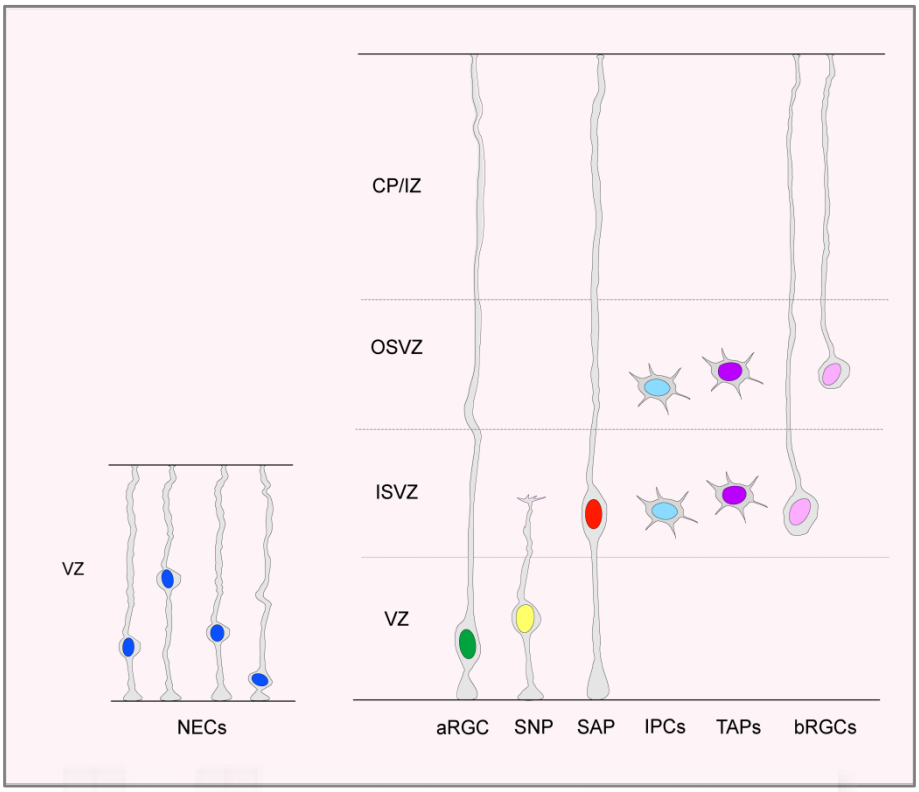

Figure 6. Progenitor cells and layering in the developing mammalian neocortex. The first germinal layer to form in neocortex at the onset of neurogenesis is the VZ. As cortical thickness increases, new cell types and germinal layers emerge. The SVZ is the secondary germinal layer, which in species with an enlarged neocortex is subdivided in ISVZ and OSVZ. In terms of progenitors, three main types are described: apical (AP), basal (BP) and subapical progenitors (SAP). Among APs there are NECs, aRGCs and SNPs; BPs include IPCs, TAPs and bRGCs.

5.1.1.1.2 Apical Radial Glia Cells

Apical Radial Glial Cells (aRGCs) retain the apical-basal polarity and neuroepithelial features typical of NECs, contacting both the ventricle and the basal lamina (Fig. 6). Similar to NECs, they also form adherens junctions with neighboring RGCs in their apical side, and undergo INM, with mitotic divisions occurring at the apical surface (Gotz and Huttner, 2005). In their apical membrane, aRGCs present a cilium exposed to the ventricle important to detect signaling molecules, such as Shh and IGF (Roessmann et al., 1980; Walsh, 1988; Marín-Padilla, 1999; Campbell and Gotz, 2002; Gotz et al., 2002; Kim et al., 2010). In contrast to NECs, aRGCs coexist with other cell types in the developing cortex (initially newborn neurons), which hence becomes multilayered (see above). While additional cortical layers form basally (under the basal lamina), the cell bodies of aRGCs remain in the apical part of the cortical primordium, forming the VZ.

In this scenario, and with the cortical thickness progressively increasing, aRGCs elongate their basal process to remain attached to the basal lamina, which then becomes known as radial fiber. This radial fiber soon becomes essential to newborn cortical neurons as substrate and guide for their radial migration. As for gene expression, aRGCs are characterized by expressing the transcription factor Pax6 (Gotz et al., 1998; Warren et al., 1999; Estivill-Torrus et al., 2002; Osumi et al., 2008) and glial markers like BLBP or GFAP (Malatesta et al., 2000; Campbell and Gotz, 2002). At the end of neurogenesis, aRGCs delaminate from the VZ and differentiate into astrocytes (Schmechel and Rakic, 1979b).

NECs and RGCs can undergo two different types of division:

Symmetric division: Cells divide to generate two daughter cells with the same identity. This identity may be the same as the mother cell (self-amplificative or proliferative), or different (self-consuming). It allows the expansion in the lateral dimension (if amplificative) and the growth in the radial dimension (if self-consuming).

Asymmetric division: This mode of division generates one daughter cell that has the same identity as the mother cell (self-renewing), and another daughter with a different identity (i.e. basal progenitor or neuron).

During cortical neurogenesis, there is a gradual switch from symmetric (proliferative) to asymmetric (neurogenic) divisions, coincident with an also gradual increase in cell cycle length (Chenn and McConnell, 1995; Takahashi et al., 1995).

5.1.1.1.3 Short neural precursors

Also known as apical Intermediate Progenitors, Short Neural Precursors (SNPs) form apical junctions and maintain contact with the ventricular surface but not with the basal lamina, as their basal process detaches from this basal lamina and is retracted for mitosis after one round of INM (Fig. 6). They typically express Pax6 and are the only aRGC daughter cell type that exhibits features of aRGCs. SNPs down-regulate astroglial genes and self-renewing potential, and undergo only one round of symmetric neurogenic division, self-consuming into a pair of neurons. Thus, the generation of SNPs is a mechanism for doubling the neuronal output per apical mitosis (Gal et al., 2006; Stancik et al., 2010; Tyler and Haydar, 2013).

5.1.1.2 Apical components of apical progenitors

Apical components include apical plasma membrane, primary cilium, centrosomes, adherens junctions and gap junctions. The juxtaposition of the apical plasma membranes of all apical progenitors forms the apical surface, facing the ventricle of the neural tube. The apical end-foot lines the ventricle filled with the cerebrospinal fluid (CSF) and plays a crucial role in signaling (Lehtinen et al., 2011; Johansson et al., 2013). To receive signals secreted into the CSF, there is a protrusion from the apical membrane into the lumen of the ventricle called primary cilium. The primary cilium is a complex organelle with two components: the centrosome and the ciliary membrane. The centrosome is the oldest centriole and forms the base of the cilium (Louvi and Grove, 2011). Furthermore, the apical domain contain gap junctions, which allow for intercellular communication and signaling (Sutor and Hagerty, 2005; Yamashita, 2013).

5.1.1.3 Basal components of apical progenitors

The basal components include the baso-lateral plasma membrane, junctional complexes and the basal process (composed by varicosities and the basal end-feet). The baso-lateral plasma membrane constitutes most of the plasma membrane of NECs and aRGCs. It surrounds and accommodates the nucleus during the different phases of INM and reaches the basal lamina. Importantly, the amount of baso-lateral plasma membrane increases during development to match the increase in the cortical wall thickness. This increase pertains mainly to the so-called basal process (Taverna et al., 2014). The distal segment of the basal process is very thin and spans all neuronal layers, reaching the basal lamina. This basal process is never occupied by the nucleus during INM and is typical feature of aRGCs, some subapical progenitors and basal radial glial cells. Originally regarded merely as a scaffold for neuron migration, the basal process is nowadays recognized as an active subcellular compartment involved in signaling and fate specification (Fietz and Huttner, 2011). The basal process presents two subcompartments: the varicosities and the basal end-foot. Varicosities are areas of swelling in which the diameter of the basal process is not homogeneous (Bentivoglio and Mazzarello, 1999). The basal end-foot is the part of the basal process that makes direct contact with the basal lamina; therefore, it is the subcellular structure that more probably receives signals generated by, or enriched in, the basal lamina.

5.1.2 Basal progenitors

Basal progenitors undergo mitosis at a location basal from the apical surface, typically in the SVZ. These progenitors are delaminated from the adherens junction belt and thus lack apical plasma membrane (Fietz et al., 2010; Hansen et al., 2010; Fietz and Huttner, 2011; Betizeau et al., 2013).

5.1.2.1 Subtypes of Basal Progenitors

There are three types of basal progenitors: Intermediate Progenitor Cells (IPCs), basal Radial Glia Cells (bRGCs; also called oRG cells) and Transit-Amplifying Progenitors (TAPs) (Fig. 6) (Haubensak et al., 2004; Miyata et al., 2004; Noctor et al., 2004; Fietz et al., 2010; Hansen et al., 2010; Reillo et al., 2011; Shitamukai et al., 2011; Wang et al., 2011b; Borrell and Reillo, 2012; Betizeau et al., 2013).

5.1.2.1.1 Intermediate Progenitor Cells (IPCs)

They are non-epithelial progenitors formed by aRGCs that, once born, lose apical-basal polarity and retract their processes acquiring a multipolar morphology, to then migrate basally and form the SVZ (Noctor et al., 2004). In terms of markers, IPCs typically express the transcription factor Tbr2 and not astroglial markers or Pax6. These progenitors divide in a self-consuming manner, undergoing only one round of symmetric neurogenic division. IPCs are viewed as the major source of neurons for all cortical layers (Kowalczyk et al., 2009).

5.1.2.1.2 Transit Amplifying Progenitors (TAPs)

TAPs are essentially similar to IPCs but, unlike these, TAPs undergo multiple rounds of cell division in which they either self-amplify or self-renew before undergoing terminal neurogenic, self-consuming division (Taverna et al., 2014).

5.1.2.1.3 Basal Radial Glia Cells (bRGCs)

They are very similar to aRGCs but differ from these by lacking an apical process contacting the ventricle (Fietz et al., 2010; Hansen et al., 2010; Reillo et al., 2011). Basal RGCs have been shown to occasionally exhibit mitotic somal translocation (MST), where the bRGC soma rapidly ascends in the basal direction shortly before mitosis (Hansen et al., 2010; LaMonica et al., 2013). This seems to be much more frequent in human embryos than in other primates (macaque) or in ferret (Betizeau et al., 2013; Gertz et al., 2014). Similar to aRGCs, the majority of bRGCs express astroglial markers and Pax6. However, because unlike aRGCs they do not contact the

apical ventricular surface and are not embedded into the apical junction belt, bRGCs do not express apically localized membrane constituents such as CD133 (PROM1), Par3 (PARD3), or aPKCλ (PRKCI) (Fietz et al., 2010). In addition, and in contrast to the initial descriptions, recent analyses demonstrate that a high proportion of bRGCs co-express Tbr2, at least in the developing macaque neocortex (Betizeau et al., 2013).

Originally, bRGCs were described in the OSVZ of human and ferret, but they are now known to exist also in mouse, a species that lacks an OSVZ, and in the ISVZ and OSVZ of the marmoset, a near-lissencephalic primate (Garcia-Moreno et al., 2012; Kelava et al., 2012; Reillo and Borrell, 2012). Marker expression analyses in the ferret indicate that a larger percentage of bRGCs reside in the OSVZ compared with the ISVZ (Reillo and Borrell, 2012). *In vitro* experiments in human and mouse show that aRGCs in VZ produce bRGCs via horizontal divisions (Shitamukai et al., 2011; Wang et al., 2011a; LaMonica et al., 2013). However, the initial phase of OSVZ expansion does not seem to occur at the expense of progenitor cells in the VZ/ISVZ, indicating that the OSVZ may be generated by self-amplification rather than by delamination and migration from VZ progenitors. Accordingly, bRGCs have occasionally been observed to divide and amplify to produce more bRGCs (Hansen et al., 2010; Reillo et al., 2011). Locally expanding the population of progenitors in a basal germinal zone would be a mechanism to greatly increase neuron production, therefore highly relevant for building large brains (Haubensak et al., 2004; Miyata et al., 2004; Noctor et al., 2004; Fietz et al., 2010; Hansen et al., 2010; Reillo et al., 2011; Shitamukai et al., 2011; Wang et al., 2011b; Borrell and Reillo, 2012; Betizeau et al., 2013; Pilz et al., 2013).

Different morphological subtypes of bRGCs have been recently described. In addition to the ‘classical’ bRGC, with an extensive basal process usually reaching the basal membrane (bRG-basal-P; P for process), two additional bRG morphotypes can be distinguished: bRG cells with a well-developed apical process (bRG-apical-P), extending as far as the ISVZ and VZ, but without however reaching the ventricular surface; and bipolar bRG cells bearing both an apical and a basal process (bRG-both-P) (Betizeau et al., 2013; Pilz et al., 2013). In addition, a fourth alternative subtype of bRG has been identified and designated as transient bRG (tbRG), which dynamically extends an apical and/or a basal process, and may even retract both, during a single cell cycle.

5.1.3 Sub-Apical Progenitors (SAPs)

Sub-Apical Progenitors (SAPs) are bipolar radial glia distinct from aRGCs in that they undergo mitosis at a sub-apical location within the VZ, at a significant distance from the apical surface. In contrast to basal progenitors, however, SAPs display an apical process contacting the ventricular surface, even during mitosis (Pilz et al., 2013). These were originally identified in the basal ganglia, where they have been best characterized, and although they are known to also exist in the neocortex little is still known about their marker expression or mode(s) of cell division in the developing neocortex.

5.2 Factors underlying interspecies variations in neural progenitor cells

5.2.1 Intrinsic factors

The evolutionary enlargement of the neocortex entails a vast increase in the numbers of neurons produced during neocortical development. The final number of neurons in a given species is determined by several parameters such as: the absolute number of neural progenitor cells (NPC) and the relative abundance of each NPC type, the modes of cell division carried out by each NPC type, the length of their cell cycle and the duration of the neurogenic period (Florio and Huttner, 2014).

The relative abundance of NPC types and their contribution to the final neuronal output are different between species. For instance, interspecies variations in the abundance of basal progenitors result in changes in the thickness of the SVZ, where their cell bodies reside. As mentioned above, in gyrencephalic species the SVZ is subdivided in ISVZ and OSVZ (this subdivision is absent in most lissencephalic species) (Fig. 7) (Smart et al., 2002; Encinas et al., 2011). The thickness of the ISVZ remains constant over the course of neurogenesis but the OSVZ grows progressively thicker (Smart et al., 2002), reflecting a dramatic increase in the number of basal progenitors. Importantly, the increase in basal progenitor abundance at the peak of neurogenesis is accompanied by considerable changes in the cell type composition of the SVZ. In mice, the SVZ is composed mainly by neurogenic IPCs (around 90% of basal progenitors) and only a small fraction of bRGCs (~5%) and proliferative IPCs (around 10%) (Noctor et al., 2004; Arai et al., 2011; Shitamukai et al., 2011; Wang et al., 2011b; Martinez-Cerdeno et al., 2012). In human and macaque, these proportions are dramatically different, as bRGCs become the most abundant basal progenitor type

(50-75%), and the remaining basal progenitors are mostly TAPs (Hansen et al., 2010; Lui et al., 2011; Betizeau et al., 2013).

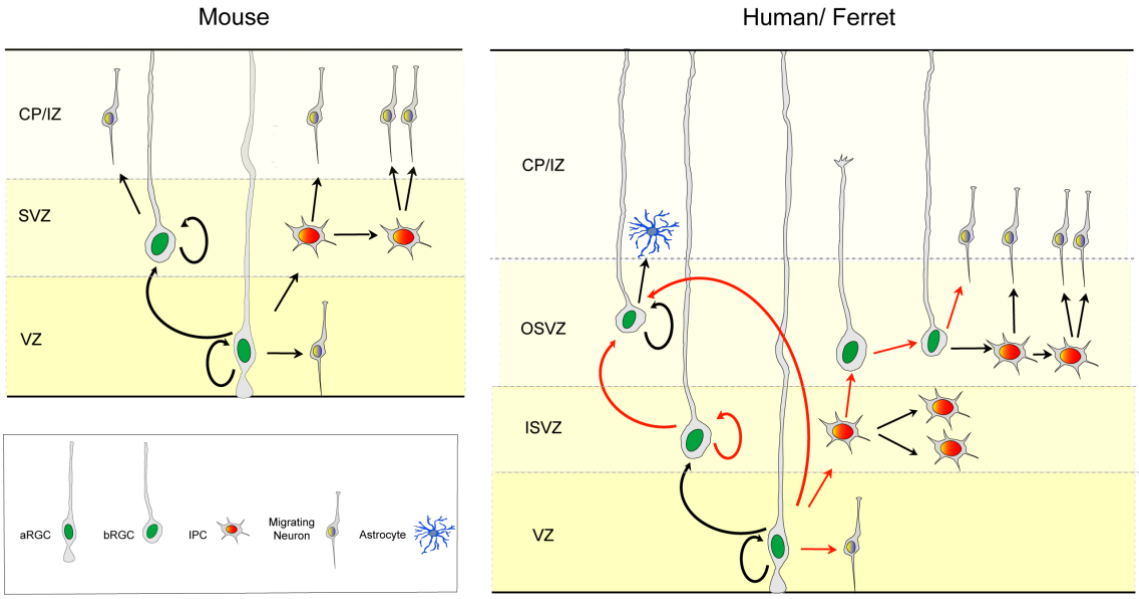

Figure 7. Interspecific variation in NPCs. Schema showing the main cortical progenitor cell types and their lineage relationships. Very significant differences exist between mouse, ferret and human developing cerebral cortex. Black arrows indicate lineage relationships demonstrated by time-lapse imaging and/or by retroviral lineage tracing. Red arrows indicate hypothetical or assumed lineage relationships, but not yet demonstrated.

5.2.1.1 *Modes of cell division*: IPCs are self-consuming neurogenic progenitors, which in lissencephalic rodents vastly predominate over the self-amplificative TAPs, whereas in gyrencephalic primates TAPs largely outnumber IPCs (Hansen et al., 2010; Betizeau et al., 2013). Similarly, bRGCs in lissencephalic rodents only undergo neurogenic divisions, whereas in gyrencephalic species these can undergo multiple rounds of self-amplification (Reillo et al., 2011; Shitamukai et al., 2011; Wang et al., 2011b; Betizeau et al., 2013).

5.2.1.2 *Cell cycle length*: differences in cell cycle length have been shown to represent a cell fate determinant, in particular the length of the G1 phase (Calegari and Huttner, 2003; Calegari et al., 2005). In mice, lengthening of the G1 phase in NPCs was shown to trigger premature neurogenesis (Calegari and Huttner, 2003; Lange et al., 2009). Conversely, G1 shortening increased NPC proliferation and delayed neurogenesis (Lange et al., 2009; Pilaz et al., 2009; Nonaka-Kinoshita et al., 2013).

5.2.1.3 *Length of the neurogenic period*: this parameter also determines critically the output of neurogenesis. A delayed onset of neurogenesis (accumulating a large number of progenitors) and a protracted neurogenic period will lead to a significant expansion of the NPC pool and hence neuron production. In primates, the onset of neurogenesis is delayed compared with rodents (Rakic, 1995b; Kornack and Rakic, 1998; Rakic, 2009), allowing for greater expansion of the NEC pool before neurogenesis begins. But also in primates neurogenesis is protracted for a much longer period of time (up to ten-fold longer) compared with rodents (Caviness et al., 1995; Rakic, 1995a), allowing for expansion of NPCs, notably bRG (Gotz and Huttner, 2005; Kriegstein A, 2009; Borrell and Calegari, 2014; Borrell and Gotz, 2014; Florio and Huttner, 2014).

5.2.1.4 *Orientation of the cleavage plane*: this is primarily determined by the axis of the mitotic spindle (Lancaster and Knoblich, 2012), which is a key element regulating the symmetry or asymmetry of cell division for aRGCs (Huttner and Kosodo, 2005; Shitamukai et al., 2011; Peyre and Morin, 2012). A vertical cleavage plane in rodents (with a cleavage furrow perpendicular to the ventricular surface) gives rise to symmetric divisions, whereas horizontal cleavage planes (parallel to the ventricular surface) lead to asymmetric divisions. Evolutionary changes in mitotic spindle orientation may have altered the way cell fate determinants are segregated during mitosis, affecting daughter cell fate and function and possibly leading to increased bRGC generation (Chenn and McConnell, 1995; Knoblich, 2008; Lancaster and Knoblich, 2012). Many studies have related mitotic spindle orientation with cell fate, such as those encoding LGN (also known as Gpsm2) and inscuteable (Konno et al., 2008; Postiglione et al., 2011), genes that carry mutations causing primary microcephaly in human (MCPH) (Fish et al., 2008; Manzini and Walsh, 2011).

5.2.1.5 *Extracellular matrix*: several studies have raised the possibility that progenitor-autonomous production of extracellular matrix constituents (ECM), may contribute to the proliferative capacity of progenitors (Arai et al., 2011; Fietz et al., 2012). Recently, *integrin* αvβ3 (ECM constituents) activation has been found to increase the cell cycle reentry of basal intermediate progenitors (Stenzel et al., 2014). Moreover, the interferences with integrin αvβ3 signaling reduce the bRG pool size in ferret (Fietz et al., 2010). Based on this, integrins, which are major receptors for ECM constituents, may have a key role in NPC proliferation. Even it has been suggested a significant role of integrins in the microenvironment of the VZ. At early stages laminins, a

heterotrimeric family of ECM molecules, are present in the VZ and their integrin receptors are expressed by NECs. It has been described that laminin/integrin interaction in anchoring NECs to the ventricular surface and maintaining the physical integrity of the neocortical niche, with even transient perturbations resulting in long-lasting cortical defects. (Lathia et al., 2007; Loulier et al., 2009). In addition integrins control different aspects of neuronal migration, neuron-glia attachment and anchoring during cortical neuronal migration (Anton et al., 1999).

5.2.2 ***Extrinsic factors***

5.2.2.1 Thalamo-cortical axons

During the period of cortical neurogenesis, axons from the thalamus grow into the neocortex to eventually form synapses with neurons in the cortical plate (Molnár and Blakemore, 1995). In this process, when traversing the intermediate zone, these axons secrete mitogenic factors that could potentially affect the proliferation of NPCs within the SVZ (Fig. 8) (Dehay et al., 2001; Dehay and Kennedy, 2007).

5.2.2.2 Cerebrospinal Fluid

The ventricles are filled with the cerebrospinal fluid (CSF), produced mainly by the choroid plexus which is a highly vascularized secretory epithelium. The composition of the CSF is conserved across species, and it is dynamically regulated during development. Main components of the CSF include insulin growth factors (IGFs), Fibroblast Growth Factors (FGFs), Sonic hedghog (Shh), Bone Morphogenic Proteins (BMPs) and Wnts (Dziegielewska et al., 2001; Johansson et al., 2008; Lehtinen et al., 2011; Johansson et al., 2013; Lehtinen et al., 2013). Importantly, IGFs (in particular IGF2) stimulate progenitor proliferation and therefore influence neurogenesis and brain size (Lehtinen et al., 2011). FGFs positively regulate progenitor proliferation and are implicated in early brain patterning and the regulation of primary cilium length and function (Iwata and Hevner, 2009; Neugebauer et al., 2009). Shh has been demonstrated to synergize with IGF signaling (Rao et al., 2004; Fernandez et al., 2010).

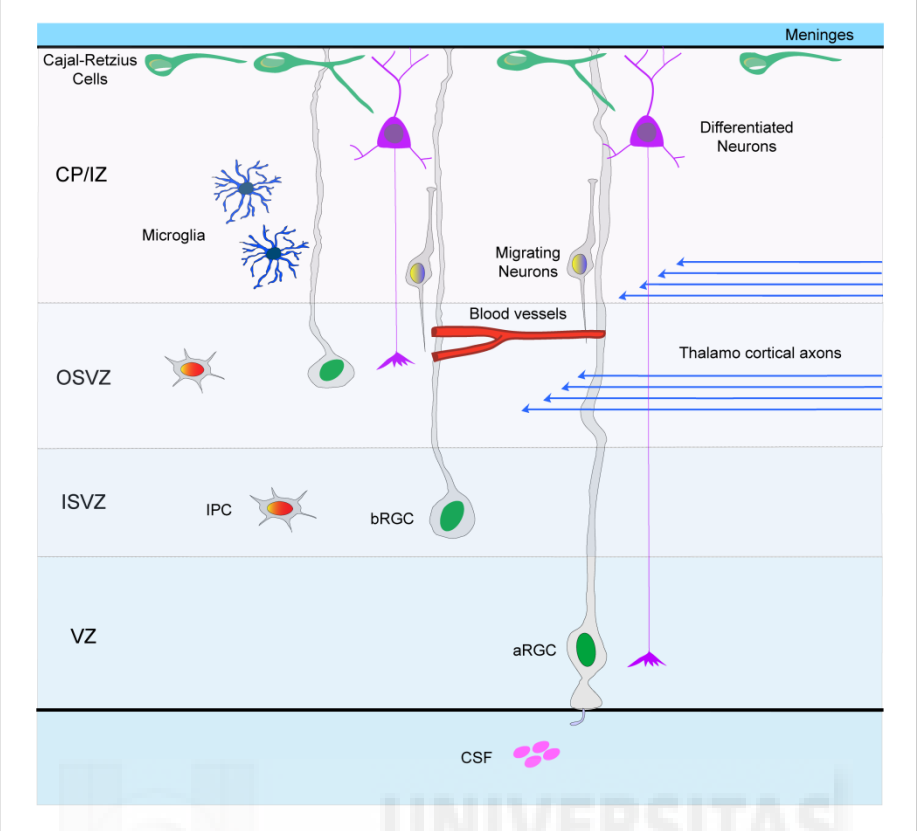

Figure 8. Factors regulating progenitor cells (NPCs). There are intrinsic and extrinsic factors affecting progenitors during cortical development. Among intrinsic: orientation of the cleavage plane, cell cycle length, mode of cell division and autonomous ECM. Respect to extrinsic factors, a large list of them has been described: thalamo-cortical axons, ventricular fluids, signals from blood vessels, microglia, neighboring stem and progenitor cells, meninges and neurons.

5.2.2.3 Stem and Progenitor Cell Niche

There are chemical signals and physical signals that stem and progenitor cells can produce, thus creating a local niche for NPCs:

Chemical signals: Gap junctions enable direct chemical communication between neighboring cells (Elias et al., 2007). Furthermore, progenitor cells secrete purines that affect proliferation of neighboring cells (Liu et al., 2010). Another example is Notch signaling, which occurs for basal intermediate progenitors and neurons binding to the Notch receptor present on aRGCs (Yoon et al., 2008). In addition, oxygen can regulate neural precursor fate. Changes in oxygen levels produce distinct stages in precursor differentiation. For instance, in mouse cortical progenitors lowered oxygen tension (2-5%) promotes clonal and long-term expansion, decreases apoptosis and prevents neuronal differentiation; in contrast, 20% oxygen induces apoptosis (Morrison et al., 2000; Chen et al., 2007; Milosevic et al., 2005).

Physical signals: Recent work suggested that progenitors may sense mechanical stress, in the sense of overcrowding, and respond to it by changing the location of their nucleus in the tissue (Kosodo et al., 2011; Leung et al., 2011; Okamoto et al., 2013). This is in agreement with classical studies that had already previously proposed that the occurrence of basal divisions is due to the congestion of the ventricular surface by apical mitoses (Smart, 1972b; Smart, 1972a).

5.2.2.4 Signals from Blood Vessels

It has been proposed that the vasculature in the developing brain acts as a niche for BPs, providing a source of nutrients and signaling molecules regulating their behavior (Javaherian and Kriegstein, 2009; Stubbs et al., 2009). Furthermore, the basal process of aRGCs serves as a guide for blood vessels invading from the pial surface, highlighting the close interrelationship between aRGCs and the vasculature (Fig. 8) (Ma et al., 2013).

5.2.2.5 Microglia

Microglia plays bidirectional roles in cortical development, by supporting cell generation and removing unnecessary cells. Microglia has been observed in the neuroepithelium where progenitor cells proliferate; these cells release trophic factors such as BDNF, FGF2, and IGF1 which may be involved in proliferation. Conversely, it has been described an opposite role of microglia restricting the number of neural progenitor cells through phagocytosis. In postnatal macaques and rats, microglia limit the production of cortical neurons colonizing the cortical proliferative zones, specifically SVZ and phagocytosing neural precursor cells (Cunningham et al., 2013). A prominent number of microglia in the VZ and SVZ has been correlated with reduction in the number of progenitor cells (Cunningham et al., 2013). Deactivating or eliminating microglia significantly increased the number of progenitor cells, whereas activating microglia decreased the number of these cells (Cunningham et al., 2013; Ueno and Yamashita, 2014).

5.2.2.6 Signals from the Meninges

The meninges release retinoic acid and key signals (such as chemokines) affecting cortical progenitor behavior, neurogenesis and growth of the cerebral cortex (Fig.8) (Borrell et al., 2006; Siegenthaler et al., 2009).

5.2.2.7 Neurons

Several types of neurons can influence progenitor behavior. For instance, Cajal-Retzius cells, which are pioneer neurons born at the very onset of neurogenesis, are known to secrete Reelin (Bar, 2000; Soriano and Del Rio, 2005), a protein implicated in neuronal migration and a proposed role in the regulation of cortical progenitor behavior (Hartfuss et al., 2003). Transient or migrating neurons of the cortical plate are another example of regulation between neurons and progenitors (Fig. 8). They are produced in the ventral telencephalon, migrate a long way and eventually invade the dorsal telencephalon but later disappear. Their ablation during development results in premature neurogenesis and depletion of the progenitor pool (Teissier et al., 2012). Finally, migrating neurons may also influence progenitor cell proliferation by the release of neurotransmitters such as GABA or glutamate. Different gradients of these peptides along development fit with activation or inhibition of proliferation (LoTurco et al., 1995; Antonopoulos et al., 1997; Fiszman et al., 1999; Haydar et al., 2000a).

6. DEVELOPMENT: NEURONAL MIGRATION

Newly specified neurons migrate before they differentiate and form synapses. Some migrations cover long distances (up to thousands of cell diameter) and follow complex routes, changing direction at landmarks along the way.

6.1 Types of Neuronal migration

Two main types of neuronal migration have been identified in the telencephalon: 1) radial migration, in which cells migrate from the germinal zone toward the surface of the brain following the radial disposition of radial fibers; and 2) tangential migration, in which cells migrate orthogonal to the direction of radial migration (Fig. 9).

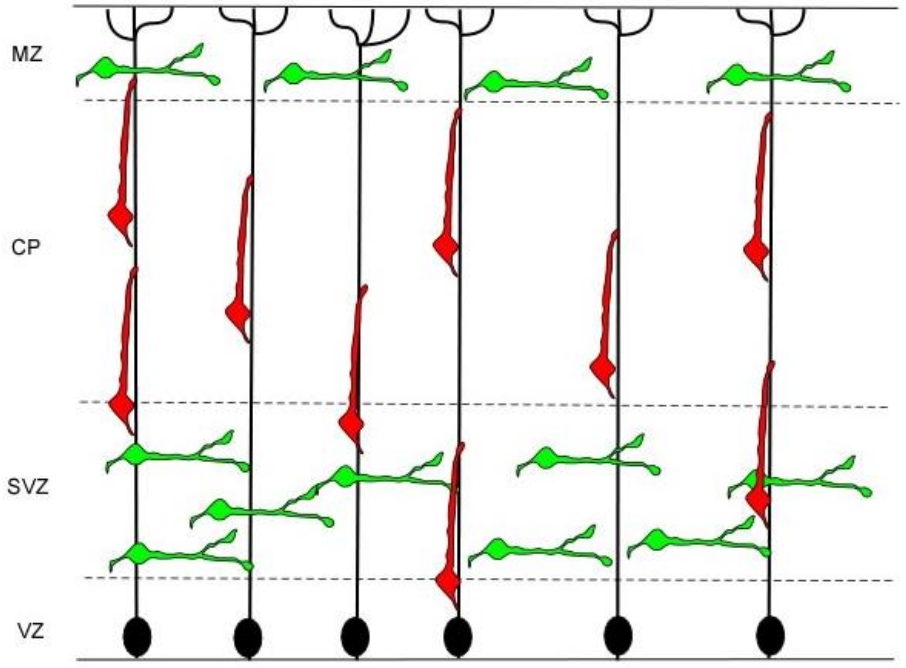

Figure 9. Neuronal migration in cerebral cortex development. Two different kinds of migration can be observed in the cortex, radial vs tangential. In the last one, neurons migrate parallel to the ventricular surface; in contrast to radial migration in which neurons go perpendicularly. Green cells are tangential migrating interneurons. Red cells are radial migrating pyramidal neurons.

6.1.1 Tangential migration

Tangential migration is typical of GABAergic interneurons, which are generated in the Ganglionic Eminences (GE) of the subpallium, and from there they migrate dorsally to reach the cerebral cortex, mainly following the SVZ (Anderson et al., 1997; Anderson et al., 2001; Marin and Rubenstein, 2001; Anderson et al., 2002: Pleasure, 2000 #2485; Marin et al., 2003; Nakajima, 2007). During tangential migration, interneurons form branches in their leading process. This mechanism allows interneurons to change their direction of movement, and has also been interpreted as a mechanism employed by the cell to explore a wide territory (Ward, 2005; Martini et al., 2009). Once in the cerebral cortex, interneurons switch from tangential to radial migration, to then migrate from the SVZ to the cortical plate (CP), where they settle in the appropriate layer of destination (Yokota, 2007; Martini et al., 2009; Marín, 2013).

6.1.2 Radial migration

Glutamatergic neurons are generated locally within the germinal layers of the cerebral cortex (VZ or SVZ) and migrate radially from there to the marginal zone (MZ) (Marin et al., 2003; Kriegstein and Noctor, 2004; Marin et al., 2010). At early stages of corticogenesis cells migrate out of the VZ independently of RGCs by somal translocation (Morest, 1970; Parnavelas et al., 2002). In this mode, cells have a long process that terminates at the pial surface and a short trailing process (Morest, 1970; Brittis et al., 1995; Miyata et al., 2001; Nadarajah et al., 2001). Translocating cells first extend this basal process to the pia as they leave the VZ, and then they lose their ventricular attachment while maintaining their pial connection (Nadarajah et al., 2001). The movement is relatively continuous and the leading process becomes progressively shorter.

As corticogenesis proceeds and the cortex becomes thicker, neurons adopt glia-guided locomotion, using the radial fiber of RGCs as scaffold and guide for their migration (Rakic, 1972). Radially migrating neurons undergoing locomotion extend a relatively short leading process, which is repeatedly extended and retracted to climb up the radial fiber. In fact, radial migration by cell locomotion involves four very different phases (Noctor et al., 2004): (1) Neurons born in the VZ move rapidly to the SVZ; (2) Migratory arrest for 24 hours or more in a multipolar state in the SVZ; (3) Retrograde migration toward the ventricle, observed only occasionally; (4) Polarity reversal and final migration toward the cortical plate. It is during this last phase that neurons migrate guided by, and in intimate relation with, radial fibers, which also serve as the physical-chemical substrate (Rakic, 1972; Sidman and Rakic, 1973; Rakic, 1974; Choi and Lapham, 1978; O'Rourke et al., 1995; Ang et al., 2003; Yoshikawa et al., 2003). In lissencephalic species, radial glia fibers display perfectly parallel trajectories, whereas in gyrencephalic species these display a dramatic divergence (Fig. 10) (Schmechel and Rakic, 1979a; Reillo et al., 2011). The tangential scatter of pyramidal neurons within the cerebral cortex, between their site of birth and their final location, is limited by the trajectory of radial glia fibers (Rakic, 1995a; Noctor et al., 2004; O'Leary and Borngasser, 2006). Accordingly, pyramidal neurons in gyrencephalic species undergo great dispersion, although the mechanism by which they change between radial fibers is completely unknown.

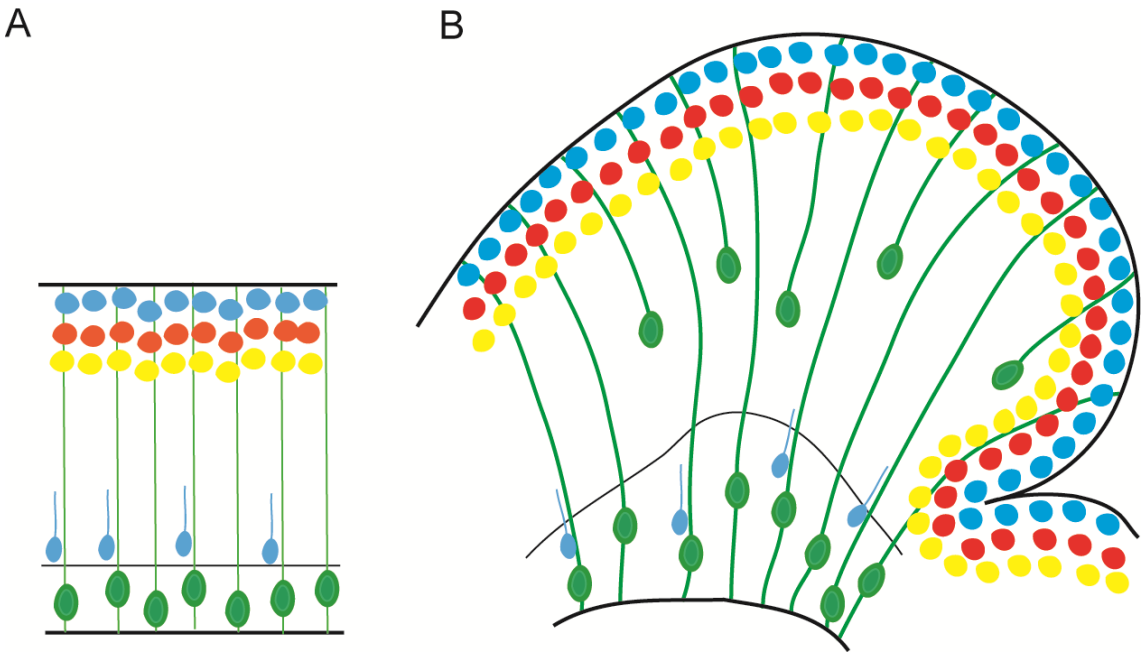

Figure 10. Different trajectories of radial fibers. (**A**) Lissencephalic species present radial glia fibers mostly parallel and neurons follow these same trajectories; in contrast to gyrencephalic (**B**), which show parallel and divergence trajectories so neurons can disperse tangentially.

6.2 Leading process

Migrating neurons are highly polarized in the direction of their movement, via the generation, maintenance, and remodeling of a leading process. The leading processes is thought to play an important role in sensing the microenvironment of migrating cells and contributing to the guidance of neurons (Kostovic and Rakic, 1990; Yee et al., 1999). Leading processes are tipped by structures similar to growth cones. These growth cones may detect short or long-range signals and as a result be differentially stabilized. Forces generated within the leading process are transmitted to the centrosome, which moves forward. Cytoskeletal forces then pull the centrosome to the base of the dominant process, thereby steering the nucleus and consolidating the displacement of the cell. The centrosome is constantly linked to the nucleus through a microtubule and the nucleus is pulled toward centrosome by dyneins associated with the microtubule network (Rivas and Hatten, 1995; Xie et al., 2003; Marin et al., 2010).

In some neurons, the leading process is branched and dynamic, with different branches growing and collapsing as migration proceeds, whereas in others there is a single, stable leading process that moves forward continuously at the tip (Fig. 11). Highly branched and dynamic leading processes are characteristic of several types of neurons that migrate tangentially, including cortical interneurons, pontine neurons, and

neuroblasts in the rostral migratory stream (Schaar et al., 2004; Bellion et al., 2005; Ward, 2005; Martini et al., 2009; Watanabe, 2009). The branching may facilitate route finding by measuring the concentrations of chemoattractants or repellents across a broad area (Ward, 2005; Martini et al., 2009; Valiente and Marin, 2010). In contrast, cortical projection neurons are bipolar with only one leading process. The leading process is unbranched and its tip moves forward without ever collapsing (Nadarajah et al., 2001). The base of the leading process, near the cell body, provides adhesion sites for nuclear movement (Nadarajah et al., 2001) During radial migration, cortical projection neurons experiment a change in morphology in the intermediate zone (from bipolar to multipolar), where there are multiple unstable processes (Tabata and Nakajima, 2003). Then, a single, stable leading process leads the way up the radial glia (Rakic, 1972; Noctor et al., 2004; Marin et al., 2010). Interestingly, defects in the interaction between pyramidal cells and radial glial fibers frequently lead to aberrant branching of the leading process (Gupta et al., 2003; Elias et al., 2007), which suggests that the bipolar morphology of radially migrating neurons, without a branched leading process, might be essential for glia-guided locomotion.

6.3 Nucleokinesis

The mechanism for translocation of the nucleus into the leading process is termed nucleokinesis, and it occurs in two steps: first, a cytoplasmic swelling forms at the base of the leading process, immediately proximal to the nucleus. The centrosome, which is generally positioned in front of the nucleus, moves into this swelling (Schaar et al., 2004; Bellion et al., 2005; Tsai et al., 2005). The centrosome is also accompanied by other organelles, including the Golgi apparatus, mitochondria, and the rough endoplasmic reticulum. Second, the nucleus follows the centrosome into the swelling. These two steps are repeated systematically, resulting in the typical saltatory movement of migrating neurons under locomotion.

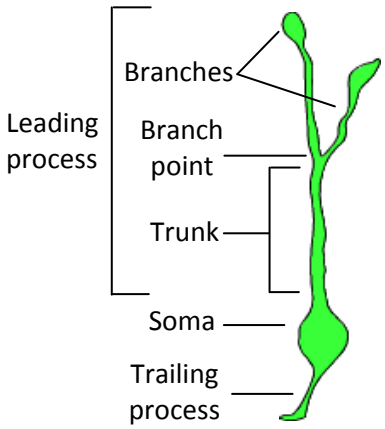

Figure 11. Structure of a radially-migrating neuron. Migrating cells present soma, trailing and leading process. Many types of cells, present branches in their leading process, in that cases, it can be subdivided in trunk, branch point and branches.

6.4 Relevance of neuronal migration

Defects in neuronal migration have been reported to cause cortical abnormalities. For example, a human brain malformation characterized by the absence of cortical folds (lissencephaly, or "smooth brain") and an abnormally thickened cerebral cortex (Jellinger, 1976; Francis et al., 2006), had been attributed to defects in neuronal migration due to mutations in two cytoskeleton-related genes: LIS1 and DCX (Kappeler et al., 2006; Nasrallah IM, 2006). Similarly, Filamin A is an actin-binding protein that binds to integrins (Loo et al., 1998) and whose mutation is responsible for causing periventricular nodular heterotopia (Sarkisian et al., 2008), which also is believed to be cause by a failure in neuronal migration (Fig. 12).

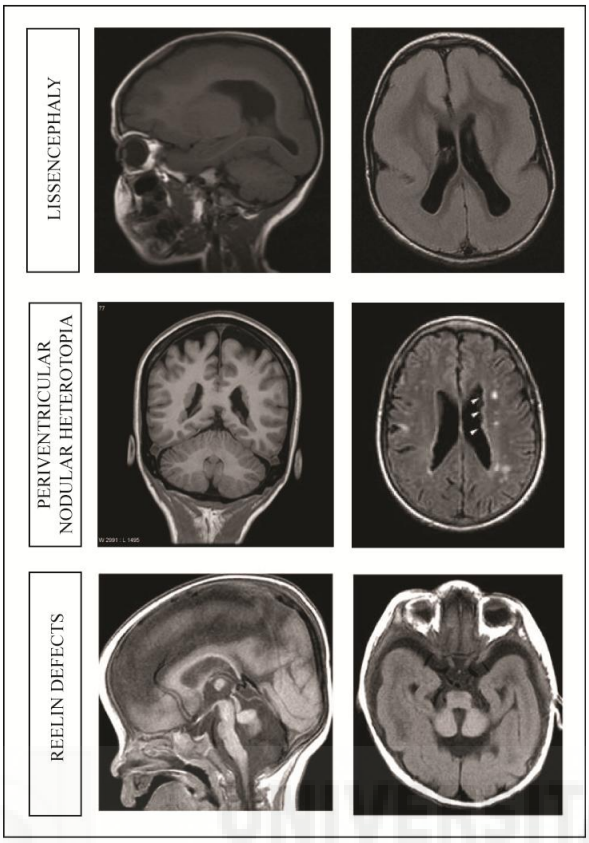

Figure 12. Human cortical abnormalities. Three different human brain disorders associated to defects in neuronal migration: lissencephaly, a lack of development of brain folds (gyri and/or sulci); periventricular nodular heterotopia, in which a subset of neurons remains as nodules lining the ventricular surface due to failures in migration; and Reelin mutant brain, with a reduced number of cortical folds that seem to contribute to the pathogenesis of autism, schizophrenia, bipolar disorder, major depression and Alzheimer's disease. [Images from Texas Children's Neurology Department and (Manto and Jissendi, 2012)].

The interaction of migrating neurons and radial glial fibers has also been shown to be important in cortical development. This interaction is mediated by various cell adhesion molecules, including astrotactin, neuregulin, and integrins (Edmondson et al., 1988; Stitt, 1990; Fishell, 1991; Anton et al., 1997; Adams et al., 2002). Mouse mutants for integrin genes show distinct cortical lamination phenotypes, demonstrating their role in neuronal migration and cortical formation (Marin and Rubenstein, 2003). Secreted extracellular molecules have also been shown to regulate the neuronal migration, including Slits, Netrins, Semaphorins and Reelin. Reelin is a secreted protein produced by Cajal-Retzius cells with critical relevance in radial migration and cortical lamination (Rice and Curran, 2001). Mice mutant for *reelin* or the Reelin signaling pathway present an inverted laminar organization of the cortex due to defects in cell migration (Caviness, 1982). Similarly, human patients with defects in Reelin have been shown to display migration defects and abnormal cortical folding. Moreover a number of

neuropsychiatric disorders including autism, schizophrenia, bipolar disorder, major depression and Alzheimer's disease share a common feature of abnormal Reelin expression in the brain (Geyer et al., 1999) (McAlonan et al., 2002; Eastwood and Harrison, 2003; Turetsky et al., 2007; Folsom and Fatemi, 2013).

Gap junctions are composed by connexins, expressed in both radial glial cells and migrating neurons, and are required for glia-guided migration due to the adhesive properties of Gap junctions between radial glial fibers and migrating neurons (Elias et al., 2007; Cina, 2009; Valiente et al., 2011). The cyclin-dependent kinase 5 (Cdk5) is mainly expressed in postmitotic neurons (Dhavan, 2001) and has crucial roles in the formation of cortical structures of the developing mouse brain, via the regulation of neuronal migration. Importantly, expression of a dominant-negative Cdk5 leads to an excessively branched leading process in migrating neurons, and a general failure to properly engage into radial migration (Ohshima et al., 1996; Gilmore et al., 1998; Ohshima et al., 2001; Hatanaka et al., 2004; Hirota et al., 2007; Yamashita et al., 2007). Also in the gyrencephalic ferret (with a divergent radial fiber scaffold) perturbation of Cdk5 function causes excessively branched morphologies in radially-migrating neurons and defects in normal radial orientation (Borrell, 2010). In summary, the majority of mouse models and human diseases producing delayed or impaired radial migration are caused mainly by an abnormal neuronal migration, frequently including excessive branching of the leading process. Hence it is critical to understand the cellular mechanisms and dynamics occurring in the leading process of cortical neurons during radial migration.

7. CEREBRAL CORTEX: TANGENTIAL EXPANSION AND FOLDING

The expansion of the mammalian and, specifically, human neocortex is a key aspect of brain evolution as it enabled the development of the higher cognitive abilities associated with the human brain. Indeed, the human brain is over 1000 times larger than the mouse brain, the period dedicated to cortical neurogenesis is 20 times longer, the transient subplate is several-fold larger and more compartmentalized, the cell cycle duration is three to four times longer, birth occurs during later stages of cortical development, and postnatal maturation lasts for much longer prior to reproduction. Structurally, humans present more than 50 distinct cytoarchitectonic cortical areas, which are also modified compared to mouse. Moreover, the human neocortex is highly folded (gyrated), whereas

the mouse brain is smooth. The gyrated cerebral cortex presents two main components: gyri and sulci. A gyrus is the outward region of cortex between two sulci or fissures.

Several cortical malformations are associated with the folding of the cerebral cortex, and many cases are also linked with defects in neurogenesis and/or migration. For instance in Primary Microcephaly, individuals present a reduction in brain size but normal cortical structure; Polimicrogyria, characterized by an excess of gyrus or Lissencephaly with an absence or reduction of folds.

Gyrification and brain size in mammals tend to increase in a directly proportional way. As a general rule, small brains are lissencephalic and large brains are gyrencephalic. Nevertheless, some exceptions have been described: manatee with a large brain presents a near-lisssencephalic cortex, mink shows a small but gyrated brain and marmoset with compact brain size, is a primate near lissencephalic.

The question about how the cerebral cortex expands and generates folds and fissures during development, as well as evolution, remains very controversial. Different theories have been postulated over the last decades to explain these features: Tension-based Hypothesis, Radial Unit Hypothesis, Epithelial-progenitor Hypothesis, Intermediate Progenitor Hypothesis and Divergent Expansion Hypothesis.

7.1 Tension-Based Hypothesis

In the CNS, axons, dendrites and glial processes are under tension. The tissue is elastic, but the elasticity is not uniform in all axes. The first cortico-cortical and cortico-subcortical tracts emerge very early, during development of the preplate. Later, the subplate forms and thalamo-cortical fibers advance into the cortical plate, and cortico-cortical pathways emerge (Kostovic and Rakic, 1990; De Carlos and O'Leary, 1992; Kostovic and Jovanov-Milosevic, 2006; Kostovic and Judas, 2010). One of the earliest hypotheses on a developmental cause for cortical folding focused on the mechanical tension of axons (Van Essen, 1997). The tension-based hypothesis states that strong, tangentially organized cortico-cortical pathways pull together the two cortical areas they interconnect to minimize the distance between them, and this pulling causes these areas to approach each other, which become localized in the walls and crests of folds; in contrast, weak and radially organized cortico-subcortical pathways offer little pulling

resistance, and the cortex involved becomes localized in the fundus of fissures. The combination of these two effects causes the outward and inward folding of the cortex, respectively (Fig. 13). A more recent extension of this hypothesis proposes that cortical folding is a function of axonal tensions through white matter connectivity (Mota and Herculano-Houzel, 2012).

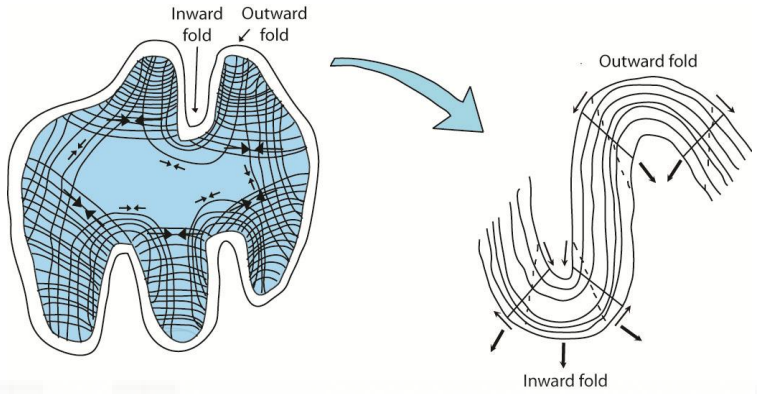

Figure 13. Tension-Based Hypothesis. This hypothesis postulates a tension-mediated folding of cerebral cortex. Outward folds bring together strongly-interconnected regions and inward folds separate weakly-interconnected regions. Cortical folding produces shearing that tends to stretch the radial axis (dashed lines). Compensatory tangential forces (small arrows) would tend to thicken the deep layers along outward folds and the superficial layers of inward folds. The converse should occur in superficial layers of outward folds and deep layers of inward folds. Additional tangential force components associated with axons in the white matter (thick arrows) should enhance these effects on deep layers and counteract them in superficial layers. [Adapted from(Van Essen, 1997)].

This hypothesis seems to be compatible with the temporal coincidence of gyral development and afferent innervations, which would optimize compact wiring (Hilgetag and Barbas, 2006b; Mota and Herculano-Houzel, 2012). In agreement, variations in axonal tension across the cortex have been suggested to affect cortical shape and influence local folding patterns (Hilgetag and Barbas, 2006a; Toro et al., 2008). However, in opposition to this hypothesis, no causal effect between gyrification and white matter myelination has been observed (Neil et al., 1998). More importantly, empirical observations in ferret have shown that while axons are under considerable tension in the developing brain, the tension is predominantly located in subcortical axon bundles, too deep to affect folding at the surface, whereas the cortical plate is actually under lateral pressure (Xu et al., 2010). In humans, no relationship is observed between

gyral formation and the establishment of cortico-cortical fiber pathways (Nakamura et al., 2012). Therefore, axonal tension is unlikely to cause cortical folding.

Although axonal tension may have a role at increasing species-specific gyrification, or providing feedback signals that trigger patterns of differential growth in the germinal zone, tension forces seem too small to drive cortical folding by sheer mechanical deformation.

7.2 Radial Unit Hypothesis

This theory proposed that RGCs are the proliferative units of the cerebral cortex (at the ventricle), which form a mosaic and a proto-map of cortical areas in the mature cortex (Rakic, 1988). Two phases are postulated along corticogenesis: "proliferative phase" with NECs dividing symmetrically to amplify the founder pool, and "differentiative phase" with aRGCs dividing asymmetrically to generate neurons (Rakic, 1995a). The neuron output is translated to cortical plate following the fiber scaffold of RGCs in order of birth (Rakic, 1995a; Noctor et al., 2001). Rakic suggested that neurons of the same ontogeny (same progenitor) would tend to migrate on a continuous fiber to the cortical plate, form a radial column of cells with related function, and project a ventricular protomap onto the developing cortex (Rakic, 1988; Rakic, 1995b; Rakic et al., 2009). The protomap formed by these units would define cortical areas of variable size, cellular composition and function (Fig. 14). Moreover, the number of radial units is different between species, whereby mammals with a larger cerebral cortex would present more radial units. As a general rule in this hypothesis, the more radial units the more surface area of the cerebral cortex, and a larger number of cells per radial unit would generate a thicker cortex.

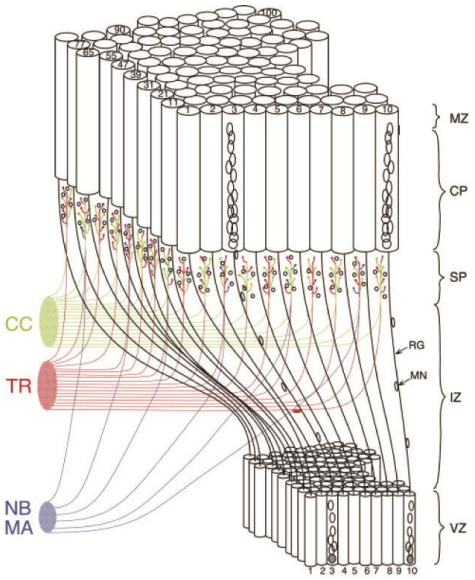

Figure 14. Radial Unit Hypothesis. RGCs act as proliferative units and they determine the number of radial columns which will form the cortex. Cortical thickness is imposed by the number of neurons in each column and neurons of the same ontogeny would migrate on a continuous fiber to the cortical plate, form a radial column of cells with related function, and project a ventricular proto-map onto the developing cortex. CC, cortico-cortical connections; TR, thalamic radiation; NB, nucleus basalis; MA, monoamine subcortical centers. [Adapted from (Rakic, 1988)].

In support of this theory, several evidences explain cortical expansion as an enlargement of the ventricular surface; this occurs as a result of regulation of cell cycle kinetics, the balance between symmetric and asymmetric divisions, and cell death of founder RGCs (Haydar et al., 1999). However, gyrated species display a massive generation of IPCs, which likely contribute to expand the cortical surface area and thickness without enlarging the VZ. These findings, made long after the formulation of the radial unit hypothesis, made it necessary to postulate alternative theories.

7.3 Intermediate Progenitor Hypothesis

This hypothesis postulates that expansion of cerebral cortex is due to an increase in the number of IPCs, which generate a large number of neurons without increasing the ventricular surface (Fig. 15) (Kriegstein et al., 2006). During development there is a switch from symmetric neurogenic to symmetric proliferative divisions. That change increases the number of IPCs which produce an exponential increment in the neuronal output. This hypothesis proposes that gyral growth is mediated by the differential proliferation of IPCs across cortical regions (Kriegstein et al., 2006). According to this

hypothesis, gyrencephalic species would accumulate IPCs locally in the SVZ, with a predominant abundance in the prospective gyrus compared to the sulcus. Moreover, these IPCs generated from RGCs, in lissencephalic species divide only once to produce two neurons (Noctor et al., 2001); in contrast, in gyrencephalic species IPCs are able to divide several times by self-amplification before generating neurons, thus explaining the enlargement of the SVZ (Smart 2002; Altman 2005. Martinez-Cerdeño 2006, Kriegstein 2006). However, a recent study demonstrated that a mouse transgenic line overexpressing Cdk4/cyclinD1, which forced IPCs to re-enter the cell-cycle, shows a laterally expanded cortex without folds; suggesting that IPCs would not be sufficient to produce gyrification (Nonaka-Kinoshita et al., 2013). More recently, the discovery of bRGCs as neurogenic progenitors introduced another cell type which could be involved in the processes of gyrification, so this theory needs to be updated (Lui et al., 2011; Reillo et al., 2011; Kelava et al., 2012).

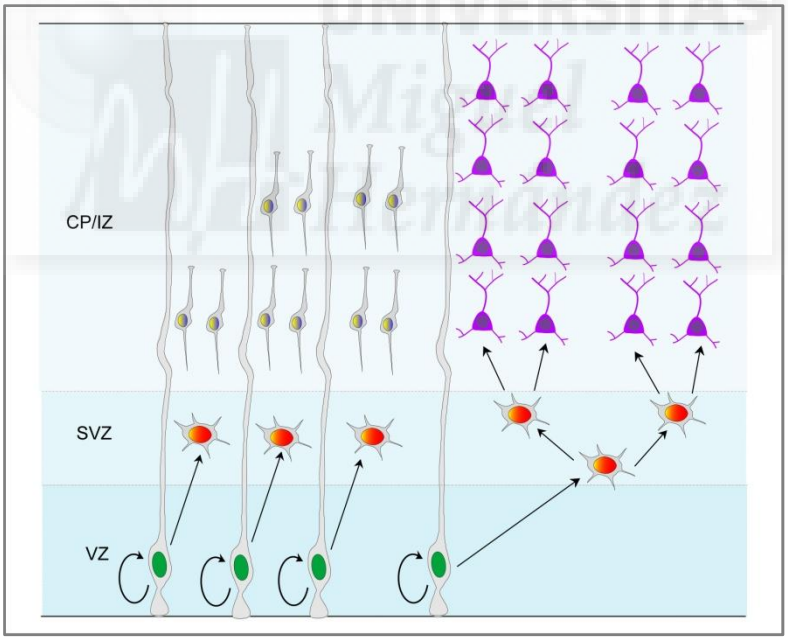

Figure 15. Intermediate Progenitor Hypothesis. Schema represents the symmetric divisions of IPCs to generate a pair of neurons (neurogenic divisions). IPCs also divide to amplify their own population (proliferative divisions) before giving rise neurons; this issue permits a huge increment in cortical neurons without increasing the ventricular surface. [Adapted from (Kriegstein, 2006)].

7.4 Epithelial-Progenitor Hypothesis

This hypothesis takes into consideration the Radial Unit Hypothesis but includes the presence of RGCs in the OSVZ. These cells would retain epithelial characteristics, radial-glial features and cell polarity like apical RGCs (in VZ). The maintenance of radial-glial identity and epithelial nature provide scaffolding for neuron migration and a better control of proliferation. Smart and colleagues (Smart et al., 2002) were the first discoverers of similar progenitors to aRGCs in ISVZ and OSVZ in primates (Lukaszewicz et al., 2005; Howard et al., 2006; Dehay and Kennedy, 2007). They proposed that the increased size of SVZ in primates would be due to the presence of RGCs in this layer, which create a more abundant number of radial units that will contribute to the lateral expansion (Lukaszewicz et al., 2005; Fish et al., 2008). Accordingly, RGCs have been observed in the OSVZ of other gyrencephalic mammals like carnivores (Fietz et al., 2010; Hansen et al., 2010; Reillo et al., 2011; Betizeau et al., 2013). However, in contraposition to this hypothesis, animals with a lissencephalic brain have also been observed to have RGCs outside of the VZ, like mouse or marmoset (Wang et al., 2011b; Kelava et al., 2012). This hypothesis complements the Radial Unit Hypothesis but does not explain clearly how the presence of RGCs in SVZ could define or impose cortical folds, and even how the radial units would allow the tangential dispersion of neurons observed in ferret and humans (Lui et al., 2011; Reillo et al., 2011; Reillo and Borrell, 2012; Kelava et al., 2013; Lewitus et al., 2013).

7.5 Divergent Expansion Hypothesis

Neocortical expansion is characterized by a huge increase in cortical surface area compared to the ventricular surface area (Fietz and Huttner, 2011; Lui et al., 2011). To explain this fact, the Divergent Expansion Hypothesis proposes a modification of radial units during neurogenesis. Accordingly, lissencephalic mammals have near-cylindrical radial units, with aRGCs in the base. In contrast, gyrencephalic species with an expanded cortical surface, present radial units with a conic shape; these radial units would incorporate subunits formed by bRGCs, each with a basal process contributing to the radial migration of neurons, but also expanding the scaffold of radial fibers laterally in a fan shape. The basal fibers of bRGCs and aRGCs would cover the entire cortex and drive migrating neurons to spread laterally, thus increasing the cortical surface area

(Reillo et al., 2011). Basal RGCs also have a proliferative capacity, being able to increase the neuron output and thus further expanding the cortical grey matter, without increasing the ventricular surface (Fietz and Huttner, 2011; Lui et al., 2011; Reillo et al., 2011).

Recently, this hypothesis has been corroborated by studies in ferret and human. These studies demonstrate a tangential expansion of the radial fiber scaffold, which would permit a huge spread of migrating neurons (Lui et al., 2011; Reillo et al., 2011; Reillo and Borrell, 2012; Kelava et al., 2013; Lewitus et al., 2013). But also analysis of gyri vs sulci show a wider fiber extension in prospective gyral regions than prospective sulcus regions (more parallel alignment) (Borrell and Reillo, 2012). These data indicate a more cylindric shape in the sulcus and a more conic shape in the gyrus, in agreement with the Divergent Expansion Hypothesis. In addition, recent studies provide evidences that an increase in bRGCs proliferation generates an increase in cortical folding. A knockdown of *Trnp1* (a DNA associated protein) in mouse neocortex produces an overproduction of bRGCs and the formation of a gyrus (Stahl et al., 2013). Similarly in ferret, containing a high proportion of bRGCs, overexpression of Cdk4/cyclin D1 causes an increase in IPC and bRGC proliferation and an increased gyrification (Nonaka-Kinoshita et al., 2013). Importantly, the Radial Divergence Hypothesis brings together in a coherent manner the previous ideas of Radial Unit, Epithelial Progenitor and Intermediate Progenitor Hypotheses, in a unique and unified hypothesis to explain the expansion and folding of the cerebral cortex.

In general terms, these five hypotheses are not incompatible and may indeed contribute to the process of cortical folding. Tension forces, RGCs (both apical and basal), IPCs and maybe more undiscovered factors may contribute to neurogenesis and cortical expansion during development and evolution.

OBJECTIVES

OBJECTIVES

1. To investigate the properties and dynamics of the leading process in radially migrating cortical neurons, both in lissencephalic and gyrencephalic mammals, and define if its branching impairs their radial movement or dynamics.

2. To identify and characterize the major progenitor cell types contributing to neurogenesis in the ferret cerebral cortex.

3. To study in the gyrencephalic ferret the embryonic origin of the OSVZ and of basal Radial Glia Cells, and the dynamics of their lineage.

MATERIALS AND METHODS

MATERIALS AND METHODS

Animals

Mouse embryos were obtained from wild-type mice *(Mus musculus)* maintained in an ICR background. Pigmented ferrets (*Mustela putorius furo*) were obtained from Marshall Bioresources (North Rose, NY) and Isoquimen (Barcelona, Spain), and kept on a 16:8 h light:dark cycle at the Animal Facilities of the Universidad Miguel Hernández. The day of vaginal plug was considered as embryonic day (E) 0.5. All animals were treated according to Spanish and EU regulations, and experimental protocols were approved by the Universidad Miguel Hernández IACUC.

Constructs

For retroviral delivery, constructs encoding *Gfp* alone, *Trnp1-Gfp* fusion protein, or a bicistronic cassette encoding *Trnp1*-IRES-*Gfp* (Stahl et al., 2013) were subcloned into an MMLV retroviral packaging vector downstream of the CAG promoter (generous gift of F.H. Gage). For electroporation, constructs encoding *Gfp, m-Yfp, E-Cadherin* (Addgene #28009) or *DN-Cdh1* (Noles and Chenn, 2007) were subcloned into a pCAG promoter-containing vector. All plasmids were produced under endotoxin free conditions (QIAGEN EndoFree Plasmid Maxi Kit).

In utero and postnatal Electroporation

For electroporation, DNA plasmids encoding *Gfp*, M-*Yfp, E-Cadherin* (*Cdh1*) or *DN-Cdh1*, under the CAG promoter were used. For postnatal electroporation in ferret, kits were deeply anesthetized and maintained with 1.5% Isoflurane during surgery, and DNA injections were aimed at the telencephalic lateral ventricle by means of stereotaxic coordinates. DNA was injected using pulled glass micropippettes. Details of postnatal electroporation of ferret kits were described previously (Borrell, 2010; Kawasaki et al., 2013). After the appropriate survival period, postnatal kits or pregnant females were overdosed with sodium pentobarbital (Nembutal), and further processed for immunohistochemistry.

For *in utero* electroporation in mouse, timed-pregnant females were deeply anesthetized and maintained in 2% Isoflurane during surgery. The abdominal cavity was open, the uterine horns exposed, and DNA solutions injected into the telencephalic lateral ventricle through the uterus wall using pulled capillaries (1B120F-4; World Precision Instruments) filled with either DNA diluted in PBS and colored with 0.5%

Fast Green (Sigma-Aldrich). DNA-injected embryos were electroporated using a 35–45 V/50 ms/950 ms/five pulses program (CUY21/CUY650P3/CUY650P5; Nepa Gene). After appropriate survival times, mice were deeply anesthetized and killed using cervical dislocation.

In utero and postnatal virus injections

High titer MMLV-based VSVG-pseudotyped retrovirus ($5x10^7$-$5x10^8$ pfu/ml) encoding *Gfp*, *Trnp1-ires-Gfp* or *Trnp1-Gfp*, under the CAG promoter were prepared, concentrated and viral titer estimated as described (Tashiro et al., 2006). High titer replication-incompetent adenovirus ($9.3x10^{11}$ vp/ml) encoding *Gfp* under the CMV promoter were obtained from QBioGene (Irvine, CA). Viral solutions were injected using pulled glass micropippettes.

For *in utero* injections in both ferret and mouse, timed-pregnant females were deeply anesthetized and maintained in 2% Isoflurane during surgery. The abdominal cavity was open, the uterine horns exposed, and retrovirus solutions were pressure injected into the telencephalic lateral ventricle of embryos through the uterine wall.

For postnatal injections, ferret kits were deeply anesthetized and maintained with 1.5% Isoflurane during surgery, and injections were aimed at the telencephalic lateral ventricle, ISVZ or OSVZ by means of stereotaxic coordinates.

Slice electroporation

V1 slices were prepared from ferrets aged P1 and maintained in culture as described previously (Borrell and Callaway, 2002). Briefly, ferret kits brains were dissected out in ice-cold *N*-2-hydroxyethylpiperazine-*N*′-2-ethane-sulfonic acid (HEPES) buffered artificial cerebral spinal fluid (140 mM NaCl, 5 mM KCl, 1 mM $MgCl_2$, 24 mM D-glucose, 10 mM HEPES, 1 mM $CaCl_2$, anf pH 7.4), the occipital pole of each hemisphere was blocked, and tissue blocks were sliced at 400 μm thickness using a vibratome. Selected slices were placed onto tissue culture inserts (Millipore, 0.4 μm pore size) and were cultured in a 37 °C, 5% CO_2 incubator with 1 ml of incubation medium (50% basal medium of eagle [BME], 25% Hanks' balanced salt solution, 25% normal horse serum, 2 mM glutamine, 0.45% D-Glucose, 10 mM HEPES, 1% Pen/Strep, 1% N2 all from GIBCO-Invitrogen). One hour later, expression vectors were pressure injected focally into the cortex of sagital slice cultures and focally electroporated as described previously (Flames et al., 2004). One day after

electroporation, slices containing fluorescent cells in the cortical plate were selected for time-lapse imaging.

Immunohistochemistry and In situ hybridization

For histological analysis, embryos were obtained by cesarean section of timed-pregnant females upon deep anesthesia with sodium pentobarbital, and perfused transcardially with 4% paraformaldehyde (PFA); postnatal ferrets were deeply anesthetized with sodium pentobarbital prior to transcardiac perfusion with PFA. After perfusion, the brains were extracted and sectioned.

For immunohistochemistry, brain sections were incubated with primary antibodies overnight (anti-GFP, 1:1000, Aves Labs; anti Vimentin, 1:400, Chemicon; anti-GABA, Sigma, 1:2000; anti-Pax6, 1:500, Millipore; anti-Tbr2 1:200, Abcam; anti-PH3, 1:1000, Upstate; anti-Ki67, 1:200, Novocastra; anti-BrdU, 1:200, Abcam; anti-GFAP, 1:1000, DAKO; anti-Olig2, 1:100, IBL), followed by appropriate fluorescently-conjugated secondary antibodies (1:200, Jackson), and counterstained with DAPI (Sigma). For anti-BrdU staining, sections were pretreated with 2N HCl for 30 min.

For *in situ* hybridization (ISH), sense and anti-sense cRNA probes were synthesized and labeled with digoxigenin (DIG; Roche Diagnostics) according to the manufacturer's instructions. ISH was performed as described previously (Reillo et al., 2011). Ferret-specific ISH probes were cloned using the following primers: *Trnp1*, fwd: 5'-TCTGGACTCCTGGATTGAGC-3', rev: 5'-TGCCGCTGTGTCTATCTGAG-3'; *Cdh1*, fwd: 5'-CGGAGCTGAGTTTTCTGGTC-3', rev: 5'-GAGGCTGTGGATTCTTCTGG-3'. These ferret-specific primers were designed based on the same ferret-specific sequences as in the microarray. PCR was performed using Go Taq Flexi DNA polymerase (Promega), and the resulting amplicons were purified with Wizard SV Gel and PCR Clean-Up System (Promega) and cloned into pGEM-T Easy Vector System I.

Slice culture

Ferret brain slices were prepared and maintained in culture as described previously (Borrell et al., 2006). Slice cultures of the embryonic mouse telencephalon were prepared as previously described (Anderson et al., 1997). To image aRGC behaviors, P1 ferrets were injected with rv::*Gfp*, and their brains obtained for slicing at P6. To image the behavior of bRGCs in OSVZ, slices were prepared from unmanipulated P18

ferrets, and one hour later slices received various injections of Ad-GFP (3-6 nl/injection site, 2-8 injection sites/slice) in the CP.

Time-lapse imaging

One day after slice preparation, slices containing fluorescent cells were selected for time-lapse imaging. Images were obtained either under a multiphoton imaging system compound by a Laser Femtosecond *Mai Tai HP* Ti: sapphire modelocked laser system (SpectraPhysics, Mountain View, CA, USA), tunable between 690-1020 nm,a Laser Scanning Spectral Confocal Microscope: Leica TCS SP2 AOBS (Leica Microsystems GmbH, Manheim, Germany). The objective used were air 20X lens in an inverted epifluorescence microscope, or under two-photon optics through HCX APO U-V-I 40x W, NA 0.8. The time-lapse were acquired with the software Leica Confocal Software (LCS). Microscope was equipped with Microscope Temperature Control System "The Cube & The Box" (37^{o}C) and gas mixer "The Brick" (5% CO_2) (Life Imaging Services, Basel, Switzerland). Frames were obtained intermittently during 30 to 142 hrs in culture. Digital images were acquired, contrast-enhanced and analyzed with Metamorph (Microbrightfield) or Imaris software (Bitplane AG Zurich, Switzerland).

Microarray and qRT-PCR

For RNA extraction, ferret kits aged P1 were deeply anesthetized, and timed-pregnant ferret females were deeply anesthetized and their living embryos were obtained by cesarean section. Subjects were then decapitated, their brains dissected and blocked in ice-cold ACSF (140 mM NaCl, 5 mM KCl, 1 mM $MgCl_2$, 24 mM D-glucose, 10 mM HEPES, 1 mM $CaCl_2$, pH 7.2). Tissue blocks containing the occipital cortex were vibrotome-cut in 300 μm-thick slices. Living cortical slices were further microdissected with microscalpels in ice-cold ACSF to isolate the VZ from the caudal pole of the cerebral cortex. Germinal layers were identified in living slices under the dissection scope, where the VZ was the most opaque layer on the apical side of the cortex. Tissue pieces were fresh-frozen in Trizol for RNA extraction, with a post-mortem interval of less than 1 hr.

Total RNA was extracted using RNeasy Mini Kit (Quiagen) followed by treatment with RNase-Free DNase Set (Quiagen). RNA quality was confirmed using the RNA 6000 Nano kit on the Agilent Bioanalyzer platform, and then 200 ng of total RNA was labeled using the one-color labeling kit from Agilent technologies according

to the manufacturer's protocol. Labeled cRNA was then hybridized for 16 h on a custom-made microarray containing 43,692 ferret-specific probes covering 17,386 genes (Camp et al., 2012). Microarray slides were scanned on an Agilent High-Resolution C Scanner, and the raw image files were processed by the Agilent feature extraction software. Raw data files were normalized using quantile normalization in Partek Genomics Suite®. Statistical analysis of microarray data was done in Multiexperiment Viewer (MEV) (Saeed et al., 2003). To identify genes with significantly different expression levels, we used ANOVA comparisons between samples, using *p*-values based on 500 permutations and Bonferroni false discovery correction, as in Ayoub et al. 2011 (Ayoub et al., 2011).

For qRT-PCR, primers for ferret gene homologs were designed based on the same ferret-specific sequences. Template cDNA was generated using Maxima First Strand cDNA Synthesis Kit for quantitative real-time PCR (qRT-PCR) (Thermo Fisher). Quantitative RT-PCR was performed using the Step One Plus sequence detection system and the SYBR Green method (Applied Biosystems), with each point examined in triplicate. Transcript levels were calculated using the comparative Ct method normalized using Actin. Primers used were: Trnp1, fwd: 5'-TTGGTCTGAGAAATCCCTGC-3', rev: 5'-CGCTGTGTCTATCTGAGGAAG-3'; Cdh1, fwd: 5'-TGCCCAGAAAACGAGAAAGG-3', rev: 5'-ACAAATACACCAACCGGAGG-3'; Actin, primers as in (Fang et al., 2010). In each experimental group we analyzed 2-3 samples, each consisting of a pool of 2-3 embryos/kits. Reactions were performed in triplicate per independent sample. Data were statistically analyzed with SPSS software using t-test.

Quantification and statistics

Cell types were identified according to the following criteria:

- *Multipolar cell*: cell with multiple short processes extended from the cell soma and without obvious polarity.
- *Migrating neuron*: cell with clear apico-basal polarity extending a relatively-think basal process much shorter than that of RGCs, and a still much shorter and thinner apical process.
- *Branched migrating neuron*: cell with a leading process that at one point is subdivided in at least two pieces longer than 5 µm.

- *Non-branched migrating neuron*: cell with a non-subdivided and entire leading process.
- *Differentiating neuron*: cell with a single basally-directed process highly branched at a distance from the cell body, frequently located at the top of the cortical plate.
- *aRGC*: cell with a single apical process contacting the ventricular surface and a very long radially-oriented basal process.
- *bRGC*: cell with a very long radially-oriented basal process, without a VZ-contacting apical process.
- *StC*: multipolar cell with several very highly branched and short processes extending from the cell soma.

In electroporation experiments, identification of GFP+ cell identity in VZ and SVZ based on morphology was unreliable due to their high density. In those experiments aRGCs were defined as Pax6+/GFP+ cells with the cell body in VZ and a distinct apical process, while bRGCs were identified as Pax6+/GFP+ cells with the cell body in SVZ.

The angle of mitosis was measured using PH3 stains and considering only cells at telophase. Angles were measured with respect to the general trajectory of the radial fiber scaffold, or with respect to the ventricular surface (Borrell and Reillo, 2012; Gertz et al., 2014). Mitoses were considered horizontal if they occurred at 60-90º with respect to radial fibers, or 0-30º with respect to the ventricular surface.

To quantify the length of different segments in migrating neurons, Neurolucida Software was used. Segments were identified in agreement with following definitions:

- *Leading process*: measurement of the micrometers that present the leading process, from soma to end of the leading process.
- *Trunk*: measure in micrometers of the segment between soma and first branch point.
- *Leading process tree or branches*: measure of the total length of segments between first branch point and the end of leading process.
- *Single branch:* measure of individual branches length in every cell.

To analyze the angle between first branch point, Neurolucida and Canvas X Sofware were used. To quantify the portion of leading process that was parallel to radial

glia fibers, we subdivided the leading process in several short segments to reproduce as much as possible the changes in direction of leading process. For each segment, we analyzed the angle with respect to RGF. The strict criterion used was that segments with angles smaller than 10 degrees were parallel to RGF, in contrast to equals or bigger angles which were non-parallel. We obtained the length of every segment and the angle, and we calculated the percentage of leading process parallel to RGF for each cell. For that measure Neurolucida Software, Canvas X Software and Imaris software (Bitplane AG Zurich, Switzerland) were used.

Double-labeling analyses.

Quantification of cell co-staining was performed by confocal microscopy (Leica) through a 40X lens and 2-4X zoom. Images were acquired from cells in 4 sections per subject, 2-3 subjects per condition and age. Images were analyzed using Imaris software (Bitplane AG Zurich, Switzerland) and Canvas X software.

Statistical analysis.

We used SPSS software to run the following tests where appropriate: independent samples or pair-wise t-test, chi-quare test, or one-way ANOVA followed by Bonferroni's test for multiple comparisons and Duncan's test for subset homogeneity.

RESULTS

RESULTS

1. A high proportion of radially-migrating pyramidal neurons in mouse have a branched leading process

To analyze the detailed morphology of radially-migrating neurons in the developing mouse cerebral cortex, we labeled them by performing *in utero* electroporation of GFP-encoding plasmids on embryonic day (E) 14.5 mouse embryos and analysis at E17.5 (Fig. 16, A and B). This resulted in a very high number of GFP+ cells in all cortical layers including the Intermediate Zone (IZ), layers V/VI and cortical plate (CP). Among all GFP-expressing cells we distinguished several stereotyped morphologies typical of excitatory neurons undergoing radial migration (Fig. 16C): *multipolar cells*, with several short processes but no obvious polarity located mainly in SVZ; *migrating neurons*, with a distinct bipolar morphology including a leading and a trailing process, and oriented radially with the leading process towards the pial surface; and *differentiating neurons*, characterized by having one single thick apical dendrite with a complex arbor of branches extended to, and seemingly contacting with, the pial surface, which appeared to have finished their radial migration and started to differentiate. Each of these morphologies predominated in specific layers: multipolar cells in SVZ, migrating neurons from IZ to CP, and differentiating neurons in the upper CP (Fig. 16, D to F).

Next we focused our analysis on cells with *migrating neuron* morphology. In this group we distinguished two different morphological subtypes: cells with a simple (unbranched) leading process, and cells with a branched leading process (Fig. 16C). Branches were distinguished from filopodia if they were longer than 5 µm. We observed many neurons with migratory morphology displaying a branched leading process across all layers of the developing cortex, so next we measured if this was a general feature of radially migrating neurons or an anecdotic event. To discard a potential confusion with multipolar cells, and to clearly include only bipolar cells with a single leading process, we restricted our analysis to IZ through CP, purposefully excluding the SVZ where multipolar neuron migration occurs (Tabata and Nakajima, 2003; Noctor et al., 2004) (Fig. 16B). In the CP and layers V/VI we found that 32.7 ± 2.4% of GFP+ cells were bipolar with a simple leading process and 30.8 ± 3.08 % had a branched leading process, whereas the remaining 36.0 ± 3.95% presented differentiating neuron morphology (Fig. 16G).

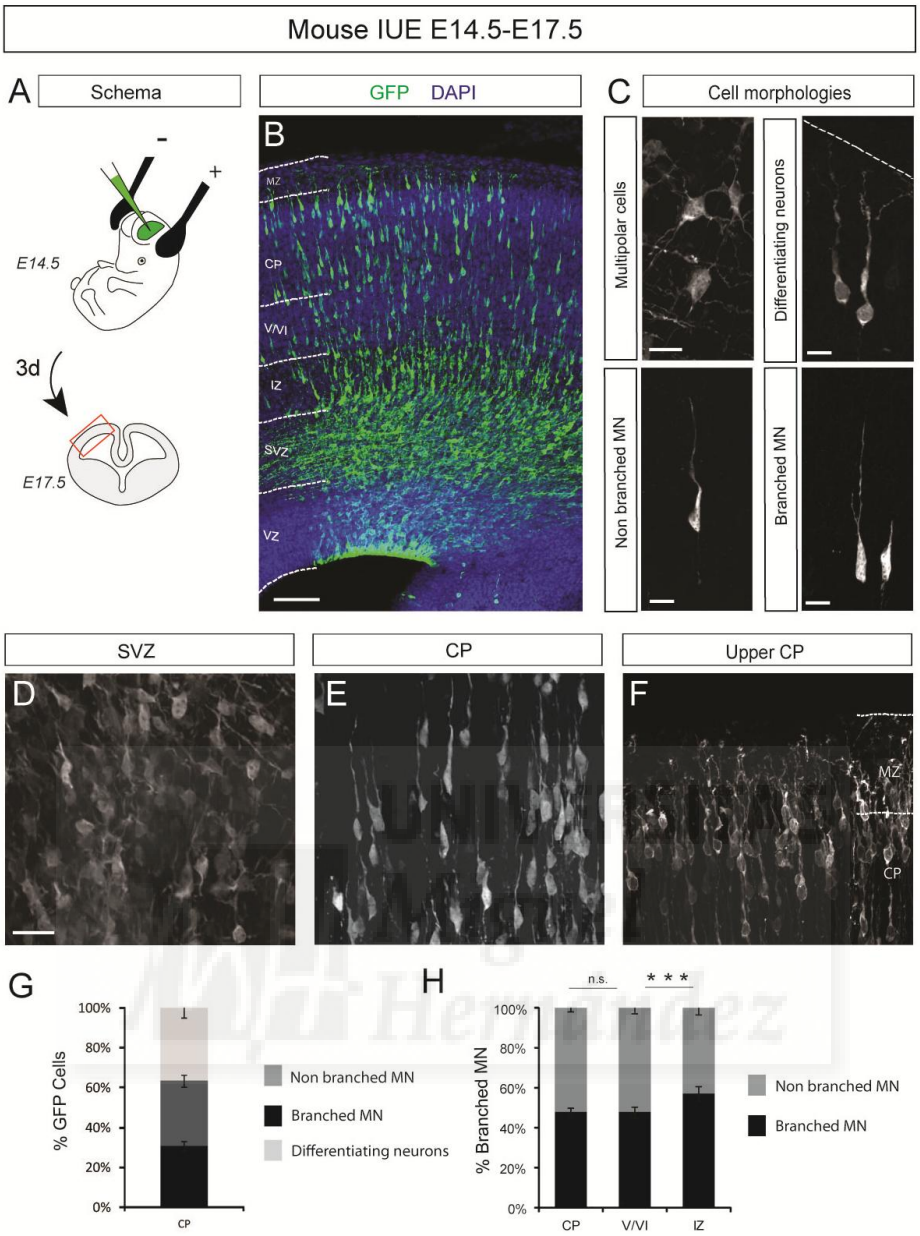

Figure 16. A high proportion of radially-migrating pyramidal neurons in mouse have a branched leading process. (**A-B**) We developed in utero electroporations with *Gfp*-encoding DNA at E14.5 and analysis at E17.5, where the majority of pyramidal neurons are in radial migration through intermediate zone and cortical plate. (**C**) Different morphologies of pyramidal neurons are observed along their movement until the pial surface: *multipolar cells (MP)*, with several short processes but no obvious polarity; *migrating neurons (MN)*, with a distinct bipolar morphology including a leading and a trailing process, and oriented radially with the leading process towards the pial surface and *differentiating neurons (DN)*, characterized by having one single thick apical dendrite with a complex arbor of branches extended to, and seemingly contacting with, the pial surface, which seemed to have finished their radial migration and started to differentiate. Cells with *migrating neurons* morphology presented two different subtypes of the leading process: single or *non-branched* leading process and *branched* leading process. We considered a branch when the fragment is longer than 5 µm. (**D-F**) High magnification of different layers to distinguish the morphologies described. (**G**) Quantification of the amount of different morphologies in CP observed in electroporated brains. 673 cells, 5 embryos; data are mean ± S.E.M. (**H**) Quantification of cells with *migrating neurons* morphology that present branched or non-branched leading process. 2251 cells; 5 embryos; data are mean ± S.E.M. (**p*<0.05, X^2 test). CP, cortical plate; V/VI, layer V/VI; IZ, intermediate zone. Scale bars: B, 100 µm; C, 20 µm; D,E,F, 50 µm.

In other words, cells displaying a branched leading process were 48.18 ± 2.02% of all migrating neurons in CP, 47.8 ± 2.69% in layers V/VI, and 57.19 ± 3.43% in IZ (Fig. 16H), confirming that radially migrating neurons with a branched leading process are very common in the mouse cerebral cortex.

2. Branched radial migration is a common mechanism in the developing ferret cerebral cortex

Given the high percentage of migrating cells with a branched leading process in the mouse cerebral cortex, we next asked if this feature might also be present in other mammals, particularly those with bigger and folded brains, and longer migration trajectories like humans. To this end we focused on the ferret, which contrary to mice and similarly to humans develops a rather large and folded cerebral cortex. Following a similar strategy as in mouse, we labeled migrating neurons in the developing ferret cortex by electroporation of *Gfp*-encoding plasmids at postnatal day (P) 1 and analysis at P8 (Fig. 17A), when transduced pyramidal neurons are in radial migration as shown previously (Borrell, 2010). Similar to mouse, in ferret we distinguished cells with multipolar, migrating and differentiating neuron morphologies (Fig. 17C), where cells with multipolar morphology were again very frequent in the SVZ (Fig. 17D), including its inner and outer subdivisions (ISVZ and OSVZ). Likewise, differentiating neurons were observed only in the upper CP (Fig. 17F). Neurons with a bipolar migratory morphology were found from IZ through MZ (Fig. 17E) and, as in mouse, these frequently showed branches in their leading process. Within the CP, we determined that 35.72 ± 3.83% of GFP+ cells were bipolar with a simple leading process and 29.87 ± 3.50% had a branched leading process (Fig. 17G) (n = 338 cells, 4 kits); hence 50.28 ± 3.38% of migrating neurons in CP and 51.28 ± 4.38% in Layer V (Fig. 17H) had a branched leading process, proportions similar to mouse. In contrast, in lower layers the proportion of GFP+ cells with a branched leading process was much higher than in mouse: 63.63 ± 3.40% in layer VI and 76.86 ± 5.38% in IZ (Fig. 17H). Taken together, our experiments in mouse and ferret indicated that branched radial migration is much more common than previously recognized. During radial migration, more than half of cortical excitatory neurons in mouse branch their leading process, a proportion that rises to 70% in gyrencephalic species, suggesting that it may be relevant for the tangential dispersion of radially-migrating neurons.

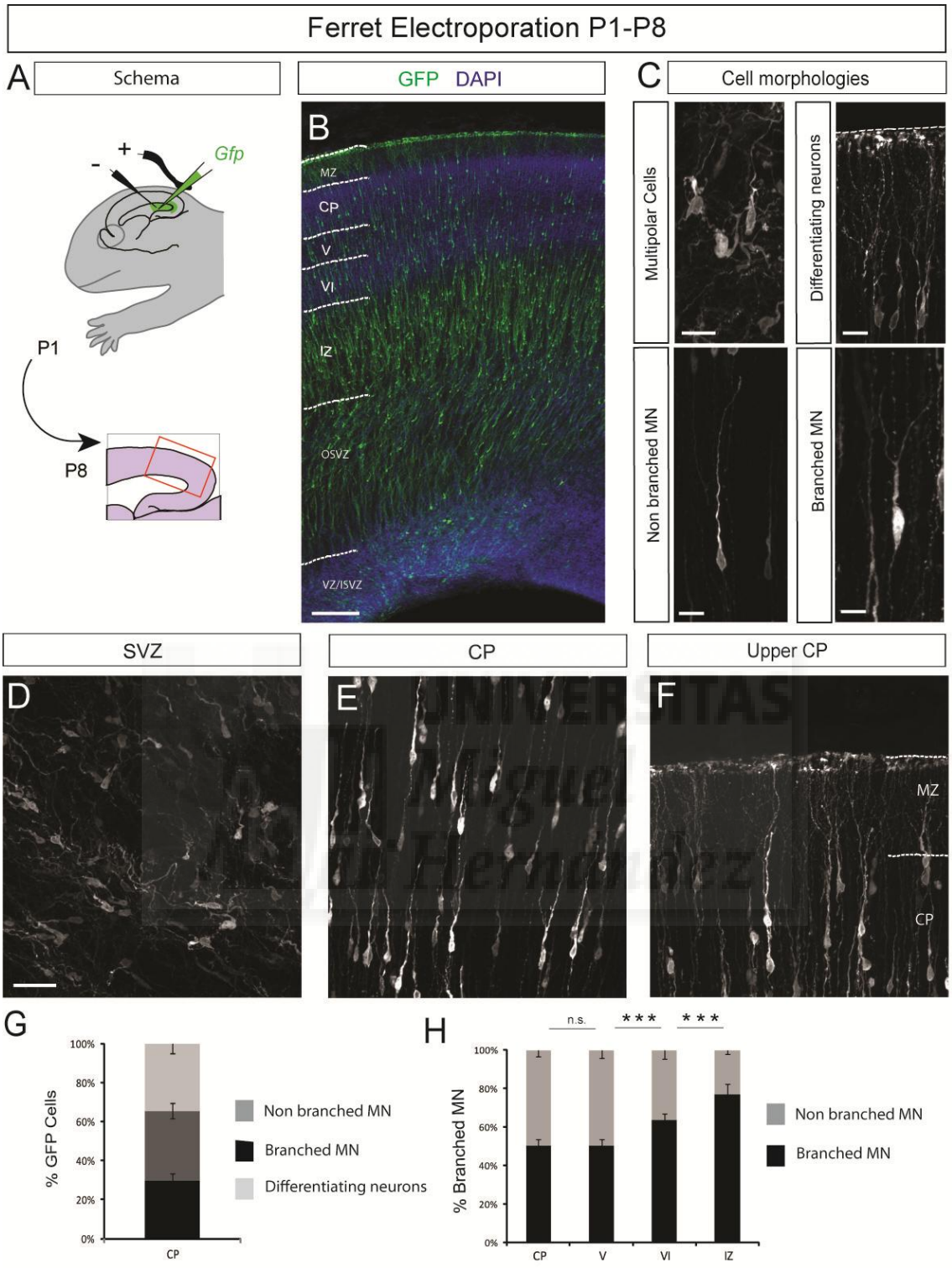

Figure 17. Branched radial migration is a common mechanism in the developing ferret cerebral cortex. (**A-B**) Ferrets were electroporated with *Gfp*-encoding DNA at P1 and analyzed at P8 when pyramidal neurons were migrating towards the marginal zone. (**C**) Different morphologies in electroporated cells: *multipolar cells (MP)*, *differentiating neurons (DN)*, and two types of *migrating neurons (MN)*, single or *non-branched* leading process and *branched* leading process. To distinguish, we followed the same morphological criteria described in figure 16. (**D-F**) High magnification of cells in different layers which reflects the morphologies described. SVZ, subventricular zone; CP, cortical plate. (**G**) Quantification of different morphologies observed in electroporated cells in CP. 338 cells, 4 kits; data are mean ± S.E.M. (**H**) The graph describes the percentage of each morphology in every layer. 6598 cells; 4 kits; data are mean ± S.E.M.(*p<0.05, X^2 test). Scale bars: B, 250 µm; C, 20 µm; D,E,F, 50 µm.

3. Multi-order branching of the leading process in radially-migrating neurons

Once we determined that radially-migrating excitatory neurons frequently branch their leading process, we next analyzed their morphology in greater detail. For this analysis we focused in layer V; this is distant from the SVZ containing many multipolar cells, and also distant from the upper CP containing numerous differentiating neurons. We also chose this layer because the percentage of migrating neurons with branched morphology in layer V was similar in mouse and ferret, making it comparable between these species. Because in mouse embryos layers V and VI were not unambiguous from each other, we combined both layers in our analysis. We found that radially-migrating cells with a branched leading process displayed up to three branch points (BPs), forming up to four branches in ferret (Fig. 18, A to D and A´ to D´). In mouse, 37.5 ± 2.45% of cells had one BP and 10.3 ± 2.45 % had two BPs (Fig. 18E). Similarly, in ferret we found that 30.48 ± 3.40% of cells displayed one BP, 14.65 ± 4.28% had two BPs and 3.87 ± 1.53% had three or more BPs (Fig. 18F). These results demonstrated a remarkable diversity of leading process morphologies among radially-migrating neurons, although cells without branches or only one branch point clearly predominated. Intriguingly, we did not observe cells with more than two branch points in mouse, as opposed to cells in the gyrencephalic ferret which exhibited three or more branch points.

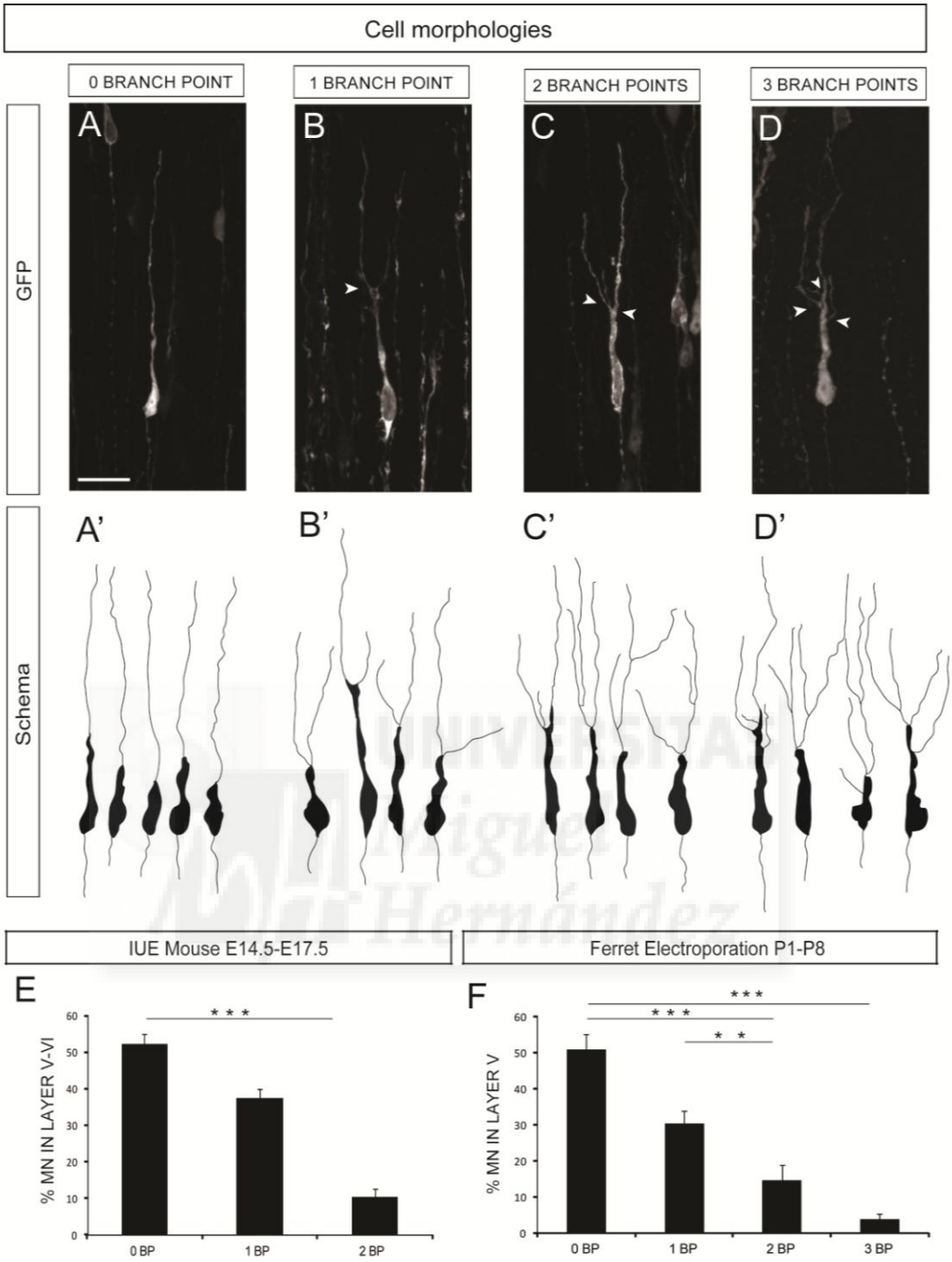

Figure 18. Multi-order branching of the leading process of radially-migrating neurons. (**A-D**) Different morphologies were observed in migrating pyramidal neurons: non-branched with zero branch points (0BP), branched with one branch point (1BP), branched with two branch points (2BP) and only in ferret brains we observed very few cells with three or more branch points (3BP). (**A´- D´**). Schema or drawing representing the different morphologies. (**E-F**) Quantification of the abundance of each type of morphology with respect to the total number of migrating neurons in mouse (**E**) and ferret brains (**F**). Mouse quantification was done in layer V-VI and ferret quantification in layer V. For mouse analysis: 165 cells, 11 embryos. Ferret analysis: 197 cells, 4 kits; data are mean ± S.E.M. (*p<0.05, X^2 test). Scale bar: 20 µm.

4. Total size of the leading process increases with its branching complexity

To analyze in greater detail the leading process of radially-migrating neurons, we distinguished two different parts: trunk, the segment between soma and the first branch point; and branch, each of the portions between the branch point and the tip of the process (Fig. 19, A to E). As a general rule, only two branches formed from each branch point. For this analysis we reconstructed every single electroporated cell in mouse layer V-VI and ferret layer V (Fig. 19, B to E). Analysis of total leading process length showed that mouse cells with zero or one BP were similar, with a leading process of 65.08 ± 1.29µm and 64.93 ± 1.69µm, respectively (Fig. 19G). Ferret neurons with zero or one BP presented a much longer leading process, 72.43 ± 1.82µm and 73.84 ± 3.62µm in length, respectively (Fig. 19L). Whereas migrating neurons in ferret had a longer leading process than in mouse, in both species the presence of one branch or none didn't change the total leading process length. In contrast, cells with more than one BP tended to have a longer leading process. In mouse, cells with two BPs had a leading process of 75.87 ± 3.75 µm (Fig. 19G), and in ferret cells with two and three BPs were 82.89 ± 5.61µm and 98.89 ± 11.34µm long, respectively (Fig. 19L). This indicated a clear tendency to having a longer leading process for migrating neurons with more than one branch point, and also that migrating neurons in ferret had a longer leading process than in mouse.

Next we wanted to determine if the tendency to increase the total length of leading process as a function of the number of branch points was due to a specific increment of the trunk or of the individual branches. When distinguishing these two parts, we found no difference in the length of the trunk in either mouse or ferret, but if anything we found a slight though not significant decrease (Fig.19, H and M). In mouse, trunk length was 17.81 ± 1.27µm for cells with one BP and 16.88 ± 2.09µm for cells with two BPs (Fig. 19H). In ferret, these measurements were 23.87 ± 1.74µm for cells with one BP, 20.29 ± 3.75µm for two BPs and 18.08 ± 1.84µm for three BPs (Fig. 19M). In agreement with differences in total leading process length between mouse and ferret, trunk length of migrating neurons was again shorter in mouse than in ferret, although the tendency to be shorter with the increment in branch number was consistent in both species. Given that differences in trunk length were not responsible for the observed increase in total leading process length, we next analyzed the length of branches, collectively and individually. Not surprisingly, the added length of all

branches in a single cell increased as a function of the number of branches (Fig. 19, I and N).

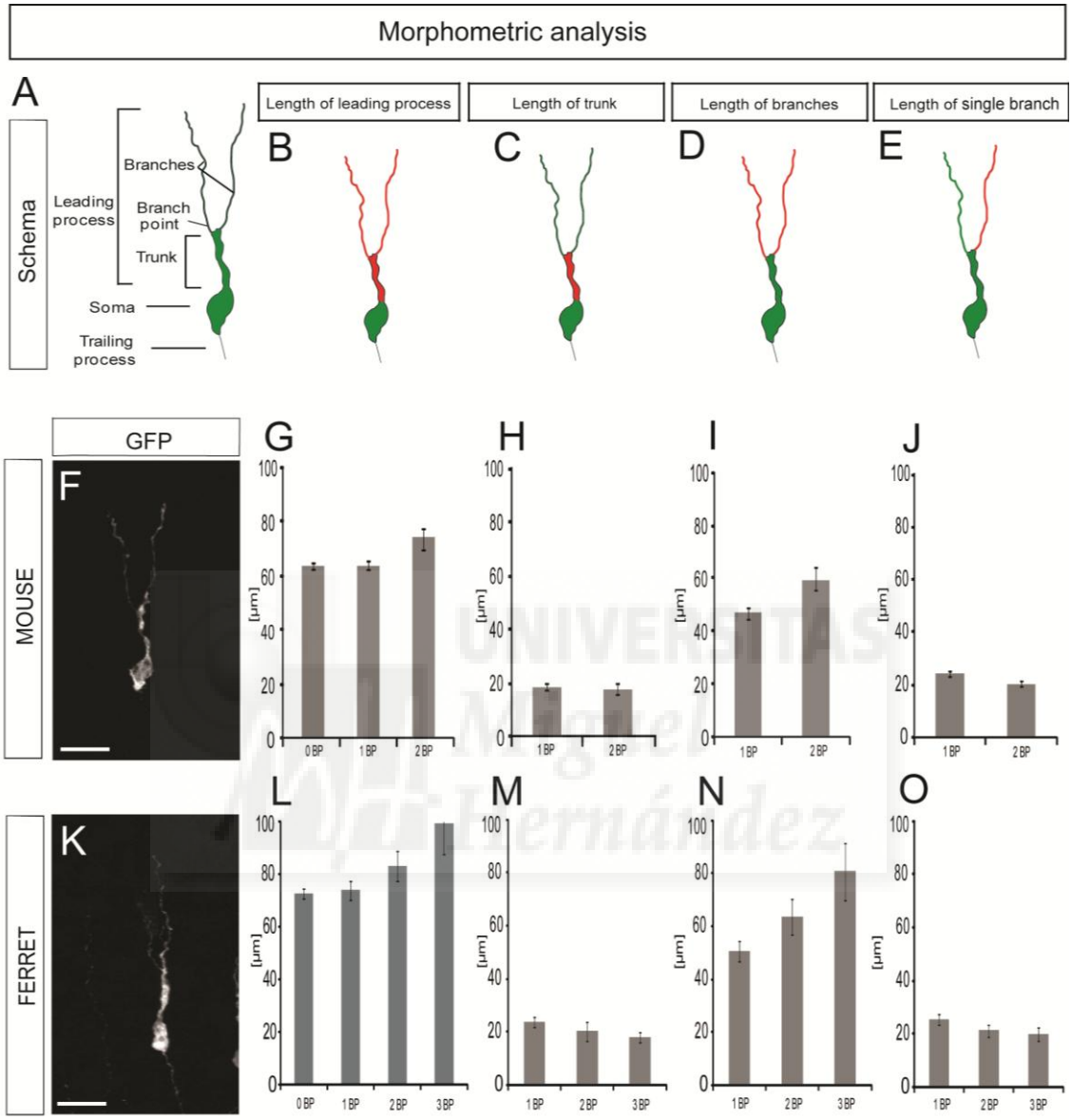

Figure 19. Total size of the leading process increases with its branching complexity. (A) Drawn of a migrating neuron with the differentiated parts: trailing process, soma and leading process subdivided in trunk, branch point and branches. (**B-E**) Schema in red color represent the parts of cell that were analyzed. (**F**) Image of a branched leading process GFP+ cell labeled by E14.5-E17.5 mouse electroporation. (**G-J**) Measure of the leading process (**G**), trunk (**H**), leading process tree (**I**) and single branch length (**J**) by groups in mouse. 165 cells, 11 embryos; data are mean ± S.E.M. (**K**) Image of a branched leading process GFP+ cell labeled by P1-P8 ferret electroporation. (**L-O**) Analysis of leading process (**L**), trunk (**M**), leading process tree (**N**) and single branch length (**O**).179 cells, 4 kits; data are mean ± S.E.M. (***p<0.001, t-test). 0BP, zero branch points; 1BP, one branch point; 2BP, two branch points; 3BP, three branch points. Scale bar: 20 µm.

In mouse, the total length of branches in cells with one BP was 47.12 ± 2.09µm, while cells with two BPs were 58.99 ± 4.25µm on average (Fig. 19I). In ferret, cells with one BP were 50.77 ± 3.87µm long, cells with two BPs were 63.66 ± 6.71µm and cells with three BPs were 80.8 ± 10.88µm (Fig. 19N). Therefore, cells with more branches had a longer leading process. As for the length of individual branches, on average these were 23.56 ± 1.04µm in cells with one BP and 19.86 ± 1.32µm in cells with two BPs in mouse (Fig. 19J). In ferret, the average length of individual branches was 25.39 ± 1.94µm for cells with one BP, 21.22 ± 2.24µm for two BPs and 20.2 ± 2.52µm for cells with three BPs (Fig. 19O). These results demonstrated that cells with fewer branch points developed longer individual branches. Taken together, our morphometric analyses of radially-migrating neurons in the mouse and ferret cerebral cortex demonstrated that cells with more branches had a longer leading process overall. This was not due to having a longer trunk, but due to the added length of the branches. Intriguingly, the length of each individual branch was smaller in cells with a larger number of branches, suggesting that the total length of the leading process may be intrinsically limited.

5. Similar angles at primary branch points between interneurons and pyramidal neurons

It has been proposed that branching of the leading process in migrating interneurons may be a cellular mechanism to increase their exploratory capacity for navigation (Bellion et al., 2005; Kappeler et al., 2006; Marin et al., 2010), and this would be limited by the angle at which the primary branches form (Martini et al., 2009). To investigate this possibility and compare the exploratory potential of migrating pyramidal neurons with interneurons, we measured the angle between branches at the first branch point (Fig. 20, A to D). In mouse, pyramidal neurons with one or two BPs displayed angles of 42.53 ± 2.48º and 49.28 ± 6.15º respectively (Fig. 20E). In ferret, cells with one BP showed slightly wider angles than in mouse (51.94 ± 3.16º), while cells with two and three BPs had a clear tendency to branch at much wider angles (64.36 ± 8.09 and 78.18 ± 16.9º, respectively; Fig. 20F). This indicated that the more branches in the leading process, the wider the angle between the primary branches, hence the more separate from each other.

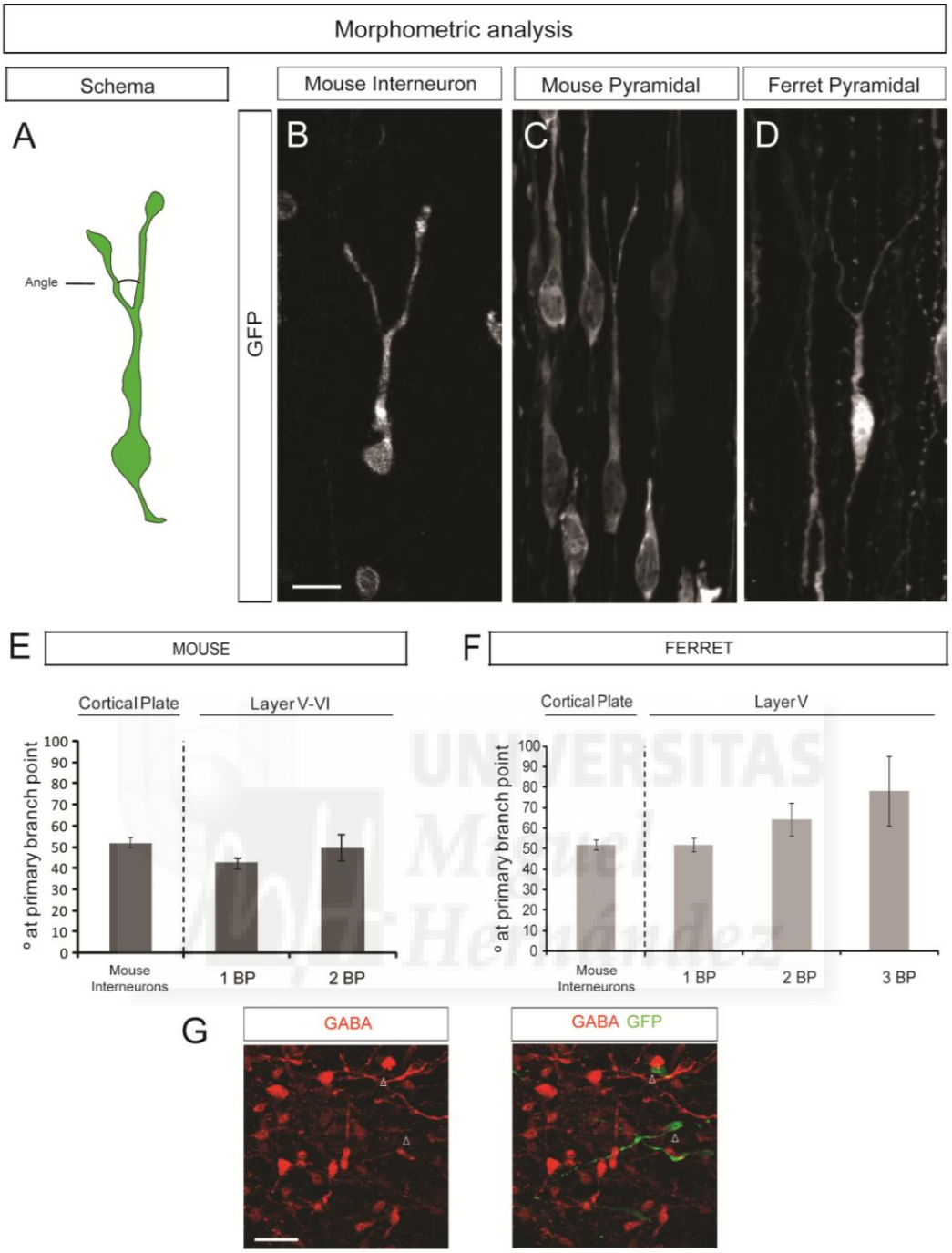

Figure 20. Similar angles at primary branch points between interneurons and pyramidal neurons. (**A**) Schema indicating the angle between branches. (**B-D**) Images of an interneuron, a branched pyramidal neuron mouse and ferret. (**E-F**) Graph represents the angle between branches at first branch point in mouse and ferret. Based in previous analysis, interneurons showed around 50 degrees when the turn from tangential to radial migration in the cortical plate. Mouse 89 cells, 11 embryos; ferret 82 cells, 4 kits; data are mean ± S.E.M. (***p<0.001, t-test). 0BP, zero branch points; 1BP, one branch point; 2BP, two branch points; 3BP, three branch points. (**G**) Immunohistochemistry in electroporated slices showed non GABA+cells in GFP electroporated neurons. Scale bars: B,C,D, 10 µm; G, 30 µm.

When cortical inhibitory interneurons change their direction of migration within the cerebral cortex from tangential to radial, they branch their leading process at wider angles than during tangential migration (Fig. 20B and E) (Martini et al., 2009). Interestingly, these angles are slightly wider than in mouse pyramidal neurons but equivalent to those in ferret pyramidal neurons with one BP. This prompted us to consider the possibility that the branched cells we were observing in ferret could be migrating cortical inhibitory interneurons. Indeed, it has been suggested that in humans cortical interneurons may be generated locally in the cerebral cortex (Jakovcevski et al., 2011; Zecevic et al., 2011). To rule out this possibility we performed immunohistochemistry against GABA (a marker of cortical interneurons) on ferret cortical slices locally electroporated with GFP. None of the GFP+ cells with a branched leading process were positive for GABA, refuting the possibility for these cells to be inhibitory interneurons (Fig. 20G). Taken together, these results suggested that just like interneurons increase the angle between their branches to change direction of migration, pyramidal neurons may widen the angle of their branched leading process for the same function. Moreover, migrating pyramidal neurons may form several branches in their leading process to explore an even wider cortical territory, and this is achieved at an even greater extent by widening the angle between their primary branches.

6. Non-branched migrating cells are more parallel to radial glia fibers than branched cells

A large body of evidence shows that the radial migration of cortical pyramidal neurons occurs in intimate physical and chemical association with the basal fibers of radial glia cells, or radial fibers. For this association to occur the leading process of migrating neurons must align parallel to radial fibers (Rakic, 1972; Sidman and Rakic, 1973; Rakic, 1974; Choi and Lapham, 1978; O'Rourke et al., 1992; Anton et al., 1999; Ang et al., 2003; Yoshikawa et al., 2003; Elias et al., 2007; Cooper, 2013). In this context, our observations of a majority of radially-migrating pyramidal neurons exhibiting a branched leading process, and that these branches form at quite wide angles, suggested that the parallel alignment and interaction of such neurons with radial fibers may be less than previously proposed for non-branched cells. As a first approximation to elucidate this question we measured, for each of our GFP-labeled cells, the extent of leading process parallel to the radial fiber scaffold, as identified with anti-vimentin stains (Fig. 21, A and B). The analysis was focused on cells in layer V of the ferret cortex, as above.

For each cell we calculated the angle of divergence between the radial fiber scaffold and different segments of the leading process (Fig. 21C).

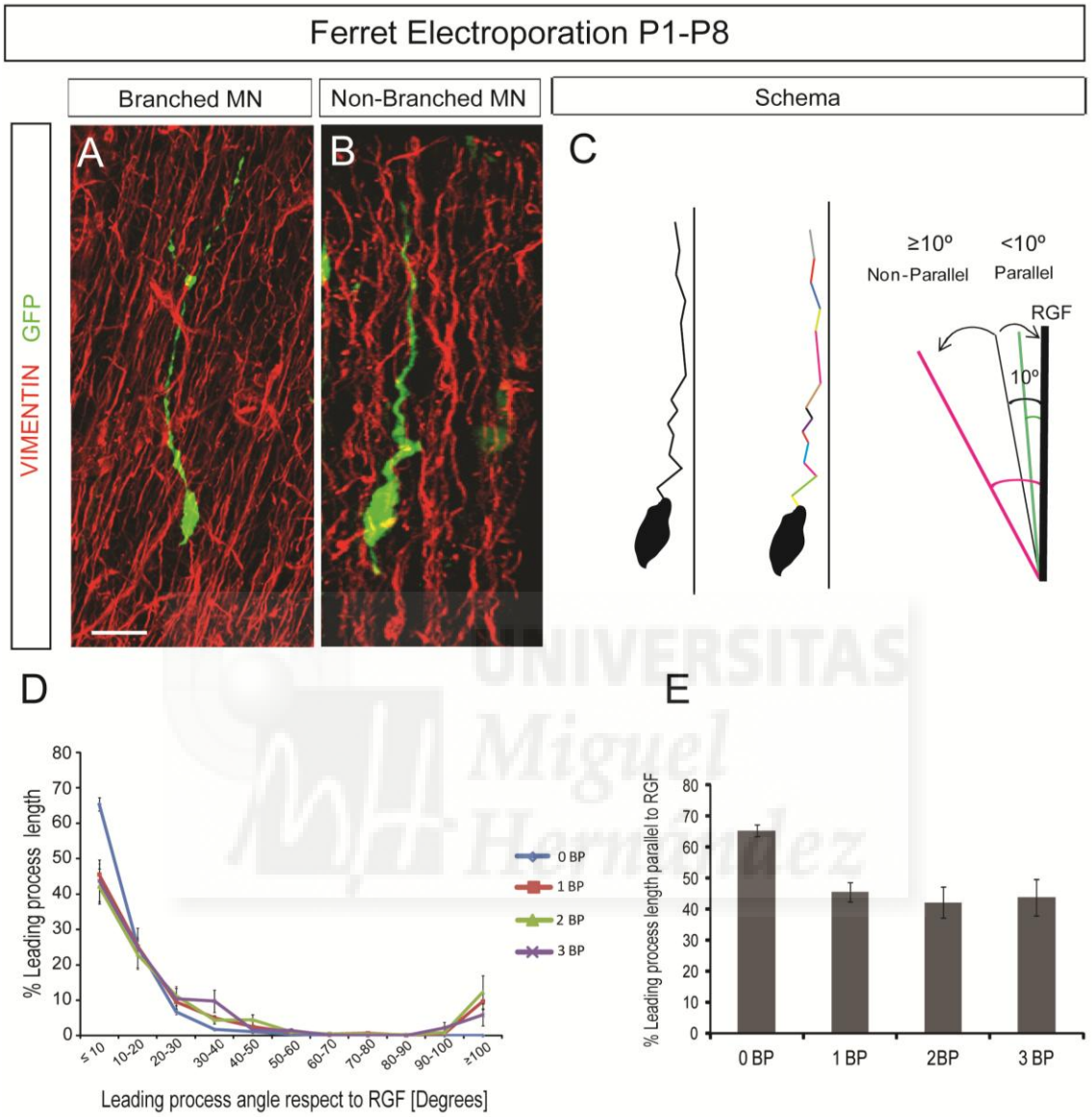

Figure 21. Non-branched migrating cells are more parallel to radial glia fibers than branched cells. (**A-B**) Pyramidal migrating neurons in ferret labeled with GFP and radial glia fibers stained with Vimentin. (**A**) Branched pyramidal neuron. (**B**) Non-branched pyramidal neuron. (**C**) The schema summarizes the subdivision in short segments of leading process. For each segment we analyzed the angle respect to the tendency of radial glial fibers. Considering segments with angles smaller than 10º are parallel and equals or bigger are non-parallel, we estimated the percentage of leading process that is parallel to RGF. (**D**) Graph shows the proportion of cells with different angles adopted by segments of leading process with respect to RGF. (0BP, n=97 cells; 1 BP, n=59 cells; 2BP, n=19 cells; 3BP, n=6 cells;4 kits per group; data are mean ± S.E.M.). (**E**) Graph represents the percentage of leading process length which is parallel to the tendency of RGF. In based of the criteria: parallel segment, angle smaller than 10º; non-parallel segment, angle equal or bigger than 10 º. (0BP, n=97 cells; 1 BP, n=59 cells; 2BP, n=19 cells; 3BP, n=6 cells;4 kits per group; data are mean ± S.E.M.). Scale bar: 10 µm.

On a first evaluation we observed that the greatest difference between cells with and without branches was in the amount of leading process oriented at 10 degrees or less, and 100 degrees or more, with respect to radial fibers (Fig. 21D). Based on this, we considered angles 10 degrees or less to represent parallel alignment, and this showed that the amount of leading process parallel to radial fibers was greater in cells without branches (65.41 ± 1.88%) than in branched cells (45.53 ± 3.01% for cells with 1 BP; 43.16 ± 4.97% for cells with 2 BPs; 43.76 ± 5.89% for cells with 3 BPs; Fig. 21E). When we looked at the distribution of angles adopted by fragments of the leading process (Fig. 21D), we observed that for all cell morphologies most of the leading process length formed angles between 0 and 30 degrees. However, branched cells had a greater proportion of their leading process oriented at 30º to 40º than non-branched cells, and this was even more dramatic for angles wider than 100º, which corresponded to 6-12% of leading process in branched cells but 0% in non-branched cells (Fig. 21D). Together, our data indicated that the leading process of cells with branched morphology may reduce their interaction with radial glia fibers during migration, hence further supporting the idea that branching of the leading process may be used by radially-migrating neurons to change direction of migration, switch between radial fibers and disperse laterally.

7. Leading process branching is dynamic and does not impair radial migration

It has been previously shown that loss-of-function of the cyclin-dependent kinase 5 (Cdk5) causes an exuberant branching of the leading process in radially-migrating neurons, and this to result in a severe impairment of cell migration (Ohshima et al., 1999; Tanaka et al., 2004; Ohshima et al., 2007; Borrell, 2010; Jacobshagen et al., 2014). Therefore the next critical question about leading process branching in radially-migrating neurons was to define whether this delays or impairs cell movement. To answer this question we performed two-photon videomicroscopy experiments in living slices of cerebral cortex from mouse embryos and ferret kits electroporated with a membrane-tethered GFP. Mouse embryos were electroporated at E14.5, allowed to further develop *in utero* until E17.5 when cortical slices were prepared, and then we started time-lapse imaging to monitor cell movement and leading process dynamics of individual GFP+ cells (Fig. 22A).

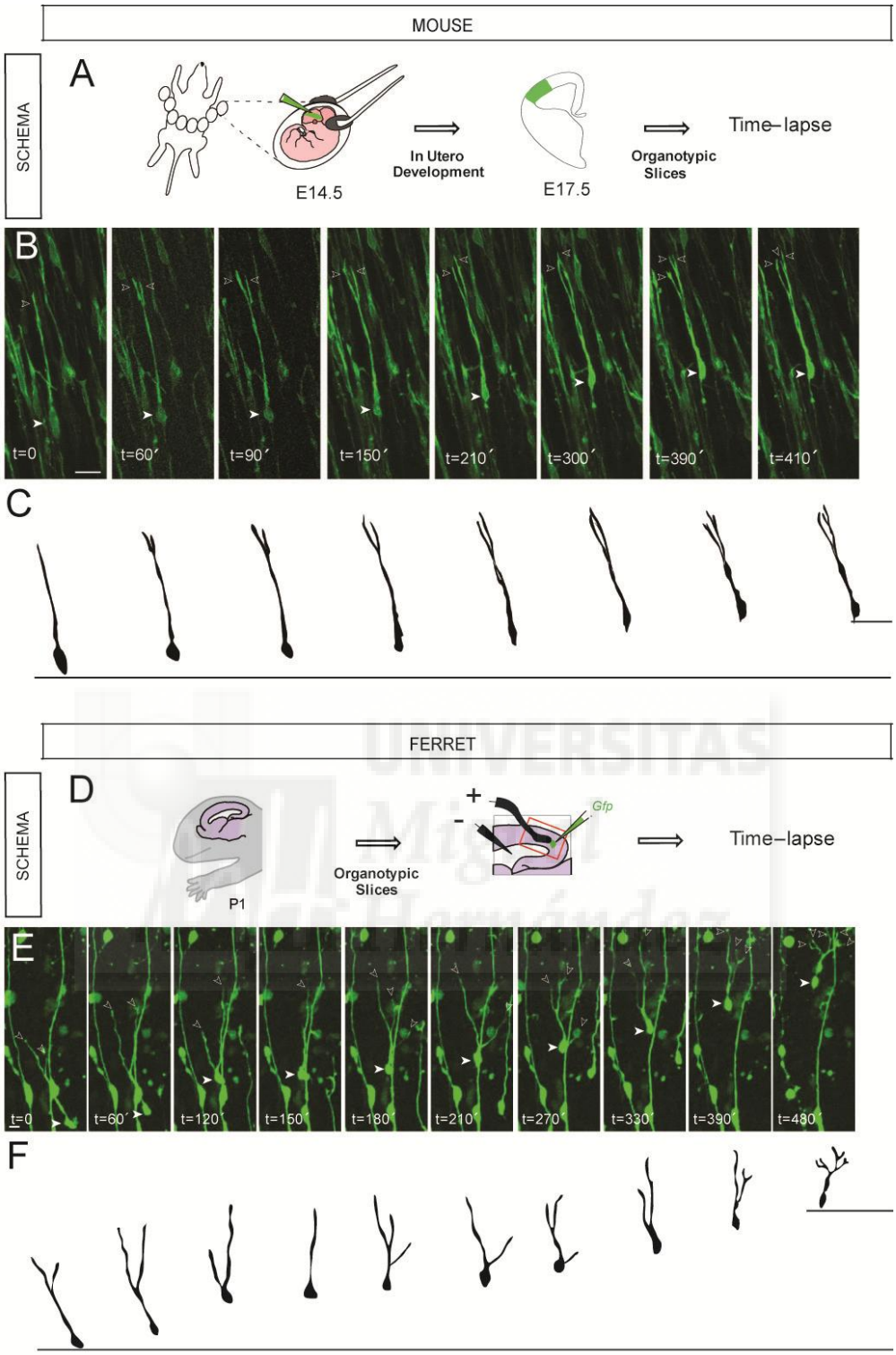

Figure 22. Leading process branching is dynamic and does not impair radial migration.
(**A**) Schema summarizing the experiment in utero electroporation in mouse from E14.5 to E17.5, organotypic slices and time-lapse. (**B**) Mouse time-lapse of a migrating neuron through cortical plate. Solid white arrowheads indicate cell soma and unfilled arrowheads point every branch. **C**) Drawing of the cell in B. Lines show the crossed distance by the cell. (**D**) Schema of the slice electroporation in ferret at P1. After labeling, we record the movement of the neuron. (**E**) Time-lapse of ferret pyramidal neuron at P1. Solid white arrowheads indicate cell soma and unfilled arrowheads point every branch. **F**) Drawing of the cell in E. Lines show the crossed distance by the cell. Scale bars: B,E, 10 µm.

To image radial migration in ferret cortex, living cortical slices were prepared from P1 kits, immediately electroporated focally, and imaged after 24 hr in culture to allow for GFP fluorescence to become detectable (Fig. 22D). As in our above analyses, the region of interest in mouse embryos was centered in the lower CP, and in ferrets in layers V/VI. As expected from our analyses in fixed tissue, cells undergoing radial migration displayed a leading process with none, one or more branches at the onset of imaging. During the course of the videomicroscopy experiments, cells underwent cycles of branching and extension of side branches, followed by translocation of the cell body inside the leading process trunk, and finalized by the selective retraction of one process combined with the stabilization and further extension of the other process (Fig. 22, B,C,E and F). All cells displaying a branched leading process migrated at similar speeds and for similar distances as non-branched cells for the duration of the imaging period (Fig. 22, B and C). These observations demonstrated first that cells with a branched leading process are perfectly motile and display no migratory handicap compared to non-branched cells. Second that branching of the leading process is transient and cells alternate between branched and non-branched morphologies, including multi-order branching (Fig. 22, E and F).

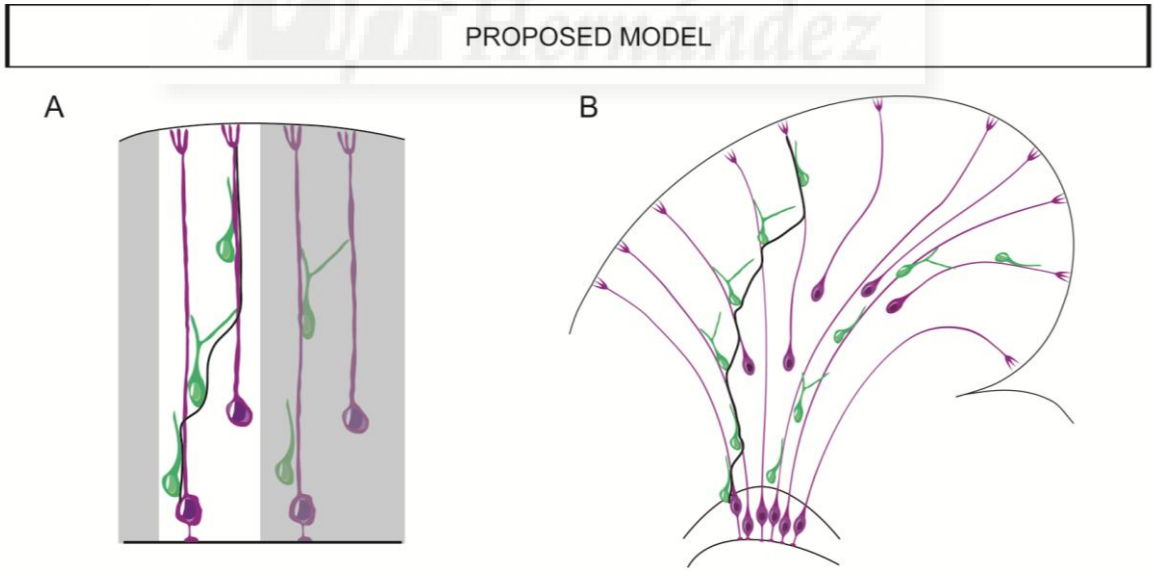

Figure 23. Proposed model. (**A**) Schema in detail representing branched migrating neurons contacting with two radial glial fibers, in contrast to non-branched that migrate following one single fiber. Branches could help that cells to move between fibers. (**B**) In gyrencephalic species, we hypothesize that branching could allow the tangential expansion of neurons through the entire cortex. One cell generated in a place in ventricular zone could move making branches, changing the radial fiber and occupying distant places.

It has been previously described, that neurons migrate guided by, and in intimate relation with RGFs, which also serve as the physical substrate for this migration (Rakic, 1972; Sidman and Rakic, 1973; Rakic, 1974; Choi and Lapham, 1978; O'Rourke et al., 1992; Ang et al., 2003; Yoshikawa et al., 2003). RGFs define the trajectory to be followed by migrating neurons. But the mechanism used by neurons to change between fibers was still unknown.

In the first part of my Thesis we reached that branching in the leading process of radially-migrating neurons is a common feature of these cells, specially significant in girencephalic species. This mechanism doesn´t stop or delay the migration, and neurons can altern between branched and non-branched morphology along their migration.

From our findings, we propose branching of the leading process as a mechanism to disparse and interchange between fibers (Fig. 23).

In agreement, the trajectory of the RGFs could permit the dispersion also. In that sense, radial glia cells play an important role in the distribution of migrating neurons. Specially in gyrencephalic species, there is an increase in divergence between radial fiber trajectories and also a high proportions of bRGCs (Fig. 23B), particularly primates, where they are highly neurogenic and accumulate prominently in the OSVZ (Schmechel and Rakic, 1979a; Schmechel and Rakic, 1979b; Fietz et al., 2010; Hansen et al., 2010; Reillo et al., 2011; Reillo and Borrell, 2012; Betizeau et al., 2013). In gyrencefalic bRGCs are intercalated between the aRGCs fibers, covering the entire cortex without increasing the thickness (proportion of nucleus) in the VZ. For all of these reasons and trying to study in deep the developmental expansion of the cerebral cortex, we wanted to determine the origin and emergence of the OSVZ. Specifically, we decided to study the origin and lineage of bRGCs, which are the main responsible of the divergent scaffold in gyrencephalic species.

8. Basal Intermediate Progenitor Cells are very scarce in ferret

To understand the origin and lineage of bRGCs and the OSVZ, we began defining the sources of OSVZ progenitor cells *in vivo* by tracing the lineage of cortical germinal layers in ferret at P1, and analyzing at subsequent developmental stages. P1 is the age of peak neurogenesis and growth in the ferret cortex, and when the size of OSVZ and abundance of bRGCs are near-maximal (Jackson et al., 1989; Reillo et al., 2011; Reillo and Borrell, 2012). The lineage of VZ progenitors was selectively labeled by transducing them with *Gfp*-encoding retroviruses (rv::*Gfp*) injected in the lateral

telencephalic ventricle, thereby infecting only progenitor cells in contact with the ventricular surface (Fig. 24A and 27A). Whereas the lineage of progenitors in ISVZ and OSVZ was labeled by local rv::*Gfp* injections into these layers (Fig. 28A and 29A). DNA delivered by retrovirus into dividing cells is randomly integrated into the genome of only one of the two daughter cells after the first mitosis. If mitoses are asymmetric the mother cell is labeled 50% of times, 100% if they are symmetric self-amplifying, and 0% if they are symmetric self-consuming (i.e. neurogenic) (Reillo et al., 2011).

Our cell lineage tracing experiments in early postnatal ferrets labeled a variety of cell types across cortical layers that progressively accumulated in IZ and CP at late stages (Fig. 24, C to G). These cell types included aRGCs, bRGCs, cells with multipolar morphology (MP), bipolar cells resembling migrating neurons (MN), differentiating neurons with a branched apical dendrite (DN) and cells with a star-like morphology (StC), the latter including cells in the astrocyte and oligodendrocyte lineages (Fig. 24, G and H). All these cell types were revealed by GFP regardless of the layer of rv::*Gfp* delivery, and systematically predominated in the OSVZ and IZ/CP, particularly MNs and DNs (Fig. 24I). As expected, DNs were only found in the upper CP and increased in abundance at later stages (P14; Fig. 24I).

Figure 24. Laminar distribution and types of cells in postnatal lineages. (A,B) Laminar distribution of GFP+ cells after injection of rv::*Gfp* in VZ (lateral ventricle), ISVZ or OSVZ at P1, and analysis at the indicated postnatal ages. Infection of VZ, *n* = 1,094 cells, 4 animals, P3; 5,544 cells, 4 animals, P6; 1,499 cells, 5 animals, P10; 4,196 cells, 3 animals, P14. Injection in ISVZ, *n* = 962 cells, 2 animals, P3; 1,063 cells, 2 animals, P6; 2,705 cells, 3 animals, P10; 3,107 cells, 2 animals, P14. Injection in OSVZ: *n* = 420 cells, 2 animals, P3; 1,092 cells, 3 animals, P6; 3,742 cells, 3 animals, P10; 1,663 cells, 2 animals, P14. IZ, intermediate zone; CP, cortical plate. (**C**-**F**) Examples of GFP+ cells with stereotyped morphologies: multipolar cells (MP), migrating neuron (MN), differentiating neuron (DN) and star-like cells (StC). Differentiating neurons typically had the cell soma in the cortical plate (CP) and a single apical dendrite branching in the marginal zone (MZ). (**G,H**) Examples of StC cells at P14 expressing Olig2 or GFAP, and quantification (*n* = 47 cells, Olig2; 47 cells, GFAP; 2 kits per group). (**I**) Relative abundance of non-RGC GFP+ cells within the indicated cortical layers bearing the identified morphologies at the indicated postnatal ages after injection of rv::*Gfp* at P1 in VZ (lateral ventricle), ISVZ or OSVZ. (**J**) Abundance of GFP+ MN and MP cells in the neocortex at the indicated postnatal ages after injection of rv::*Gfp* at P1 in VZ, ISVZ or OSVZ. Number of cells and animals analyzed is the same as above. Data are mean ± S.E.M. Scale bars, 20 μm.

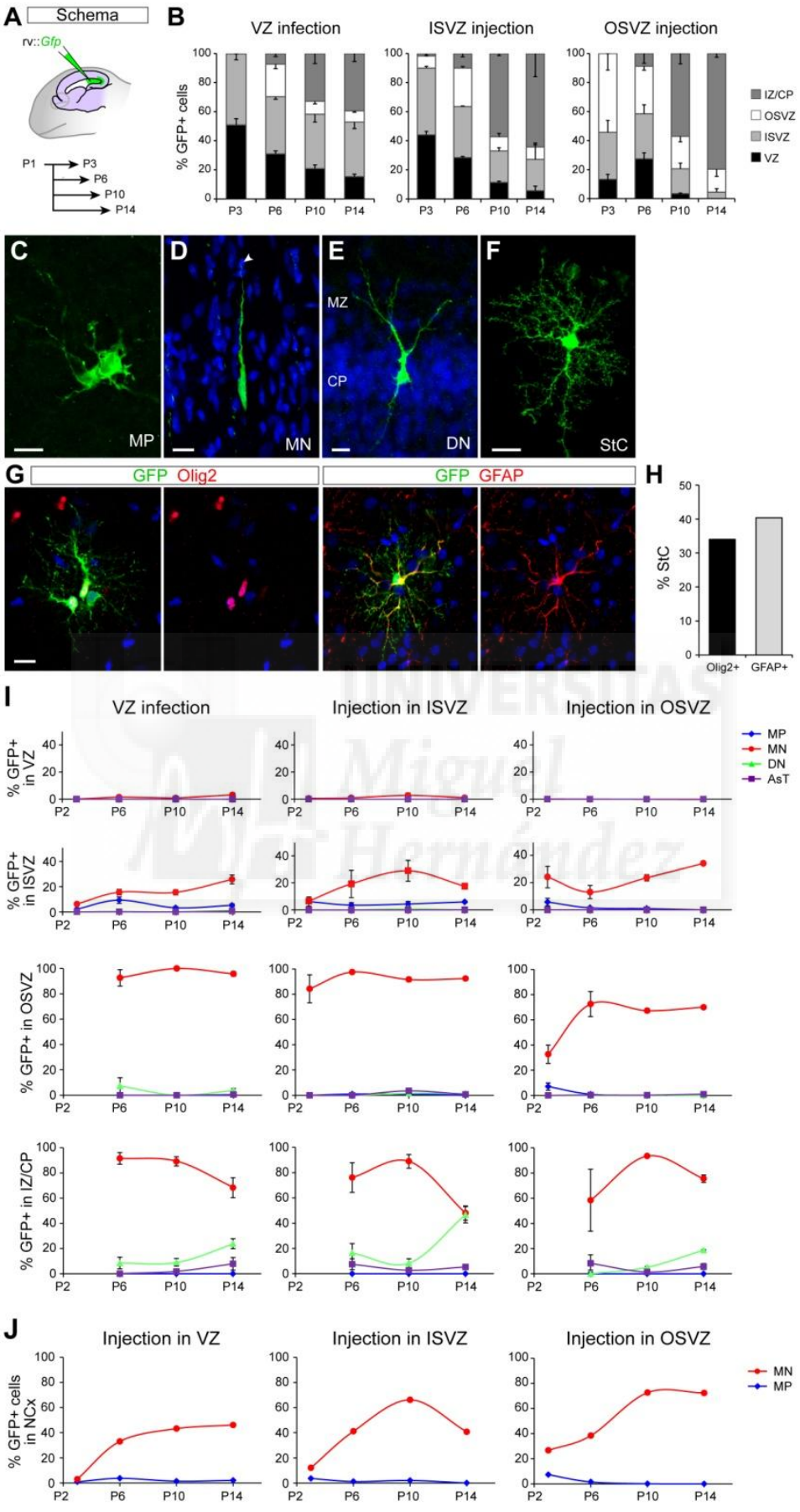
A
Schema
rv::Gfp
P1
P3
P6
P10
P14
B
VZ infection
ISVZ injection
OSVZ injection
% GFP+ cells
IZ/CP
OSVZ
ISVZ
VZ
C
MP
D
MN
E
MZ
CP
DN
F
StC
G
GFP Olig2
GFP GFAP
H
% StC
Olig2+
GFAP+
I
VZ infection
Injection in ISVZ
Injection in OSVZ
% GFP+ in VZ
% GFP+ in ISVZ
% GFP+ in OSVZ
% GFP+ in IZ/CP
MP
MN
DN
AsT
J
Injection in VZ
Injection in ISVZ
Injection in OSVZ
% GFP+ cells in NCx
MN
MP

MP cells had the typical morphology of neurogenic IPCs (Fig. 24C), but their relative abundance was very low (<10% of GFP+ cells; Fig. 24, I and J), not only compared to the mouse SVZ (Noctor et al., 2004; Kowalczyk et al., 2009) but especially considering that many cells in GFP+ clones eventually differentiated as neurons (Fig. 24I). Moreover, SVZ cells with multipolar morphology include IPCs and newborn neurons (Tabata and Nakajima, 2003). To specifically identify IPCs we stained against Tbr2 (marker of IPCs and newborn neurons not expressed by aRGCs) and Ki67 (marker of cycling cells). This analysis was performed at P6 after rv::*Gfp* injection in VZ at P1, to obtain the largest number of GFP+ MP cells (Fig. 25A to D). Whereas 100% of MPs were Tbr2+, only 14.3% were Ki67+, indicating that only a minority of the already few MPs were IPCs (Fig. 25, B and D). In contrast to the unexpected scarcity of MP cells, MN cells were very abundant (Fig. 24, I and J), so we analyzed if these could be IPCs with bipolar morphology. Only 25.0% of MNs were Tbr2+ and none were Ki67+ (Fig. 25, C and D), consistent with these cells not being IPCs but rather newborn cortical neurons.

The above results seemed to indicate that IPCs were extremely rare in ferret, contrary to mouse. An alternative was that our pleiotropic retroviral vectors might somehow have a different cellular specificity between mouse and ferret. To discard this possibility we injected rv::*Gfp* in mouse embryos at E14.5 and analyzed at E16.5, a period of cortical development equivalent to P1-P6 in ferret (Fig. 25, E and F). MP cells represented 29.7% of all GFP+ cells in mouse, eight times more than in ferret (3.6%; Fig. 25H). Ki67 stains revealed that in mouse embryos 12.4% of all GFP+ cells were putative IPCs (Ki67+ MP cells; Fig. 25,G and H), while these represented only 0.5% in ferret (Fig. 25H). This further supported that IPCs may be very scarce in ferret, representing very few of the already small population of MP cells. To further confirm the unexpected scarcity of IPCs in ferret we electroporated *Gfp*-encoding plasmids in VZ of newborn kits, because this method labels abundant pyramidal neurons in the juvenile ferret cortex (Borrell, 2010) and so it must label their cellular lineage earlier in development (Fig. 25, I and J).

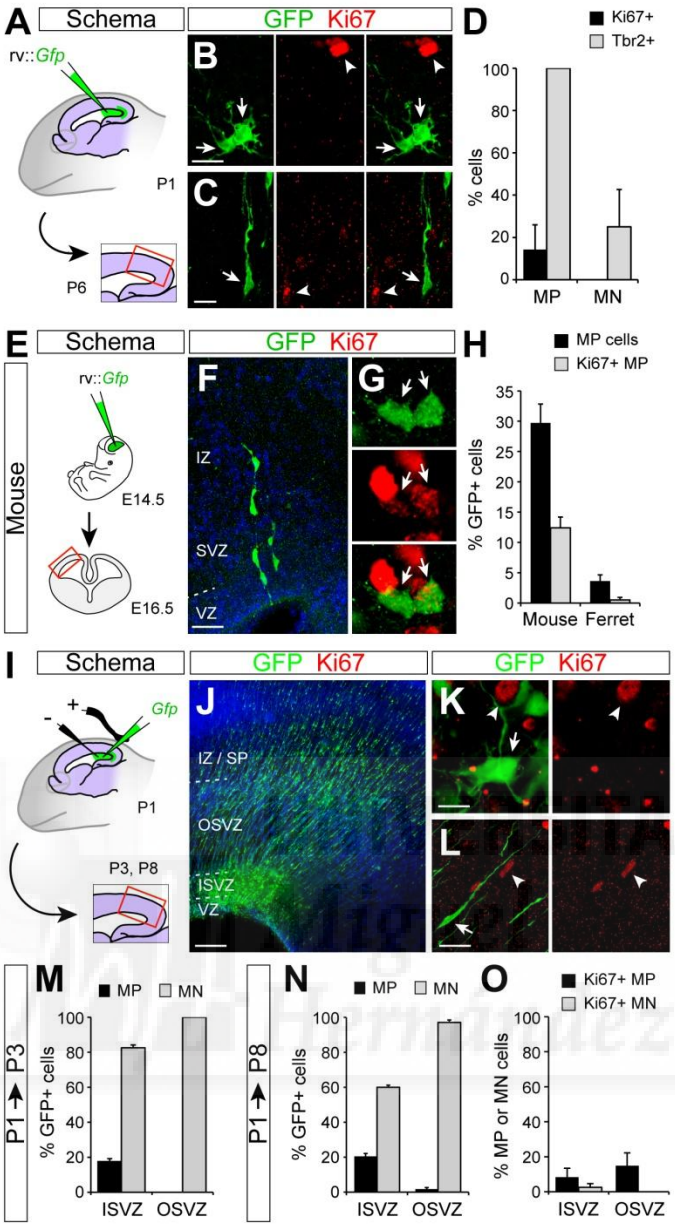

Figure 25. Intermediate Progenitor Cells are very infrequent in ferret. (**A-D**) GFP-labeling of MP and MN cells after intraventricular delivery of rv::*Gfp* at P1 and analysis at P6. All MP cells were positive for Tbr2 but few for Ki67 (B,D; *n* = 15 cells, 3 animals, Ki67; 17 cells, 3 animals, Tbr2), while few MN cells were Tbr2+ and none were Ki67+ (C,D; *n* = 38 cells, 3 animals, Ki67; 40 cells, 3 animals, Tbr2). (**E-H**) GFP-labeling of mouse MP and MN cells after intraventricular delivery of rv::*Gfp in utero* at E14.5 and analysis at E16.5, stages of cortical development equivalent to P1-P6 in ferret. Arrows in (**G**) indicate Ki67+ MP cells. (**H**) The abundance of MP cells (total) and Ki67+ MP cells in mouse was much higher than in ferret (Mouse: MP, *n* = 338 cells, 7 embryos; Ki67+ MP, *n* = 76 cells, 7 embryos. Ferret: MP, *n* = 5,544 cells, 4 animals; Ki67+ MP, *n* = 15 cells, 3 animals). (**I-O**) Ferrets were electroporated with *Gfp*-encoding DNA at P1 and analyzed at P3 or P8. (**K,L**) Examples of MN (K) and MP (L) cells at P8 negative for Ki67. (**M,N**) Abundance of GFP+ MP and MN cells at P3 and P8, showing that very few GFP+ cells in ISVZ and OSVZ were MP at both stages, although their frequency was higher after electroporation than after rv::*Gfp* infection (compare to H) (P3: *n* = 1,749 cells, ISVZ; 39 cells, OSVZ; 3 animals per group. P8: *n* = 2,314 cells, ISVZ; 3,799 cells, OSVZ; 4 animals per group). (**O**) Quantification of GFP+ MP and MN cells within ISVZ and OSVZ positive for Ki67, demonstrating that very few MP and nearly none of the MN cells were Ki67+ (ISVZ, *n* = 172 cells, MP; 112 cells, MN; OSVZ, *n* = 38 cells, MP; 282 cells, MN; 3 animals per group). Data are mean + S.E.M. Scale bars: B,C, 10 µm; F, 30 µm; J, 150 µm; K, 5 µm; L, 20 µm.

In contrast to retroviral infection, electroporation labeled a much greater proportion of cells with MP and MN morphology along the same developmental period (Fig. 25, J to N). However, the proportion of MP and MN cells positive for Ki67 was again extremely low or null (Fig. 25O), demonstrating that their vast majority was non-proliferative and, thus, that IPCs are extremely scarce in the early postnatal ferret.

In summary, analyses of abundance and marker expression demonstrated that neurogenic IPCs (multipolar, Ki67+, Tbr2+ cells) were a very small minority of progenitors in ISVZ and OSVZ, in contrast to the mouse SVZ (Fig. 24 and 25).

9. A large proportion of aRGCs and bRGCs express the neurogenic marker Tbr2, pointing out RGCs as the main source of neurons in the gyrencephalic ferret cortex

Given the extremely low abundance of IPCs found in ferret, we next explored which other progenitor cell types might be the major contributors to cortical neurogenesis in ferret, turning our attention to aRGCs and bRGCs. To define the basic molecular features of aRGCs and bRGCs as cortical progenitors we performed a marker expression analysis. The vast majority of GFP+ cells morphologically identified as aRGCs and bRGCs were positive for Ki67 and Pax6 (Fig. 26, A, B and E), in agreement with their current definition (Reillo et al., 2011; Reillo and Borrell, 2012; Betizeau et al., 2013). Unexpectedly, 23.7% of aRGCs and 34.3% of bRGCs also expressed Tbr2 (Fig. 26, C to E). This was surprising because in mouse Tbr2 is a marker of IPCs but not RGCs (Englund et al., 2005; Kowalczyk et al., 2009; Wang et al., 2011a), also reported previously in ferret and human (Fietz et al., 2010; Hansen et al., 2010; Reillo et al., 2011; Gertz et al., 2014). However, these observations were fully consistent with more recent analyses in macaque embryos (Betizeau et al., 2013). To confirm these findings we performed anti-phosphovimentin (PhVim) stains, to reveal the morphology of progenitor cells at mitosis and thus to distinguish progenitor cells with a basal process (putative RGCs) from those without one (putative IPCs) (Weissman et al., 2003; Fietz et al., 2010; Wang et al., 2011b; Reillo and Borrell, 2012). At two different developmental stages we found nearly identical results, and very similar to the above using rv::*Gfp*: Pax6 was expressed by 96.0-100% of cells with a PhVim+ basal process, but then also by 90-100% of cells without a PhVim+ basal process (Fig. 26, F and I). Similarly, Tbr2 was expressed at similar frequencies by cells with and without a

PhVim+ basal process in all three germinal layers (Fig. 26, G to I). This was contrary to mouse, where aRGCs and bRGCs are Pax6+/Tbr2-, and IPCs are mostly Pax6-/Tbr2+ (Kowalczyk et al., 2009; Arai et al., 2011; Wang et al., 2011b). To confirm these findings we investigated the pattern of PhVim labeling in morphologically-identified GFP+ bRGCs, which revealed that 43.1% of bRGCs positive for PhVim (in mitosis) lacked a PhVim+ basal process (Fig. 26, J to L). These results indicated that bRGCs in gyrencephalic species are molecularly diverse, varying in Tbr2 expression and PhVim pattern. In addition, the frequent expression of Tbr2 in bRGCs suggested that these might be the main neurogenic progenitors in the ferret cortex as recently shown in macaque embryos, where IPCs are also very scarce as we found in ferret (Betizeau et al., 2013).

Given the multiple similarities between ferret and macaque bRGCs mentioned above, we next analyzed the existence of diverse bRGC morphotypes as described recently in macaque (Betizeau et al., 2013). To this aim we studied ferret kits injected with rv::*Gfp* in VZ at P1 and analyzed at P6, containing abundant bRGCs in ISVZ (Fig. 24 and 27). As opposed to macaque OSVZ, all bRGCs in ferret ISVZ had a basal process and none had an apical process. However, bRGCs were distinguished by having a long or a short basal process, the former being much more abundant than the latter (Fig. 26M). Interestingly, we also distinguished three types of aRGC based on the length of their basal process: long, short or absent. These included RGCs with the cell body in ISVZ but with an apical process reaching the ventricular surface of the telencephalon, as described previously (Pilz et al., 2013). Similar to bRGCs, aRGCs with a long basal process were the most abundant so that, overall, aRGCs and bRGCs with a long basal process accounted for nearly 70% of RGCs in ferret (Fig. 26M).

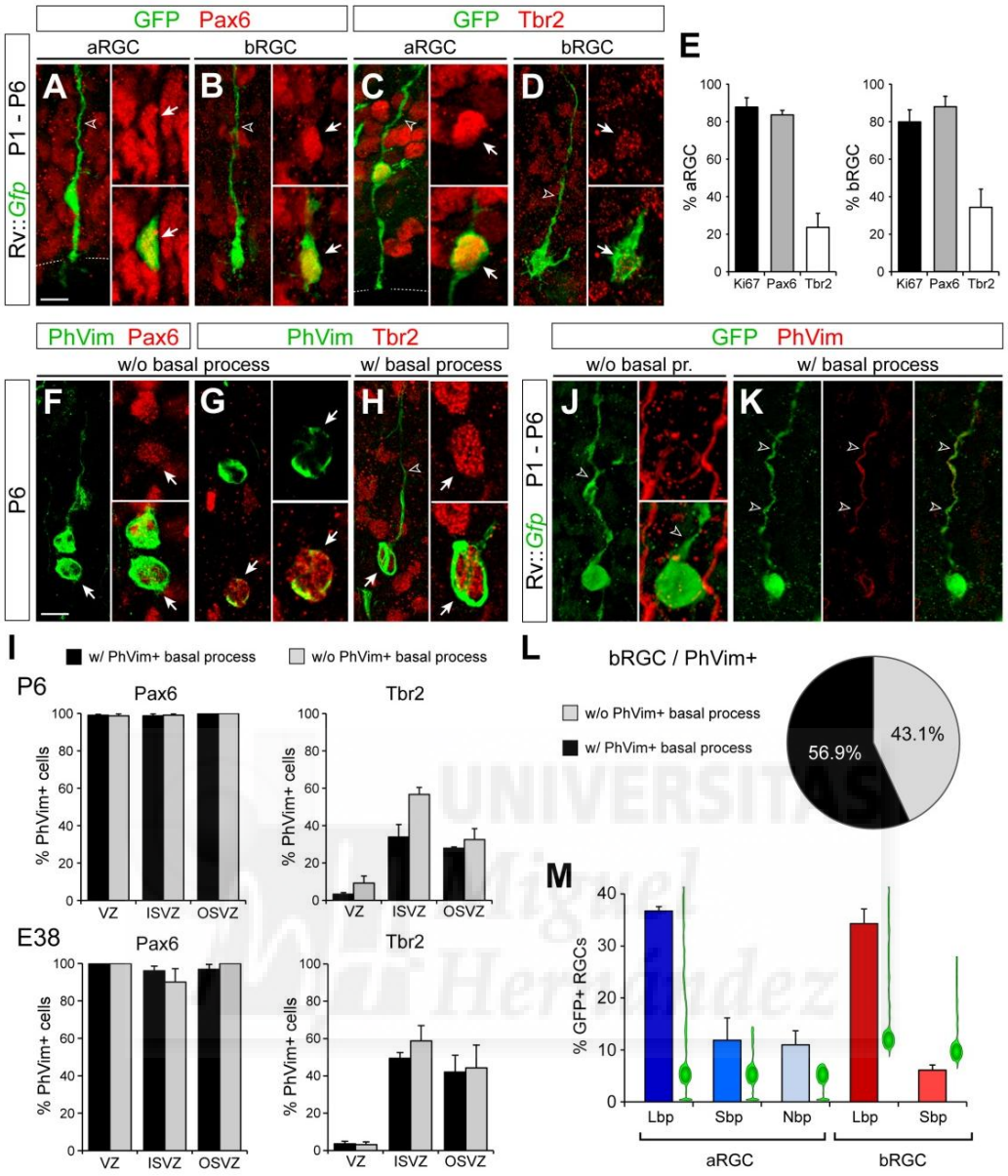

Figure 26. aRGCs and bRGCs are molecularly diverse and include a Tbr2+ subpopulation. (**A-E**) GFP+ aRGCs in VZ (**A,C**) and bRGCs in ISVZ (**B,D**) at P6 after ventricular injection of rv::*Gfp* at P1, showing expression of Pax6 (**A,B**) and Tbr2 (**C,D**) in both populations. (**E**) Abundance of aRGCs and bRGCs expressing Ki67, Pax6 or Tbr2 (aRGCs, *n* = 57 cells, Ki67; 82 cells, Pax6; 61 cells, Tbr2; 3 animals. bRGCs, *n* = 72 cells, Ki67; 59 cells, Pax6; 31 cells, Tbr2; 3 animals). (**F-I**) PhVim+ cells in VZ, ISVZ and OSVZ at P6 and E38, without or with a basal process, expressing Pax6 or Tbr2, and relative abundance (I) (P6: Pax6, *n* = 788 cells in VZ, 692 cells in ISVZ, 292 cells in OSVZ, 3 animals; Tbr2, *n* = 514 cells in VZ, 1,012 cells in ISVZ, 526 cells in OSVZ, 3 animals. E38: Pax6, *n* = 126 cells in VZ, 215 cells in ISVZ, 118 cells in OSVZ, 3 animals; Tbr2, *n* = 456 cells in VZ, 420 cells in ISVZ, 237 cells in OSVZ, 3 animals). (**J-L**) GFP+ bRGCs in ISVZ labeled after injections as in (A-D), displaying PhVim label without or with a basal process, and relative abundance (*n* = 54 cells, 4 animals). (**M**) Morphotypes of RGCs at P6 after rv::*Gfp* delivery in VZ at P1 (*n* = 314 cells, 3 kits). The majority were aRGCs with a long basal process (Lbp) and bRGCs with a long basal process (Lbp). Apical RGCs with a short basal process (Sbp) or no basal process (Nbp), and bRGCs with a short basal process (Sbp) were a minority. Not a single example of bRGC with an apical process was observed. Data are mean + S.E.M. Detail images demonstrating co-localization are single confocal planes. Scale bar, 10 µm.

Taken together, our analyses demonstrated that RGCs (apical and basal) represented the vast majority of progenitor cells in the developing ferret cerebral cortex, and that while nearly all expressed Pax6, they were heterogeneous in Tbr2 expression and in the pattern of PhVim stain, where presence or absence of a PhVim+ basal process did not recapitulate actual progenitor cell morphology at mitosis. Importantly, our analyses demonstrated that non-RGC progenitors are extremely infrequent in ferret compared to RGCs. Therefore, ferret cortical neurogenesis does not rely on multipolar IPCs, as in rodents (Miyata et al., 2004; Noctor et al., 2004; Kowalczyk et al., 2009), but RGCs seem to be the main neurogenic progenitors, as in macaques.

10. bRGCs in OSVZ are not generated in VZ or ISVZ postnatally

After markers analysis of aRGCs and bRGCs, we analyzed the origin and lineages of these cells. Importantly, aRGCs and bRGCs represented the vast majority of progenitor cells in all three germinal layers: upon infection of VZ progenitors with rv::*Gfp* at P1, by P3 we found that 50.6% of GFP+ cells were aRGCs and 45.3% bRGCs (Fig. 27, C and E). The production of bRGCs from aRGCs was confirmed by 2-photon videomicroscopy in slice cultures (Fig. 27 and 29), in agreement with previous reports (Wang et al., 2011b; LaMonica et al., 2013; Pilz et al., 2013; Gertz et al., 2014).

Remarkably, all bRGCs were found in ISVZ and none in OSVZ (Fig. 27E). Because two days might be insufficient time for bRGCs generated in VZ to reach the OSVZ, we next allowed longer survivals. GFP labeling was traced for up to two weeks post-injection, but bRGCs continued absent from the OSVZ while very abundant in ISVZ (Fig. 27, D and E). Next we reasoned that if bRGCs in OSVZ were not produced directly from the VZ, they might be generated indirectly via bRGCs in ISVZ. The above results seemed to rule out this possibility as GFP+ bRGCs were not seen in OSVZ even long after these had been observed in ISVZ (Fig. 27, B and E). An alternative possibility was that bRGCs in OSVZ were produced by other types of progenitor cells resident in ISVZ and/or not derived from the postnatal VZ. In such case, bRGCs in OSVZ would only be revealed by direct labeling of ISVZ progenitors. To test this we performed injections of high titer rv::*Gfp* locally into the ISVZ of P1 ferrets (Fig. 28A). Two days after rv::*Gfp* injection abundant aRGCs and bRGCs were labeled in VZ and ISVZ, respectively, but were virtually absent from OSVZ (Fig. 28, B,C and E). At longer survival times bRGCs continued to represent the vast majority of GFP+ cells in

ISVZ (65.9-77.2%), but they remained absent from the OSVZ (Fig. 28, D, E and F), demonstrating that bRGCs in OSVZ were not produced by progenitor cells in the ISVZ. Taken together, these results provided the first demonstration *in vivo* that aRGCs are an abundant source of bRGCs in gyrencephalic species, but also that at late stages of cortical development these are solely destined to the ISVZ, without contributing to the OSVZ.

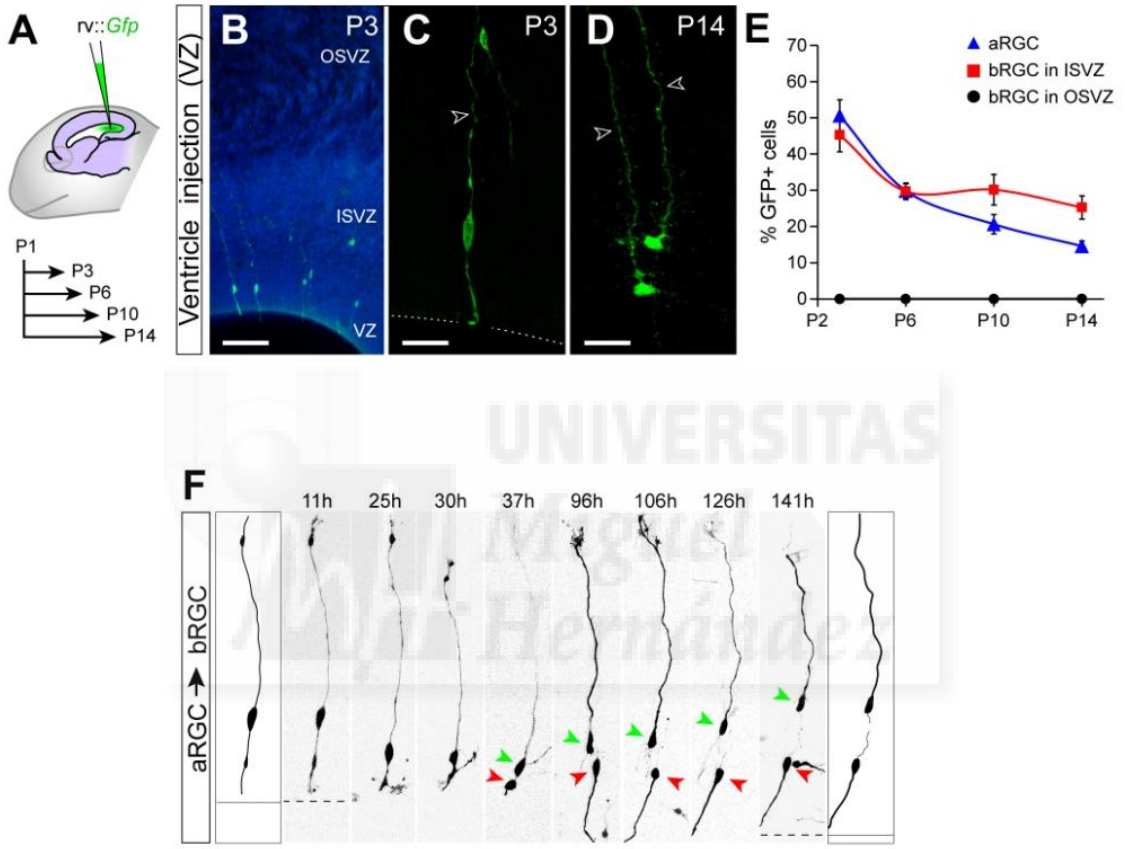

Figure 27. Postnatal VZ do not generate bRGCs for the OSVZ. (**A-F**) P1 ferrets were injected with rv::*Gfp* into the lateral telencephalic ventricle to infect VZ, and analyzed at various subsequent stages. Cell lineages from these layers contained aRGCs in VZ (**C**) and abundant bRGCs in ISVZ throughout development (**D**); arrowheads indicate the basal process, but null presence in OSVZ (**E**) (*n* =1094 - 5,544 cells per group; Table 1, Annex). (**F**) Time-lapse imaging frames of an aRGC dividing apically, between 30 and 37h of imaging time, to generate a bRGC (green arrowhead) retaining the basal process. The apical cell (red arrowhead) retained the apical process. Scale bars: 100 µm low magnifications, 20 µm details.

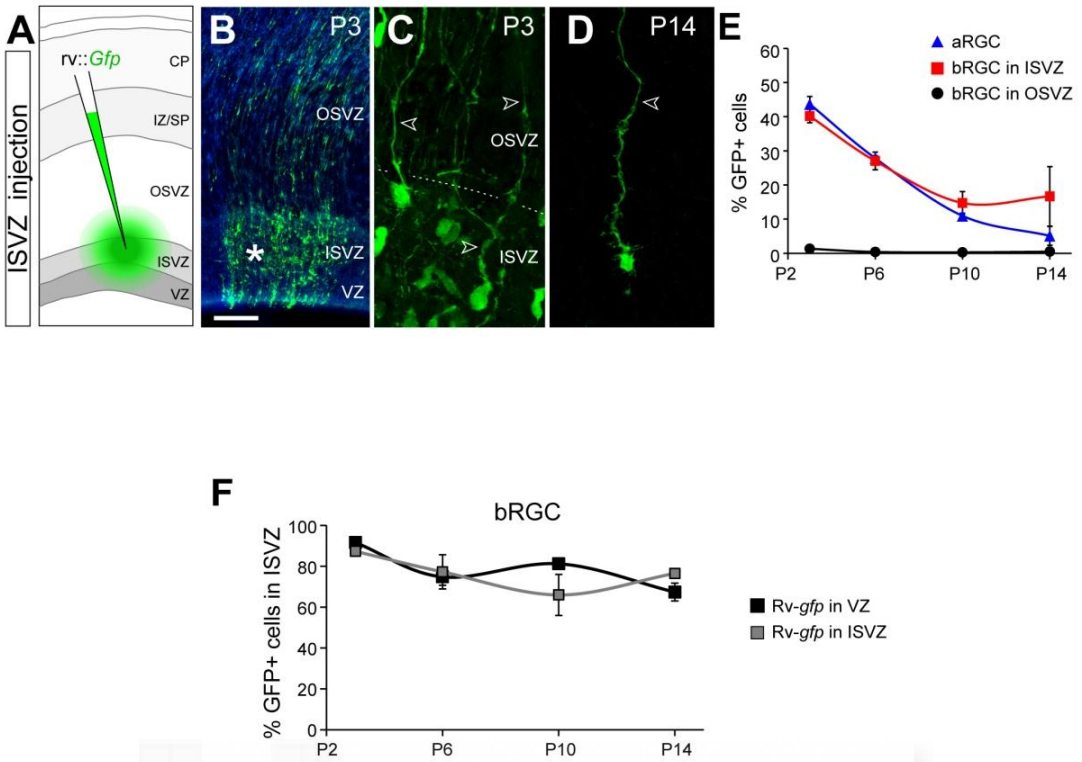

Figure 28. Postnatal ISVZ do not generate bRGCs for the OSVZ. (**A-F**) Ferrets were injected with rv::*Gfp* locally in ISVZ at P1 and analyzed at later stages. GFP+ bRGCs were abundant in ISVZ at all survival times (**E**), but none bRGCs was observed in OSVZ. (*n* = 962 cells-3107 cells per group; Table 1, Annex). Images in (**B**) show clusters of GFP+ cells at the injection site (asterisks). (**F**) Abundance of GFP+ bRGCs located in ISVZ after VZ and ISVZ infections (VZ, *n* = 1,094 cells, 4 animals, P3; 5,544 cells, 4 animals, P6; 1,499 cells, 5 animals, P10; 4,196 cells, 3 animals, P14. ISVZ, *n* = 962 cells, 2 animals, P3; 1,063 cells, 2 animals, P6; 2,705 cells, 3 animals, P10; 3,107 cells, 2 animals, P14). Scale bars: 100 µm low magnifications, 20 µm details.

11. Abundant generation of bRGCs in the postnatal OSVZ

To elucidate if bRGCs in the postnatal OSVZ were generated locally, we injected rv::*Gfp* in the OSVZ (Fig. 29, A and E). At P3 we found 60.4% of GFP+ cells in the OSVZ displaying bRGC morphology (Fig. 29, B, C and E), a proportion that decreased by P6 to then remain similar until P14 (Fig. 29, D and E). To investigate the dynamics of bRGC production in OSVZ we injected rv::*Gfp* at various stages and analyzed after two days. At P3 and P8 bRGCs represented 60-52% of cells born in OSVZ (Fig. 29F), indicating their net increase. Videomicroscopy in slice cultures demonstrated self-amplification of bRGCs, including *de novo* generation of a basal process (Fig. 29G) as in primates (Hansen et al., 2010; Betizeau et al., 2013). Unfortunately, virus injections in OSVZ had the limitation that numerous cells in the underlying ISVZ and VZ were also labeled (Fig. 29B), likely infected via their basal process (Reillo et al., 2011).

Nevertheless, our above analyses showed that these layers never generate OSVZ bRGCs, and therefore they were being generated only locally within the postnatal OSVZ. Similarly, we found that the few IPCs in OSVZ were not generated by VZ or ISVZ progenitors, but mainly locally within OSVZ (Fig. 24).

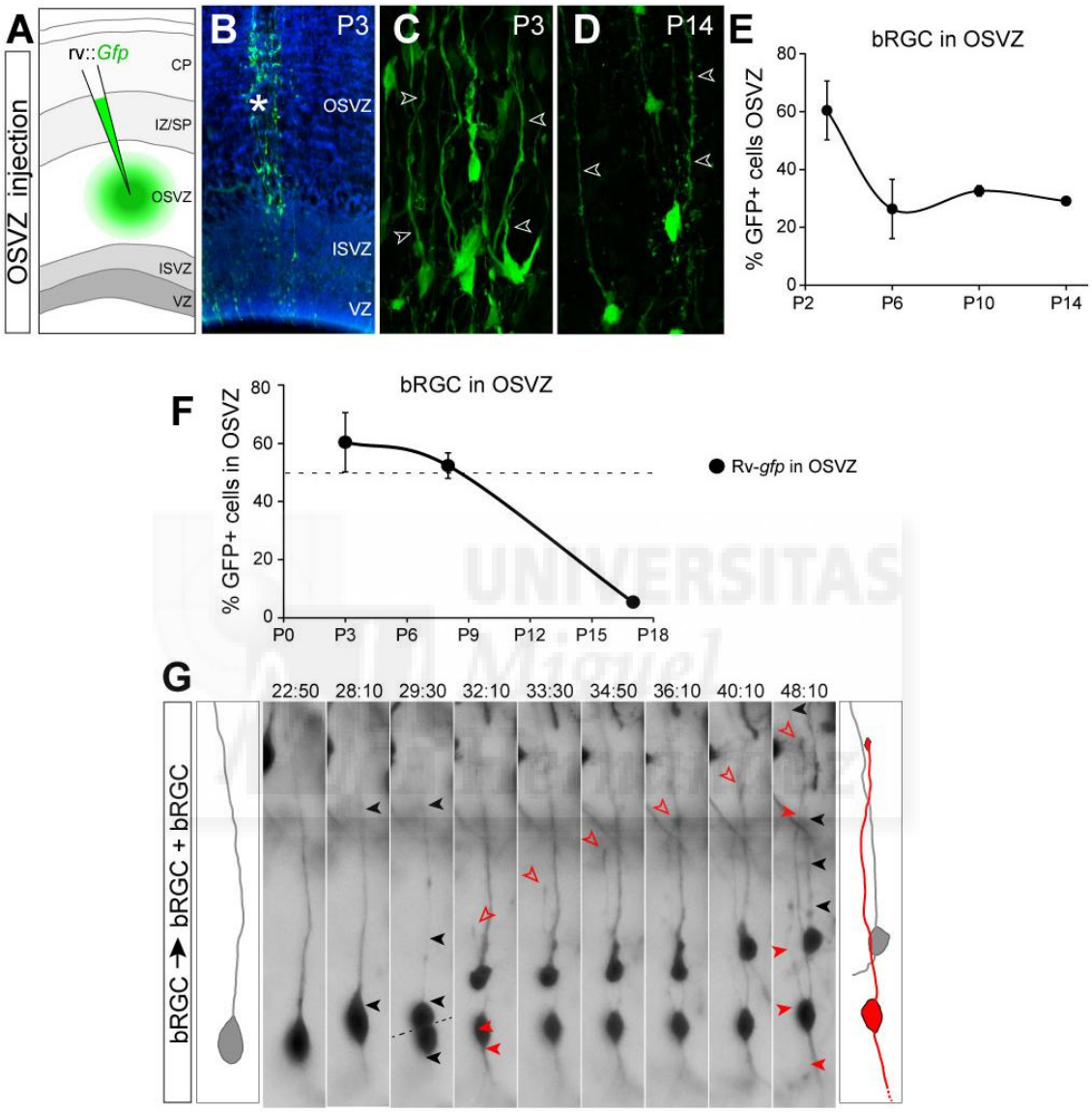

Figure 29. Postnatal OSVZ bRGCs are generated by self-amplification. (**A-E**) Ferrets were injected with rv::*Gfp* locally in OSVZ at P1 and analyzed at later stages. GFP+ bRGCs were abundant in OSVZ at all survival times (**E**), demonstrating local bRGC production (*n* = 420 - 3,742 cells per group; Table 1, Annex). Images in (**B**) show clusters of GFP+ cells at the injection site (asterisks). (**F**) Abundance of GFP+ bRGCs in OSVZ at the indicated postnatal stages after injections of rv::*Gfp* in OSVZ and 2-3 days of survival. Data are mean ± S.E.M. (*n* = 420 cells, 3 animals, P1-P3; 1288 cells, 4 animals, P6-P8; 819 cells, 2 animals, P14-P17). (**G**) Time-lapse imaging frames of a bRGC in OSVZ with a basal process (black arrowheads), undergoing a near-horizontal division at t=29:30 hr (dashed line) to generate two bRGCs. The basal daughter cell (top) retained the maternal basal process, whereas the apical daughter (bottom) grew a new basal process (solid red arrowheads) tipped with a small growth cone (red open arrowheads).

Taken together, our findings demonstrated that the OSVZ is a unique niche of progenitor cell production at postnatal stages, following a lineage independent from progenitors in VZ and ISVZ, and where the vast majority of progenitors are bRGCs that expand by self-amplification.

12. OSVZ is initiated embryonically by founder bRGCs seeded directly from VZ progenitors

Our above analyses demonstrated that at postnatal stages bRGCs in ISVZ and OSVZ follow completely independent lineages. In ISVZ, bRGCs are continuously generated by aRGCs in the VZ, whereas in OSVZ they are exclusively generated locally, within the OSVZ**.** However the key question of where and when OSVZ progenitors (mainly bRGCs) arise originally remained open. Given that all cortical cells derive from the early embryonic neuroepithelial progenitors at some point (Gotz and Huttner, 2005), we focused on earlier stages to determine the origin of bRGCs. In ferret the OSVZ is first distinguishable at E36, six days prior to birth (E42/P0) (Fig. 30A), so we traced VZ progenitors with rv::*Gfp* at E34 and E36 *in utero*.

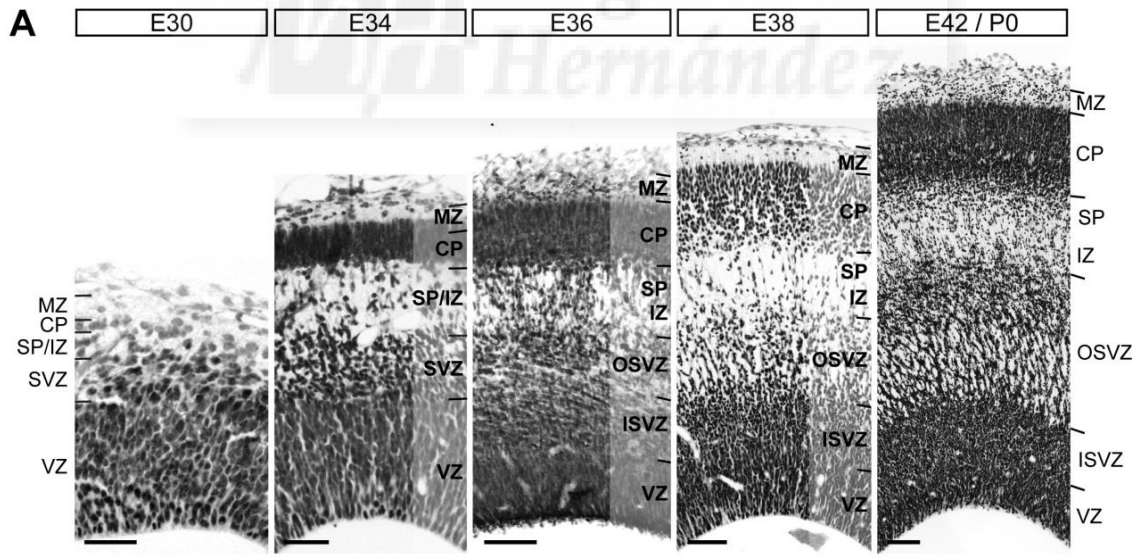

Figure 30. The OSVZ forms between E34 and E36. (**A**) Nissl stains of the ferret embryonic neocortex illustrate the developmental progression of germinal layers and the formation of OSVZ between E34 and E36. Scale bars: 30 µm (E30 and E34), 100 µm (E36), 150 µm (E38), 200 µm (E42/P0).

When we injected rv::*Gfp* in the ventricle of E34 embryos and analyzed them at E36, we found GFP expression in numerous bRGCs in ISVZ, but none in OSVZ (Fig. 31, A to C). Next we injected rv::*Gfp* at E36 and analyzed at E38, and again we found numerous GFP+ bRGCs in ISVZ but none in OSVZ (Fig. 31C). Because 1.5 days might be insufficient time for new bRGCs to migrate from VZ to OSVZ, we repeated the injections at E34 but now analyzing at E38. In these embryos we found that 37.1% of GFP+ cells were bRGCs, and 21.7% of these were located in OSVZ (8.0% of all GFP+ cells; Fig. 31, A to C). Extending the survival period we continued to find a significant amount of GFP+ bRGCs in OSVZ at postnatal stages (Fig. 32). These results demonstrated that bRGCs in the postnatal OSVZ had been originally produced by aRGCs at embryonic stages, although not anymore at postnatal stages.

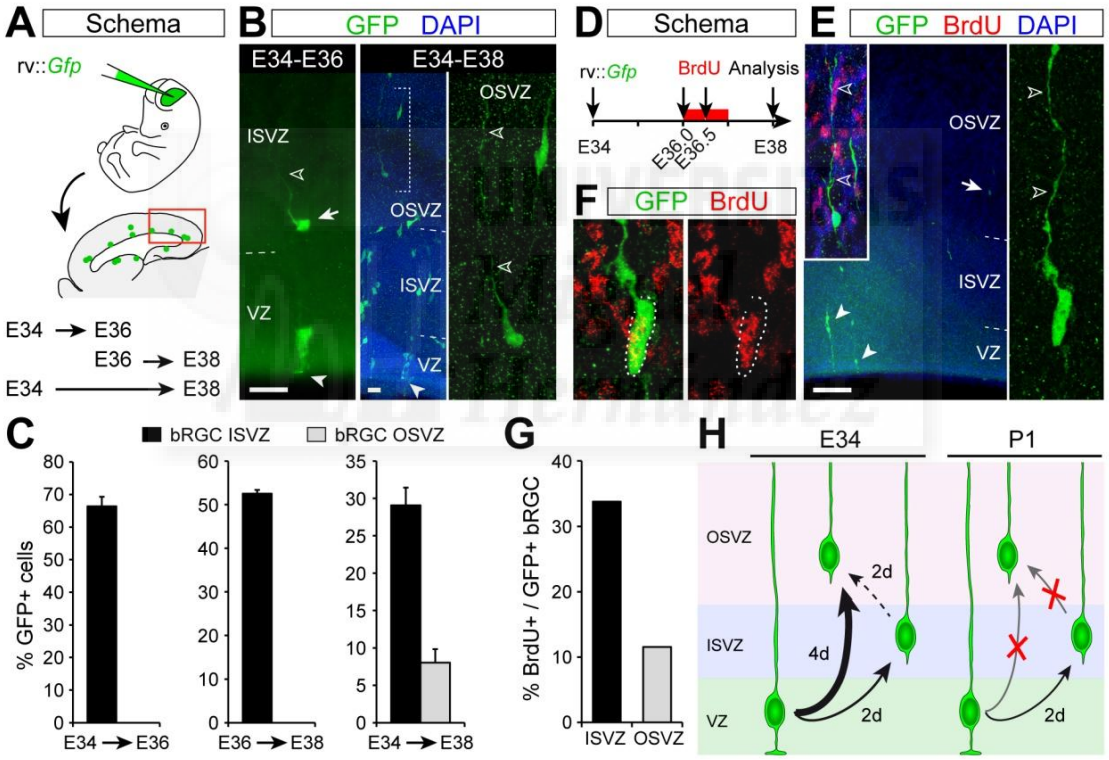

Figure 31. Embryonic aRGCs generate directly bRGCs for the OSVZ. (**A-C**) Ferret embryos received a ventricular injection of rv::*Gfp* at E34 or E36, and developed *in utero* until E36 or E38. (**B,C**) GFP+ bRGCs were found in OSVZ after 4 days of survival (E34-E38, detail), but only in ISVZ after 2 days (E34-36, arrow; *n* = 931 cells, 8 embryos; E36-38, *n* = 104 cells, 2 embryos; E34-38, *n* = 1,830 cells, 7 embryos). (**D-G**) VZ progenitors were labeled with rv::*Gfp* at E34, BrdU was administered two days later, and were analyzed at E38 (**E,F**). Arrow in (**E**) indicates bRGC magnified in inset. Very few GFP+ bRGCs in OSVZ contained BrdU (E, right; F,G) (*n* = 229 cells, 5 embryos), indicating that most were directly generated from VZ. In (**B,E**) solid arrowheads indicate aRGCs, open arrowheads indicate basal process of bRGCs. (**H**) At E34 aRGCs generate bRGCs that reach the ISVZ two days later (E36) and OSVZ four days later (E38). Few bRGCs in OSVZ are generated between E36 and E38 (likely from ISVZ), the majority being generated between E34 and E36 directly from VZ. Postnatally, aRGCs generate bRGCs for the ISVZ, but neither generates bRGCs for the OSVZ. Scale bars: B, 25 µm; E, 150 µm.

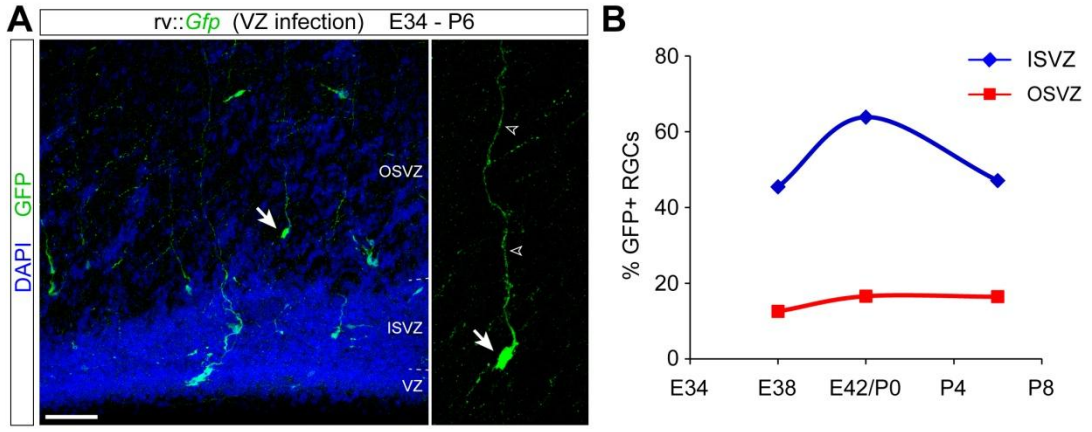

Figure 32. Long-time experiment for ventricular injection of rv::*Gfp* at E34. (**A-B**) Abundance of GFP+ bRGCs in ISVZ and OSVZ with respect to all RGCs, at the indicated ages after intraventricular injection of rv::*Gfp* at E34 (E38: *n* = 1,830 cells, 7 embryos; P0, *n* = 624 cells, 3 kits; P6, *n* = 5,240 cells, 2 kits). Note that embryonic VZ progenitors generate bRGCs that populate the postnatal OSVZ, in contrast to postnatal VZ progenitors which did not. Data are mean + S.E.M. Scale bars: 100 µm.

The lineage tracing between E34 and E38 allowed for several rounds of cell division, so we could not distinguish whether bRGCs in OSVZ had been generated in a single step directly from aRGCs at E34, or whether from E34 to E36 aRGCs generated bRGCs in ISVZ, and from E36 to E38 these divided to generate OSVZ bRGCs. To distinguish if bRGCs in OSVZ had been generated directly by aRGCs in VZ, or indirectly following division in ISVZ, we injected rv::*Gfp* at E34, administered BrdU at E36.0 and E36.5 to label cells cycling between E36 and E37 (S-phase ≈12 hr) (Reillo and Borrell, 2012), and analyzed at E38 (Fig. 31D). BrdU administration was interrupted at E37 to avoid labeling bRGCs that might have reached the OSVZ early, as they were cycling cells themselves. Only 11.5% of bRGCs in OSVZ contained BrdU (Fig. 31, E to G), indicating that the majority had been directly generated by aRGCs in VZ before E36. In addition, rv::*Gfp* infection of VZ at E34 labeled some IPCs in OSVZ at E38 (MP, Ki67+; 0.46±0.37% of GFP+ cells), unlike their null labeling at postnatal stages (Fig. 24). Hence aRGCs in the embryonic VZ produce bRGCs and IPCs that migrate through the ISVZ *en route* to the OSVZ, a process not occurring after birth (E42) in ferret cerebral cortex (Fig. 31H). Together, our results demonstrated that the OSVZ develops in two distinct phases: an early period of progenitor cell seeding from the VZ, and a later period of self-amplification independent from other germinal layers.

13. Generation of bRGCs is dynamic and involves self-consuming VZ divisions

To precisely define the embryonic period during which bRGCs are produced from the VZ, we monitored the developmental dynamics of their generation from aRGCs during embryonic development with rv::*Gfp* injections *in utero* in the telencephalic ventricle at various stages and performed 2-day cell lineage tracing analyses (Fig. 33A).

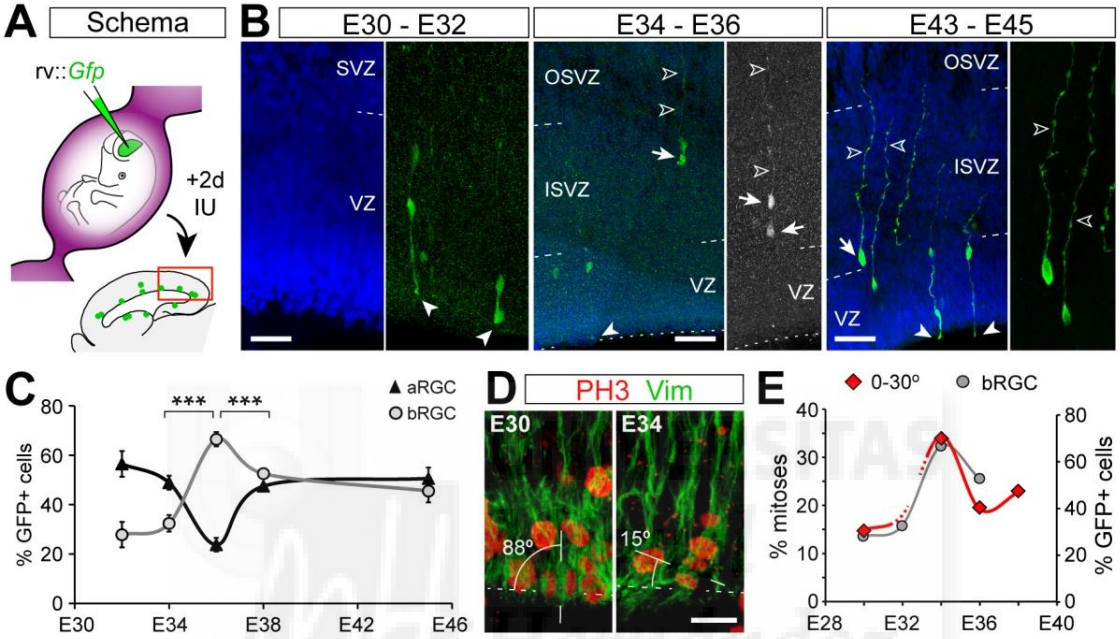

Figure 33. Transient peak of bRGC production from aRGCs at the onset of OSVZ. (**A-C**) Tracing of bRGC production from aRGCs along development. Ferret embryos aged E30, E32, E34, E36, and P1 kits received intraventricular injection of rv::*Gfp* and were analyzed 2 days later. (**B**) GFP labeling in embryos injected as indicated; solid arrowheads indicate ventricular end-feet of aRGCs, arrows indicate bRGCs, open arrowheads indicate basal process. (**C**) Abundance of GFP+ aRGCs and bRGCs at the indicated ages. Production of bRGCs peaked at E36, when aRGCs self-consumed (<50%); ***p<0.001, X^2-test; n = 170 cells, E32; 304 cells, E34; 931 cells, E36; 104 cells, E38; 1094 cells, E45; 2-8 embryos per group. (**D,E**) Orientation plane of VZ mitoses with respect to ventricular surface (dashed lines) (n = 91 cells, E30; 90 cells, E34; 124 cells, E36; 69 cells, E38; 2-8 embryos per group). Variation in horizontal mitoses (0-30°, red curve) was paralleled by bRGC production after rv::*Gfp* infection of VZ at those ages (grey curve). Scale bars: B, 40 µm (E32), 75 µm (E36, E45); D, 15 µm.

At all ages virtually all cells born from VZ (GFP+) were aRGCs or bRGCs (Fig. 33, B and C), but their proportions changed significantly along development. At E32 and E34, 47-56% of GFP+ cells were aRGCs, and only 29-34% bRGCs. Between E34 and E36 the production of bRGCs increased dramatically to represent 66% of GFP+ cells at E36. The transient peak of bRGC production between E34 and E36 was paralleled by the self-consumption of aRGCs, representing only 24% of GFP+ cells

(Fig. 33C). This situation lasted only two days, and by E38 and P1 the production of bRGCs was down to 53-45% of GFP+ cells, respectively, and aRGCs were 47-51% (Fig. 33).

Given the short survival time of our lineage experiments, and that the originally-infected cells were aRGCs, we interpreted changes in the percentage of GFP+ aRGC as changes in cell-fate decisions at the population level: self-amplification (>50% of GFP+ cells are aRGCs), self-renewal (50%) or consumption (<50% are aRGCs). Cell-fate decisions are known to co-vary with the angle at which aRGCs undergo mitosis, where vertical mitoses occur in symmetric self-amplifying divisions and horizontal mitoses occur in asymmetric divisions generating bRGCs (Shitamukai et al., 2011; LaMonica et al., 2013; Stahl et al., 2013; Xie et al., 2013; Gertz et al., 2014; Paridaen and Huttner, 2014).

In agreement with developmental dynamics of bRGC production, the proportion of horizontal mitoses in VZ, as revealed by PH3 stains, peaked transiently at E34 (indicating changes in mitotic activity), following a temporal dynamics parallel to their production of bRGCs, maximal by progenitors infected at E34 (Fig. 33, D and E; Fig. 34).

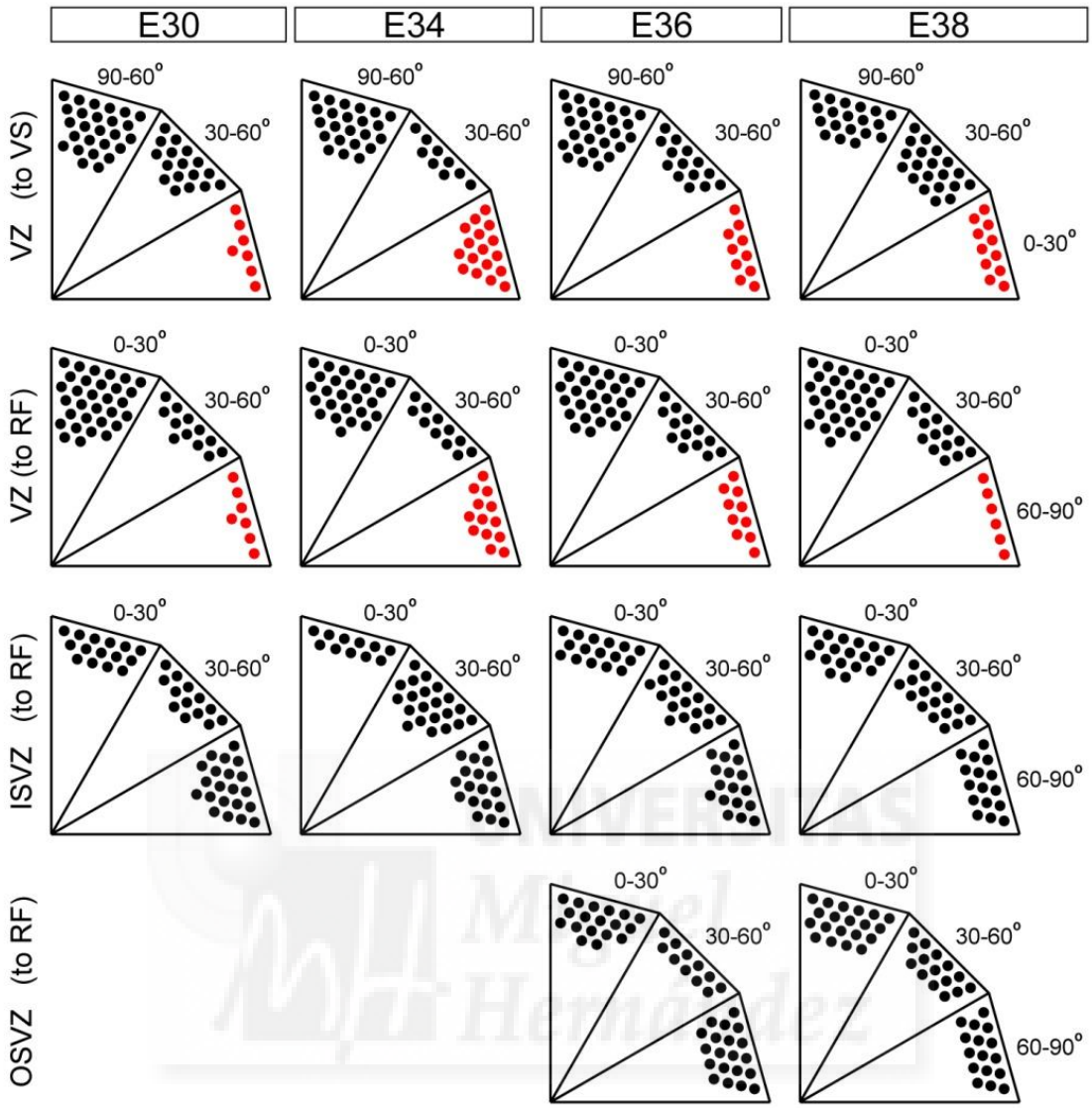

Figure 34. Transient increase of horizontal mitoses by VZ progenitors at E34. Distribution of orientations for apical mitoses in VZ with respect to the ventricular surface (VS) or Radial Fiber scaffold (RF), and for basal mitoses in ISVZ and OSVZ with respect to RF, across embryonic stages. Each dot represents 2% of mitoses (VZ: *n* = 91 cells, 8 embryos, E30; 90 cells, 2 embryos, E34; 124 cells, 2 embryos, E36; 69 cells, 3 embryos, E38. ISVZ: *n* = 128 cells, 8 embryos, E30; 40 cells, 2 embryos, E34; 96 cells, 2 embryos, E36; 81 cells, 3 embryos, E38. OSVZ: *n* = 49 cells, 2 embryos, E36; 61 cells, 3 embryos, E38). Horizontal mitoses (parallel to VZ or perpendicular to RF, labeled in red) in VZ doubled in abundance transiently at E34, coincident with the onset of bRGC peak production.

Our experiments so far demonstrated that aRGCs and bRGCs represent the vast majority of progenitor cells in the developing cerebral cortex of the gyrencephalic ferret, and that at early stages of cortical development aRGCs mostly undergo amplifying divisions, generating only a few bRGCs that begin accumulating in a nascent SVZ (Fig. 35). At E34, and for a brief time window, aRGCs change the orientation of their mitoses and generate massive amounts of bRGCs by self-consuming divisions. Many of these bRGCs migrate to the basal part of the SVZ and become founder cells of the emerging OSVZ. At E36-E38 the production of bRGCs from aRGCs decreases sharply, to continue decreasing gradually thereafter while ISVZ and OSVZ expand. At birth (onset of layer 2/3 neurogenesis) the OSVZ already follows a lineage completely independent from VZ and ISVZ, sustained by bRGC self-renewal and amplification, while the VZ continues to seed bRGCs to the ISVZ (Fig. 35).

Thus, bRGCs are generated in a burst between E34-36 by aRGCs in horizontal self-consuming divisions (Fig. 33C). This is an unprecedented mechanism of generating this important cell type involved in expansion and gyrification of the neocortex, which also highlights a peak of developmental vulnerability during 2 gestational days, as a failure to seed bRGCs into the OSVZ may never be corrected at later stages.

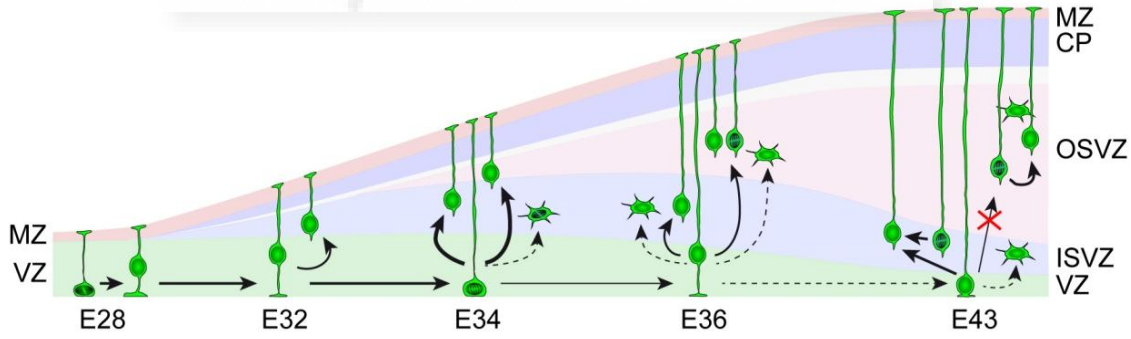

Figure 35. Different behaviors of the aRGCs during the development of the OSVZ. After an early period of self-renewal, aRGCs switch transiently to horizontal self-consuming divisions between E34 and E36, generating bRGCs massively. These early bRGCs become founder cells of the OSVZ, which later follow a lineage independent from VZ and ISVZ, sustained by bRGC self-amplification, while VZ continues to seed bRGCs to ISVZ.

14. Timing of the critical period for bRGC production and OSVZ generation depends on developmental variations of *Cdh1* and *Trnp1* expression

To identify candidate genes regulating the dynamics of bRGC production by aRGCs we searched for differential gene expression in VZ between three key stages: E30, E34 and P1. Using a ferret-specific microarray (Bruder et al., 2010) we identified 1,852 differentially-expressed genes (DEGs) between at least two stages (FDR <0.05, fold-change >2; Fig. 36A). Only 59 DEGs were found between E30-E34 (27 up-regulated, 32 down-regulated), whereas 1,822 genes changed between E34-P1 (871 up-regulated, 951 down-regulated; Fig. 36B, Tables 2 and 3, Annex).

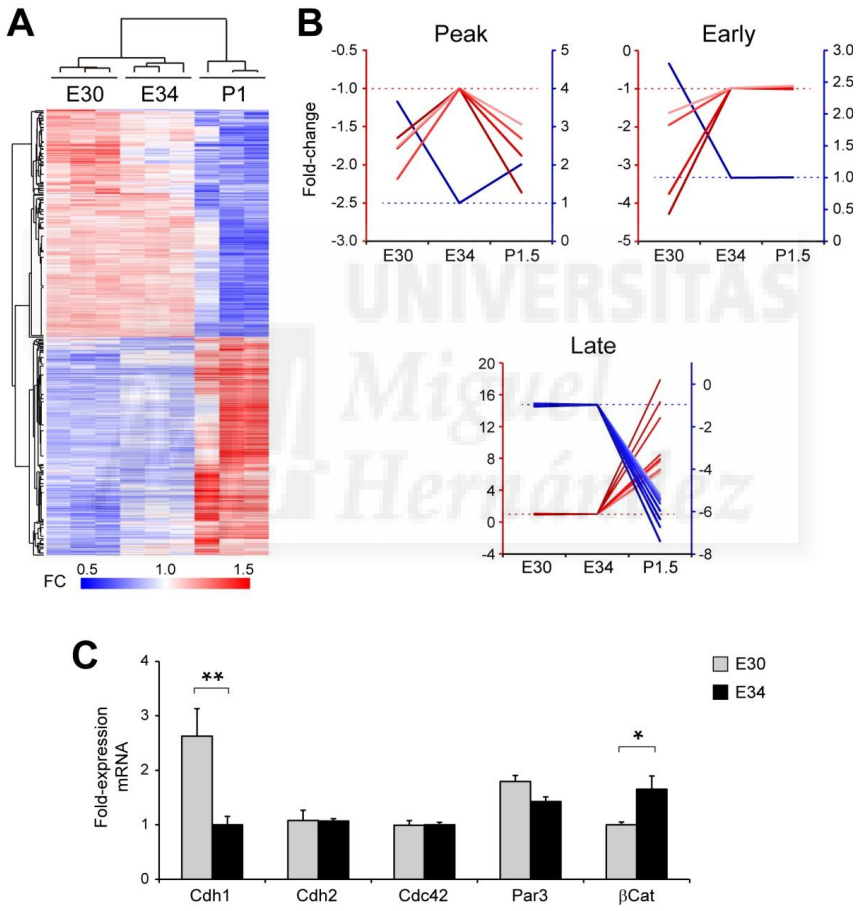

Figure 36. Differential gene expression in VZ across developmental stages. (**A**) Heatmap of unsupervised hierarchical clustering of gene probes differentially-expressed in VZ between E30, E34 and P1 (FC, fold-change with respect to average), and dendrogram of similarity between samples. Each lane is a biological replica. The vast majority of probes were differentially-expressed between embryonic and postnatal stages, but not between embryonic stages (Tables 2 and 3, Annex). (**B**) Examples of developmental expression trends of differentially-expressed gene probes. The vast majority of genes had late change profile (increase, red axis; decrease, blue axis), whereas much fewer had "Early" or "Peak" profiles. Red axes are for data represented in red, and blue axes for data in blue. (**C**) Quantitative RT-PCR data for candidate gene expression in VZ between E30 and E34 (mean + S.E.M.) demonstrating a >2.5-fold decrease in *Cdh1* expression, whereas *β-Cat* increased 1.6-fold and other apical complex protein genes remained unchanged.

Among the late-stage DEGs we identified *Trnp1*, a gene previously involved in bRGC generation in mouse (Stahl et al., 2013), but none of the early-stage DEGs seemed attractive candidates. Because production of bRGCs from aRGCs involves their delamination from the apical junction belt (Itoh et al., 2013; Borrell and Calegari, 2014; Taverna et al., 2014), we re-screened our early-stage samples by qRT-PCR to analyze adherens junction-related genes (Gotz and Huttner, 2005). *Cadherin1* (*Cdh1*) was the only candidate with lower mRNA levels at E34 compared to E30, consistent with increased RGC detachment from VZ (Fig. 33, A to C, Fig. 36C) (Itoh et al., 2013). To test the involvement of Cdh1 in bRGC production from aRGCs we performed *in utero* electroporation to express a dominant-negative Cdh1 at E30, which caused a 2.5-fold increase in bRGC abundance and a significant decrease in aRGCs (Fig. 37, D to F).

Conversely, electroporation of *Cdh1* at E34 was sufficient to abrogate the massive bRGC production normally occurring between E34 and E36, down to 33% of control embryos (Fig. 37F). Thus, reduced expression of Cdh1 is instrumental for the burst production of bRGCs destined for the OSVZ.

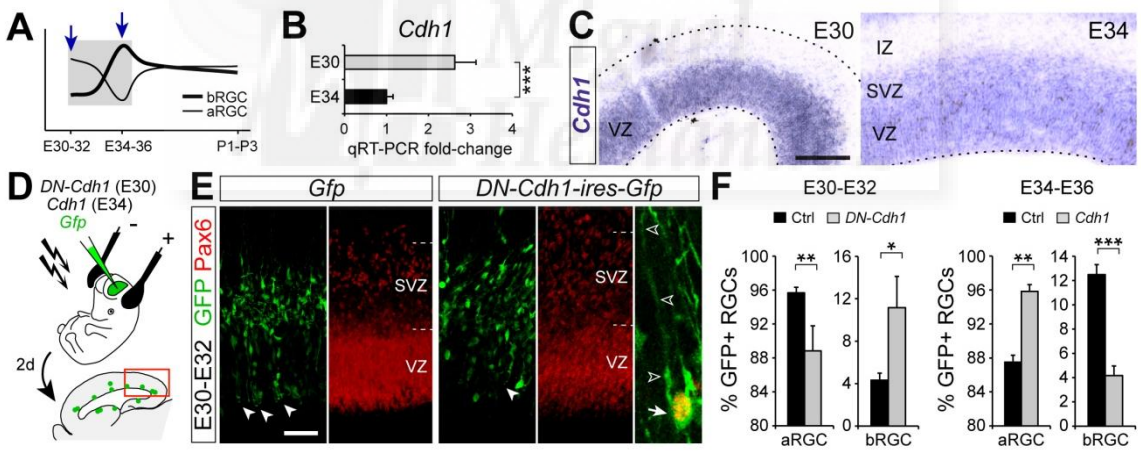

Figure 37. Timing of the critical period for bRGC production and OSVZ generation depends on developmental variations of *Cdh1* and *Trnp1* expression. Cdh1 is affecting to the early period of bRGCs generation. (**A**) Early period of bRGC generation from aRGCs. (**B,C**) Candidate gene screening by qRT-PCR revealed *Cdh1* as differentially-expressed in VZ between E30 and E34 (B), also shown by ISH (C). (**D-F**) Electroporation of *DN-Cdh1* from E30 to E32 increased bRGC production (GFP+/Pax6+ cells in SVZ) and decreased aRGCs, whereas overexpression of *Cdh1* from E34 to E36 had the opposite effect. Numbers of cells and embryos analyzed, Table 1, Annex; **p*<0.05, ***p*<0.01, ****p*<0.001; Scale bars: C, E, 75 µm.

Next we tested the involvement of Trnp1 in regulating bRGC production for the OSVZ at late stages. Down-regulation of *Trnp1* in mouse causes overproduction of bRGCs (Stahl et al., 2013), so our data suggested that low levels of endogenous *Trnp1* in VZ at E34 may favor bRGC production for the OSVZ, while high levels at later stages may close this critical period (Fig. 38, A to F). To test potential role of *Trnp1* in regulating bRGC production from aRGCs we used retroviruses to overexpress *Trnp1* in VZ of E34 embryos and analyzed the cellular output at E36 (Fig. 38D). GFP+ bRGCs were nearly half as abundant in *Trnp1* embryos compared to controls, concomitant with a 2-fold increase in aRGC abundance (Fig. 38, E and F). This demonstrated that low levels of endogenous *Trnp1* expression are important for bRGC production between E34 and E36. Conversely we tested the influence of high endogenous *Trnp1* levels on the low bRGC production at P1, by overexpressing a dominant-negative Trnp1 between P1 and P3 (Trnp1-GFP fusion protein; Fig. 38J) (Stahl et al., 2013). Compared to GFP-injected controls, expression of DN-Trnp1 increased significantly the production of bRGCs, while reducing aRGCs (Fig. 38F).

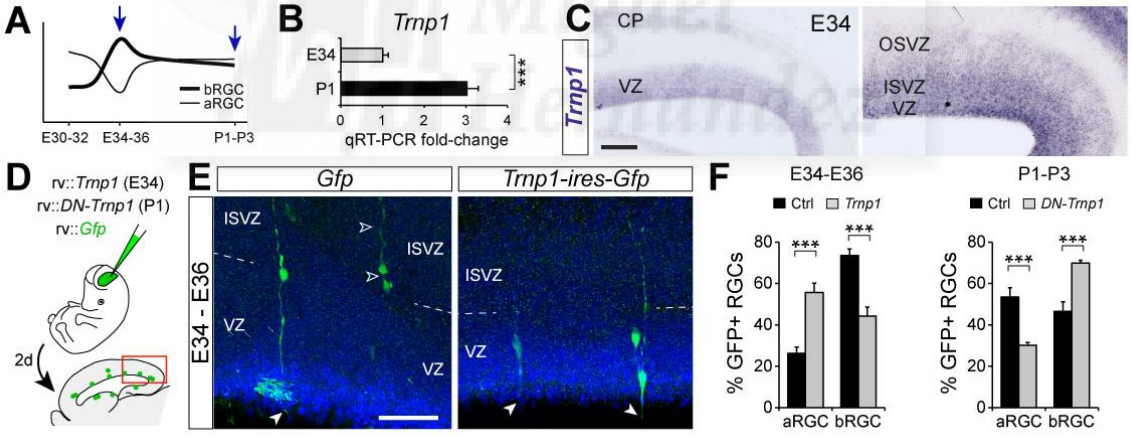

Figure 38. ***Trnp1* controls the later period of the bRGC production and OSVZ generation.** (**A-C**) Validation by qRT-PCR and ISH of differential expression of *Trnp1* between E34 and P1, as revealed by microarray analysis (Fig. 33). (**D-F**) Overexpression of *Trnp1* by retroviral delivery from E34 to E36 decreased bRGC production and increased aRGC abundance, whereas expression of dominant-negative (DN) *Trnp1* from P1 to P3 had the opposite effect. Numbers of cells and embryos analyzed, Table 1, Annex; **p*<0.05, ***p*<0.01, ****p*<0.001; Scale bars: B, 150 µm; E, 75 µm.

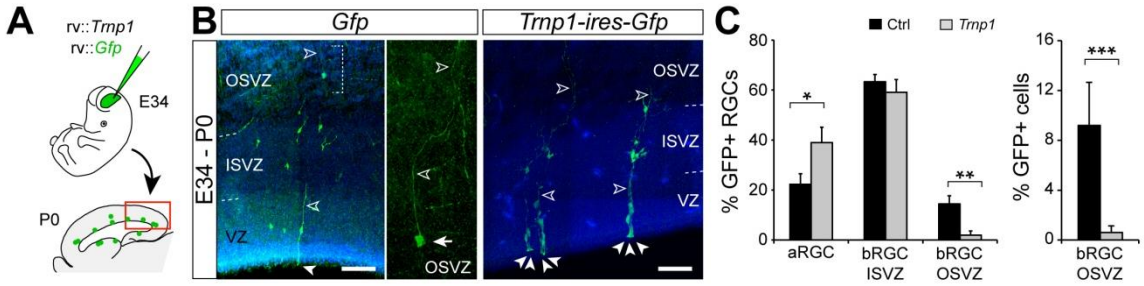

Figure 39. Long time experiment for overexpression of *Trnp1*. (**A-C**) Sustained overexpression of *Trnp1* from E34 to P0 by retroviral delivery dramatically blocked bRGC production for the OSVZ. Measures are relative to GFP+ RGCs, or all GFP+ cells in lineage. In all panels, solid arrowheads indicate apical end-feet of aRGCs, open arrowheads indicate basal fibers of bRGCs. Numbers of cells and embryos analyzed, Table 1, Annex; **p*<0.05, ***p*<0.01, ****p*<0.001; Scale bar: B, 75 µm.

To define if the above decrease in bRGC generation indeed affects seeding of the OSVZ, we overexpressed *Trnp1* in VZ cells at E34 followed by long-term survival until E42/P0 (Fig. 39A). The OSVZ of *Trnp1*-overexpressing ferrets was nearly devoid of GFP+ bRGCs, concomitant with a relative increase in aRGCs, but remarkably with no relative alteration of ISVZ (Fig. 39, B and C). This demonstrated that in our short-survival experiments many bRGCs observed in ISVZ were *en route* to the OSVZ and that the period between E34 and E36 is largely dedicated to the generation of bRGCs that will seed and found the OSVZ.

Taken together, these results demonstrated that the dynamic temporal regulation of *Cdh1* and *Trnp1* expression is both necessary and sufficient to control the variations in bRGC production from aRGCs during cortical development. Accordingly, high expression of either *Cdh1* or *Trnp1* is sufficient to limit bRGC production, whereas low expression of both genes simultaneously is necessary for the massive self-consumption of aRGCs to produce bRGCs, and thus for the critical period of OSVZ generation.

DISCUSSION

DISCUSSION

I. Radially-migrating pyramidal neurons: morphological aspects

Our findings indicate that pyramidal neurons can adopt several morphologies during their radial migration, mainly related to the branching or not of their leading process. We have observed a tendency to increase the leading process length with the number of branches, and that this is caused by a larger leading process tree whereas the length of the trunk does not change. Intriguingly, cells with more branches showed a reduced size of each individual branch, suggesting that the total leading process size of migrating cells may be limited. Regarding the potential role of leading process branching, our results suggest that it may allow cells to better explore their cellular environment and discriminate variations in guidance cues for directional migration.

We have observed a remarkable diversity of leading process morphologies among radially-migrating neurons, with a clear predominance of cells without branches or only one branch point. Intriguingly, the number of branches generated is not random, as in mouse we did not observe cells with more than two branch points, whereas in ferret cells exhibited up to three or more branch points, even if only in a few cases. A possible interpretation of these observations is that gyrencephalic species may develop more branches because they navigate along a larger territory. Due to the tangential expansion of the radial glia scaffold in ferret, migrating neurons may move in more directions that in mouse. Hence, elaborating multiple branches might enable a more reliable detection of attractant and repellent guidance cues, and side branches may be eliminated once the direction of movement has been selected.

It has been published that branches in the leading process of cortical interneurons form at wider angles when these enter the cortex and change from tangential to radial mode of migration, than when they migrate tangentially from the basal ganglia (Polleux et al., 2002; Ang et al., 2003; Martini et al., 2009; Marin et al., 2010; Valiente and Marin, 2010). We have found that these wide angles are equivalent to those in ferret pyramidal neurons with one branch point. Perhaps in the same way that interneurons increase this angle to drastically change their direction of migration (from tangential to radial), pyramidal neurons in ferret may also widen this angle to drastically switch direction of migration and cross from one radial fiber to another. These results suggest that migrating pyramidal neurons may generate several branches to explore more territory, and also that these cells produce more branches and broaden

the angle between primary branches to cover a wider sampling territory, thus being able to better decide the next direction of migration. Moreover, because the cerebral cortex in gyrencephalic species has a much greater surface area that in animals with a smooth cortex like mouse (Gotz and Huttner, 2005; Kriegstein et al., 2006; Reillo et al., 2011; Borrell and Calegari, 2014), the combination of making many branches and at wider angles may be important for migrating neurons in gyrencenphalic species to disperse over a rapidly increasing cortical surface area. Indeed, we found that more than 50% of migrating cortical excitatory neurons in mouse branch their leading process, a proportion that rises to 70% in gyrencephalic species. Hence radial migration with a branched leading process is more frequent in animals with a larger and more complex cerebral cortex. Taken together, our experiments in mouse and ferret indicate that branched radial migration is much more common than previously recognized, and further suggest that this may contribute to the tangential dispersion of radially-migrating neurons.

II. Branching: functional and evolutionary impact

Using time-lapse videomicroscopy we observed that migrating cells with a single leading process generate two branches as part of their normal cycle during radial migration. Contrary to previous reports (Noctor et al., 2001; Gupta et al., 2003; Weissman et al., 2003; Xie et al., 2003; Kriegstein and Noctor, 2004; Noctor et al., 2004; Xie 2006; Ohshima et al., 2007), cells with branched morphologies had the same migratory capacity and dynamics than non-branched cells. We propose that branching is a common mechanism for mammalian pyramidal neurons during their radial migration though the cortex. Branching is adopted during normal migration by pyramidal neurons, which at one time point they develop branches while continue moving. In addition, branched migration may allow migrating neurons to contact with two or more radial glia fibers simultaneously, as opposed to non-branched cells that would only migrate along a single radial fiber. Accordingly, in gyrencephalic species branching may allow a very prominent tangential dispersion of radially-migrating neurons (which does not occur in mouse), where one cell generated in a given point in VZ may switch between radial fibers multiple times along the migratory path to finally occupy a position laterally very distant from its site of origin (Fig. 10 and 23).

It has been proposed that the trajectory of radial glia fibers between their site of birth and their final location limits the tangential scatter of pyramidal neurons within the

cerebral cortex. Accordingly, gyrencephalic species display a prominent divergence between radial fiber trajectories, and new born neurons are greatly dispersed (Reillo et al., 2011). This divergence is created by the addition of radial fibers during development, which are being intercalated into the preexisting scaffold mainly due to the abundant presence of bRGCs in the OSVZ. Hence the combination of aRGCs and bRGCs provides radially migrating neurons with a fanned array of radial trajectories, enabling them to spread tangentially and to expand the CP laterally (Smart et al., 2002; Zecevic et al., 2005; Kriegstein et al., 2006; Reillo et al., 2011). Therefore, our results suggest that the combination of branched migration with a fanned array of radial fibers leads to the tangential expansion of the cerebral cortical mantle and, by extension, its eventual folding.

What are the mechanisms that underlie the abundant presence of bRGCs in the OSVZ, and the emergence of the OSVZ itself during cortical development? Our results demonstrate that the formation of the OSVZ depends on a critical period of massive bRGC generation from the VZ, after which the OSVZ follows a lineage completely independent from the other germinal layers (VZ and ISVZ), and thereon relies on the self-amplification of its progenitor cells for further expansion. These highly unexpected findings extend on the complexity of the mechanisms that regulate cortical development (Rakic, 2009; Lui et al., 2011; Borrell and Calegari, 2014; Borrell and Gotz, 2014). Importantly, we find that the critical period for bRGC seeding to form the OSVZ depends on the combined temporal regulation of *Cdh1* and *Trnp1* expression and function in VZ, two genes previously shown to play key roles in the balance between self-renewal and delamination of aRGCs in the mouse VZ (Noles and Chenn, 2007; Rasin et al., 2007; Pilz et al., 2013; Stahl et al., 2013). Given the relevance of the OSVZ in the development of gyrencephaly (Lui et al., 2011; Reillo and Borrell, 2012; Borrell and Calegari, 2014), the temporal regulation of *Trnp1* and *Cdh1* expression during embryogenesis may have evolved as a conserved mechanism generating cortical phenotypic diversity among mammals.

III. Origin and expansion of the OSVZ

Previous videomicroscopy analyses of slice cultures *in vitro* from primate cortex revealed a wide variety of progenitor cell types in the OSVZ and complex lineage transitions (Hansen et al., 2010; Betizeau et al., 2013). In this Thesis we have defined the cellular substrates for the developmental origin and expansion of the OSVZ *in vivo*. We show that the OSVZ is initiated by the accumulation of bRGCs generated directly by apical progenitors in the VZ. This seeding of cells from VZ to OSVZ is only transient, and eventually the lineage of OSVZ cells becomes completely independent from VZ. During this transition, seeded bRGCs become founders of the OSVZ, which then self-amplify to expand this layer to its remarkable size at late stages. This process is completely different in mouse, where basal progenitors rarely self-renew and the SVZ is formed by transient populations of progenitor cells, continuously seeded by the VZ and self-consumed shortly after (Haubensak et al., 2004; Miyata et al., 2004; Noctor et al., 2004; Attardo et al., 2008; Noctor et al., 2008). Intriguingly we find that the ISVZ shares features with both OSVZ and mouse SVZ, as it continuously receives bRGCs from the VZ with self-renewing capacity. Given that seeding of the OSVZ occurs only during a critical period, the rate of self-amplification of its constituent progenitor cells may become a major factor for its expansion and size. This notion is consistent with the dynamics of bRGC proliferation in the OSVZ of non-human primates, where this layer undergoes a massive increase in size during a period of rapid bRGC self-amplification (Betizeau et al., 2013). Expansive cell lineages are also frequent in the mouse LGE (Pilz et al., 2013), suggesting the evolutionary co-option of this developmental strategy (Borrell and Calegari, 2014).

IV. Diversity of progenitor cell lineages

Our experiments demonstrate for the first time that neocortical germinal layers follow independent lineages. After an embryonic period of frequent cell seeding from VZ to ISVZ and OSVZ, two lineages diverge with the OSVZ becoming completely independent, while VZ and ISVZ remain interrelated. This is consistent with previous videomicroscopy analyses in human and ferret, showing VZ-to-SVZ cell seeding but also SVZ progenitor self-renewal (Hansen et al., 2010; LaMonica et al., 2013; Gertz et al., 2014). As opposed to the single lineage in lissencephalic rodents, the multiple and complex lineages in gyrencephalic mammals allow for the independent regulation of

each individual lineage (Betizeau et al., 2013), providing a richer palette of developmental and evolutionary possibilities.

V. Critical periods in development, evolution and disease

The rate at which aRGCs in the VZ produce bRGCs is inversely proportional to their self-amplification (Kriegstein et al., 2006; Dehay and Kennedy, 2007; Fietz and Huttner, 2011). If building a large OSVZ required a prolonged period of intensive bRGC generation from aRGCs, this would significantly reduce the size of the VZ and of telencephalic vesicles (Rakic, 1988; Chenn and Walsh, 2002). In contrast, limiting the production of bRGCs to a critical period, combined with their subsequent self-amplification, is a sound strategy to limit VZ depletion while maximizing OSVZ size. This dual strategy may be particularly relevant in species with large brains and a very prominent OSVZ, especially primates. Similar to the abundant self-amplification of OSVZ bRGCs in the perinatal ferret, also in macaque monkey embryos the self-amplification of bRGCs becomes exceptionally prominent during a brief time window, immediately preceding OSVZ expansion and the massive generation of upper-layer neurons (Betizeau et al., 2013). Thus critical periods are emerging as a wide-spread strategy across phylogeny to regulate and maximize cellular resources during cortical development.

Generation of bRGCs from aRGCs is favored by oblique and horizontal mitoses, combined with the apical detachment of daughter cells (Shitamukai et al., 2011; LaMonica et al., 2013; Stahl et al., 2013; Gertz et al., 2014). The onset of the critical period for bRGC generation is bookmarked by a two-fold increase in horizontal mitoses and a significant decrease in *Cdh1* expression, a crucial component of apical adherens junctions previously implicated in regulating apical cell delamination, and whose expression is regulated by epithelial-mesenchymal transition (EMT) genes (Gotz and Huttner, 2005; Itoh et al., 2013). Likewise, the closure of the critical period is marked by an increase in *Trnp1* expression, which favors vertical mitoses and represses bRGC formation (Stahl et al., 2013). We show that the early blockade of *Cdh1* function in aRGCs induces a premature onset of the critical period, and the late down-regulation of *Trnp1* delays its closure, whereas up-regulation of one or the other blocks the onset of this period. Importantly, abrogation of the critical period by sustaining elevated *Trnp1* levels resulted in a severe reduction of OSVZ size in the long term. Hence the dynamic regulation of expression levels of both these genes may determine the timing and

abundance of OSVZ cell seeding versus VZ depletion. The evolution of molecular mechanisms controlling the spatial-temporal expression of critical period genes may have been key in the phylogenic emergence and expansion of the OSVZ, and ultimately in the extraordinary diversity of cortical phenotypes across mammals (Welker, 1990; Borrell and Calegari, 2014).

Our studies identify a completely novel mechanism of cortical development, whereby the formation of a germinal layer (OSVZ) depends on the seeding of founder progenitor cells during a brief critical period. Large amounts of founder bRGCs are generated during this period via the transient depletion of aRGCs from the VZ, after which the OSVZ lineage becomes independent from the other germinal layers and thereon relies on the self-amplification of its progenitor cells for further expansion. Limiting the VZ production of bRGCs to a brief period, combined with their subsequent self-amplification, allows limiting VZ depletion while maximizing OSVZ size, which is particularly beneficial in species with large brains and a prominent OSVZ, especially primates (Betizeau et al., 2013). The combined regulation of *Cdh1* and *Trnp1* levels along development is necessary and sufficient to control bRGC production from aRGCs (Itoh et al., 2013; Pilz et al., 2013; Stahl et al., 2013), which is key to precisely open and close the critical period of OSVZ formation. Critical periods are unique windows of opportunity during development, but also periods of high susceptibility to developmental perturbation or vulnerability to disease (LeBlanc and Fagiolini, 2011; Levelt and Hubener, 2012). Given the central role of the OSVZ in cortical development including neurogenesis and surface area expansion (Hansen et al., 2010; Reillo et al., 2011; Betizeau et al., 2013; Nonaka-Kinoshita et al., 2013) (and this study), the critical period of OSVZ seeding is a time of susceptibility to cortical disease, where subtle or acute defects may have magnified long-term consequences. Indeed, acute abrogation of cell proliferation in ferret embryos at the onset of the critical period leads to reduced OSVZ expansion and lissencephaly (Poluch and Juliano, 2013). Human cortical malformations due to acute insults during fetal development are rarely traced, but defects in VZ integrity, progenitor proliferation and precise gene expression regulation, are emerging as critical in malformations of cortical development (Nicholas et al., 2010; Yu et al., 2010; Barkovich et al., 2012; Cappello et al., 2013; Bae et al., 2014; Kielar et al., 2014). Defining the role of genes with transient and precisely regulated timing of expression during corticogenesis holds promise for future research, and understanding the molecular mechanisms for their precise spatial-temporal regulation becomes an

exciting challenge. In agreement, the identification in my thesis of the critical period for OSVZ formation allows better framing the mechanistic effect of mutations perturbing cerebral cortex development in humans.

CONCLUSIONS

CONCLUSIONS

1. Branched radial migration of pyramidal cells is very frequent in the developing cerebral cortex, particularly in gyrencephalic species.
2. Cells with a branched leading process are perfectly motile and display no migratory handicap compared to non-branched cells. Branching of the leading process is transient and cells alternate between branched and non-branched morphologies, including multi-order branching.
3. Radially migrating neurons with a highly branched leading process form wide angles between the primary branches, and the portion of this leading process parallel to radial glia fibers is small. This supports the notion that branching of the leading process may be used by radially-migrating neurons to change direction of migration, by switching between radial fibers and dispersing tangentially.
4. In the ferret cerebral cortex IPCs are a very small minority of basal progenitors, both in ISVZ and OSVZ, in contrast to the mouse SVZ.
5. aRGCs and bRGCs are very abundant in the ferret cerebral cortex and are molecularly diverse, including the expression of markers typical of neurogenic progenitors. bRGCs are the main population of progenitors in ISVZ and OSVZ.
6. VZ and ISVZ maintain a direct lineage relationship throughout cortical development, where bRGCs populating the ISVZ are continuously generated by aRGCs during the embryonic and postnatal periods.
7. The OSVZ follows a lineage completely independent from VZ and ISVZ during most of its development. Accordingly, only during a brief critical period of embryonic development aRGCs in VZ generate a burst of bRGCs destined to seed the OSVZ, and after this critical period the OSVZ does not receive more exogenous progenitor cells but grows exclusively by the self-amplification of its founder bRGCs.
8. *Cdh1* and *Trnp1* function are both necessary and sufficient to define the developmental time of onset, and duration, of the critical period for OSVZ formation, by regulating aRGCs to self-amplify versus to produce OSVZ bRGCs.

CONCLUSIONES

1. La generación de ramas durante la migración radial es un mecanismo muy común en el desarrollo de la corteza cerebral, particularmente en especies girencefálicas.
2. Las células que poseen ramas en su proceso de guía son perfectamente capaces de moverse del mismo modo que lo hacen las que no tienen ramas y no presentan problemas para la migración. Además, la generación de ramas es un proceso transitorio y las células alternan morfologías con ramas y sin ellas, incluyendo formación de múltiples ramas.
3. Las neuronas con un gran número de ramas que migran radialmente forman grandes ángulos en la primera ramificación, y presentan una menor proporción del proceso de guía paralelo a las fibras de glia radial en comparación con las que no poseen ramas. Esto sugiere que la generación de ramas en el proceso de guía podría ser utilizado por las neuronas que migran de forma radial para cambiar su dirección de migración, mediante el cambio de fibra radial y la dispersión tangencial.
4. Los IPCs en la corteza cerebral del hurón representan una pequeña minoría del total de progenitores basales, tanto en ISVZ como en OSVZ, en contra de lo que ocurre en la SVZ de ratón.
5. Las aRGCs y bRGCs son muy abundantes y molecularmente diversas en la corteza cerebral de los hurones, incluyendo la expresión de marcadores de progenitores típicamente neurogénicos. Las bRGCs son la principal población de progenitores de ISVZ y OSVZ
6. VZ e ISVZ mantienen una relación de linaje directa durante el desarrollo cortical, donde bRGCs localizadas en ISVZ son generadas continuamente por aRGCs tanto durante el periodo embrionario como postnatal.
7. La OSVZ sigue un linaje completamente independiente de VZ e ISVZ durante la mayor parte de su desarrollo. Sólo durante un corto periodo crítico del desarrollo embrionario las aRGCs de VZ generan masivamente bRGCs destinadas a sembrar la OSVZ, y tras este periodo crítico la OSVZ no recibe más células progenitoras de manera exógena, sino que crece exclusivamente por la auto-amplificación de las bRGCs fundadoras.

8. La función de *Cdh1* y *Trnp1* es necesaria y suficiente para definir, durante el desarrollo, el momento de inicio y la duración del periodo crítico de formación de la OSVZ, mediante la regulación entre la auto-amplificación de aRGCs y la producción de bRGCs para la OSVZ.

REFERENCES

Adams NC, Tomoda T, Cooper M, Dietz G, Hatten ME (2002) Mice that lack astrotactin have slowed neuronal migration. Development 129:965-972.

Aguzzi A, Barres B, Bennett M (2013) Microglia: scapegoat, saboteur, or something else? Science 339:156-161.

Anderson SA, Eisenstat DD, Shi L, Rubenstein JL (1997) Interneuron migration from basal forebrain to neocortex: dependence on Dlx genes. Science 278:474-476.

Anderson SA, Kaznowski CE, Horn C, Rubenstein JL, McConnell SK (2002) Distinct origins of neocortical projection neurons and interneurons in vivo. Cereb Cortex 12:702-709.

Anderson SA, Marin O, Horn C, Jennings K, Rubenstein JL (2001) Distinct cortical migrations from the medial and lateral ganglionic eminences. Development 128:353-363.

Ang ES, Jr., Haydar TF, Gluncic V, Rakic P (2003) Four-dimensional migratory coordinates of GABAergic interneurons in the developing mouse cortex. The Journal of neuroscience : the official journal of the Society for Neuroscience 23:5805-5815.

Anton ES, Kreidberg JA, Rakic P (1999) Distinct functions of alpha3 and alpha(v) integrin receptors in neuronal migration and laminar organization of the cerebral cortex. Neuron 22:277-289.

Anton ES, Marchionni MA, Lee KF, Rakic P (1997) Role of GGF/neuregulin signaling in interactions between migrating neurons and radial glia in the developing cerebral cortex. Development 124:3501-3510.

Antonopoulos J, Pappas I, Parnavelas J (1997) Activation of the GABAA receptor inhibits the proliferative effects of bFGF in cortical progenitor cells. Eur J Neurosci 9:291-298.

Arai Y, Pulvers JN, Haffner C, Schilling B, Nusslein I, Calegari F, Huttner WB (2011) Neural stem and progenitor cells shorten S-phase on commitment to neuron production. Nat Commun 2:154.

Ascoli GA, Alonso-Nanclares L, Anderson SA, Barrionuevo G, Benavides-Piccione R, Burkhalter A, Buzsaki G, Cauli B, Defelipe J, Fairen A, Feldmeyer D, Fishell G, Fregnac Y, Freund TF, Gardner D, Gardner EP, Goldberg JH, Helmstaedter M, Hestrin S, Karube F, Kisvarday ZF, Lambolez B, Lewis DA, Marin O, Markram H, Munoz A, Packer A, Petersen CC, Rockland KS, Rossier J, Rudy B, Somogyi P, Staiger JF, Tamas G, Thomson AM, Toledo-Rodriguez M, Wang Y, West DC, Yuste R (2008) Petilla terminology: nomenclature of features of GABAergic interneurons of the cerebral cortex. Nat Rev Neurosci 9:557-568.

Attardo A, Calegari F, Haubensak W, Wilsch-Brauninger M, Huttner WB (2008) Live imaging at the onset of cortical neurogenesis reveals differential appearance of the neuronal phenotype in apical versus basal progenitor progeny. PLoS One 3:e2388.

Ayoub AE, Oh S, Xie Y, Leng J, Cotney J, Dominguez MH, Noonan JP, Rakic P (2011) Transcriptional programs in transient embryonic zones of the cerebral cortex defined by high-resolution mRNA sequencing. Proc Natl Acad Sci U S A 108:14950-14955.

Bacon Ga (1996) Local circuit neurons in the medial prefrontal cortex (areas 24a,b,c, 25 and 32) in the monkey: I. Cell morphology and morphometrics. J Comp Neurol 364:567-608.

Bae BI, Tietjen I, Atabay KD, Evrony GD, Johnson MB, Asare E, Wang PP, Murayama AY, Im K, Lisgo SN, Overman L, Sestan N, Chang BS, Barkovich AJ, Grant PE, Topcu M, Politsky J, Okano H, Piao X, Walsh CA (2014) Evolutionarily

dynamic alternative splicing of GPR56 regulates regional cerebral cortical patterning. Science 343:764-768.

Bar IG, AM. (2000) Evolution of cortical lamination: the reelin/Dab1 pathway. Novartis Found Symp 228.

Barkovich AJ, Guerrini R, Kuzniecky RI, Jackson GD, Dobyns WB (2012) A developmental and genetic classification for malformations of cortical development: update 2012. Brain 135:1348-1369.

Bayatti N, Moss JA, Sun L, Ambrose P, Ward JF, Lindsay S, Clowry GJ (2008) A molecular neuroanatomical study of the developing human neocortex from 8 to 17 postconceptional weeks revealing the early differentiation of the subplate and subventricular zone. Cereb Cortex 18:1536-1548.

Bellion A, Baudoin JP, Alvarez C, Bornens M, Metin C (2005) Nucleokinesis in tangentially migrating neurons comprises two alternating phases: forward migration of the Golgi/centrosome associated with centrosome splitting and myosin contraction at the rear. The Journal of neuroscience : the official journal of the Society for Neuroscience 25:5691-5699.

Bentivoglio M, Mazzarello P (1999) The history of radial glia. Brain Res Bul 49:305-315.

Betizeau M, Cortay V, Patti D, Pfister S, Gautier E, Bellemin-Menard A, Afanassieff M, Huissoud C, Douglas RJ, Kennedy H, Dehay C (2013) Precursor diversity and complexity of lineage relationships in the outer subventricular zone of the primate. Neuron 80:442-457.

Borrell V (2010) In vivo gene delivery to the postnatal ferret cerebral cortex by DNA electroporation. J Neurosci Methods 186:186-195.

Borrell V, Calegari F (2014) Mechanisms of brain evolution: Regulation of neural progenitor cell diversity and cell cycle length. Neurosci Res.

Borrell V, Callaway EM (2002) Reorganization of exuberant axonal arbors contributes to the development of laminar specificity in ferret visual cortex. The Journal of neuroscience : the official journal of the Society for Neuroscience 22:6682-6695.

Borrell V, Gotz M (2014) Role of radial glial cells in cerebral cortex folding. Curr Opin Neurobiol 27C:39-46.

Borrell V, Kaspar BK, Gage FH, Callaway EM (2006) In vivo evidence for radial migration of neurons by long-distance somal translocation in the developing ferret visual cortex. Cereb Cortex 16:1571-1583.

Borrell V, Reillo I (2012) Emerging roles of neural stem cells in cerebral cortex development and evolution. Dev Neurobiol 72:955-971.

Brittis PA, Meiri K, Dent E, Silver J (1995) The earliest patterns of neuronal differentiation and migration in the mammalian central nervous system. Exp Neurol 134:1-12.

Brodmann K (ed.) (1909) Localization in the Cerebral Cortex. London: Imperial College Press.

Bruder CE, Yao S, Larson F, Camp JV, Tapp R, McBrayer A, Powers N, Granda WV, Jonsson CB (2010) Transcriptome sequencing and development of an expression microarray platform for the domestic ferret. BMC Genomics 11:251.

Bulfone A, Wang F, Hevner R, Anderson S, Cutforth T, Chen S, Meneses J, Pedersen R, Axel R, Rubenstein JL (1998) An olfactory sensory map develops in the absence of normal projection neurons or GABAergic interneurons. Neuron 21:1273-1282.

Bystron I, Blakemore C, Rakic P (2008) Development of the human cerebral cortex: Boulder Committee revisited. Nat Rev Neurosci 9:110-122.

Bystron I, Rakic P, Molnar Z, Blakemore C (2006) The first neurons of the human cerebral cortex. Nat Neurosci 9:880-886.

Calegari F, Haubensak W, Haffner C, Huttner W (2005) Selective lengthening of the cell cycle in the neurogenic subpopulation of neural progenitor cells during mouse brain development. J Neurosci 25:6533-6538.

Calegari F, Huttner W (2003) An inhibition of cyclin-dependent kinases that lengthens, but does not arrest, neuroepithelial cell cycle induces premature neurogenesis. J Cell Sci 116:4947-4955.

Callaway EM (1998a) Local circuits in primary visual cortex of the macaque monkey. Annu Rev Neurosci 21:47-74.

Callaway EM (1998b) Prenatal development of layer-specific local circuits in primary visual cortex of the macaque monkey. The Journal of neuroscience : the official journal of the Society for Neuroscience 18:1505-1527.

Camp JV, Svensson TL, McBrayer A, Jonsson CB, Liljestrom P, Bruder CE (2012) De-novo transcriptome sequencing of a normalized cDNA pool from influenza infected ferrets. PLoS One 7:e37104.

Campbell K, Gotz M (2002) Radial glia: multi-purpose cells for vertebrate brain development. Trends Neurosci 25:235-238.

Cappello S, Gray MJ, Badouel C, Lange S, Einsiedler M, Srour M, Chitayat D, Hamdan FF, Jenkins ZA, Morgan T, Preitner N, Uster T, Thomas J, Shannon P, Morrison V, Di Donato N, Van Maldergem L, Neuhann T, Newbury-Ecob R, Swinkells M, Terhal P, Wilson LC, Zwijnenburg PJ, Sutherland-Smith AJ, Black MA, Markie D, Michaud JL, Simpson MA, Mansour S, McNeill H, Gotz M, Robertson SP (2013) Mutations in genes encoding the cadherin receptor-ligand pair DCHS1 and FAT4 disrupt cerebral cortical development. Nat Genet 45:1300-1308.

Caviness VS, Jr. (1982) Neocortical histogenesis in normal and reeler mice: a developmental study based upon [3H]thymidine autoradiography. Brain Res 256:293-302.

Caviness VS, Jr., Takahashi T, Nowakowski RS (1995) Numbers, time and neocortical neuronogenesis: a general developmental and evolutionary model. Trends Neurosci 18:379-383.

Charvet C, Darlington R, BL. F (2013) Variation in human brains may facilitate evolutionary change toward a limited range of phenotypes. Brain Behav Evol 81:74-85.

Chen H, Pistollato F, Hoeppner D, Ni H, McKay R, Panchision D (2007) Oxygen tension regulates survival and fate of mouse central nervous system precursors at multiple levels. Stem Cells Sep;25:2291-2301.

Chenn A, McConnell SK (1995) Cleavage orientation and the asymmetric inheritance of Notch1 immunoreactivity in mammalian neurogenesis. Cell 82:631-641.

Chenn A, Walsh CA (2002) Regulation of cerebral cortical size by control of cell cycle exit in neural precursors. Science 297:365-369.

Choi BH, Lapham LW (1978) Radial glia in the human fetal cerebrum: a combined Golgi, immunofluorescent and electron microscopic study. Brain Res 148:295-311.

Cina CM, K. Theis, M. Willecke, K. Bechberger, JF. Naus, CC. (2009) Involvement of the cytoplasmic C-terminal domain of connexin43 in neuronal migration. J Neurosci 29:2009-2021.

Cobos IP, L. Martínez, S. (2001) The avian telencephalic subpallium originates inhibitory neurons that invade tangentially the pallium (dorsal ventricular ridge and cortical areas). Dev Biol 239:30-45.

Cooper (2013) Cell biology in neuroscience: mechanisms of cell migration in the nervous system. J Cell Biol 202:725-734.

Cunningham CL, Martinez-Cerdeno V, Noctor SC (2013) Microglia regulate the number of neural precursor cells in the developing cerebral cortex. The Journal of neuroscience : the official journal of the Society for Neuroscience 33:4216-4233.

Davalos D, Grutzendler J, Yang G, Kim J, Zuo Y, Jung S, Littman D, Dustin M, Gan W (2005) ATP mediates rapid microglial response to local brain injury in vivo. Nat Neurosci 8:752-758.

De Carlos JA, O'Leary DD (1992) Growth and targeting of subplate axons and establishment of major cortical pathways. The Journal of neuroscience : the official journal of the Society for Neuroscience 12:1194-1211.

deAzevedo LC, Fallet C, Moura-Neto V, Daumas-Duport C, Hedin-Pereira C, Lent R (2003) Cortical radial glial cells in human fetuses: depth-correlated transformation into astrocytes. J Neurobiol 55:288-298.

DeFelipe J, Alonso-Nanclares L, Arellano J (2002) Microstructure of the neocortex: comparative aspects. J Neurocytol Mar-Jun;31:299-316.

Dehay C, Giroud P, Berland M, Smart I, Kennedy H (1993) Modulation of the cell cycle contributes to the parcellation of the primate visual cortex. Nature 366:464-466.

Dehay C, Kennedy H (2007) Cell-cycle control and cortical development. Nat Rev Neurosci 8:438-450.

Dehay C, Savatier P, Cortay V, Kennedy H (2001) Cell-cycle kinetics of neocortical precursors are influenced by embryonic thalamic axons. The Journal of neuroscience : the official journal of the Society for Neuroscience 21:201-214.

Dhavan RT, LH. (2001) A decade of CDK5. Nat Rev Mol Cell Biol 2:749-759.

Douglas RM, KA. (2004) Neuronal circuits of the neocortex. Annu Rev Neurosci 27:419-451.

Dziegielewska K, Ek J, Habgood M, Saunders N (2001) Development of the choroid plexus. Microsc Res Tech 52:2-5.

Eastwood SL, Harrison PJ (2003) Interstitial white matter neurons express less reelin and are abnormally distributed in schizophrenia: towards an integration of molecular and morphologic aspects of the neurodevelopmental hypothesis. Mol Psychiatry 8:821-831.

Edmondson JC, Liem RK, Kuster JE, Hatten ME (1988) Astrotactin: a novel neuronal cell surface antigen that mediates neuron-astroglial interactions in cerebellar microcultures. J Cell Biol 106:505-517.

Elias LA, Wang DD, Kriegstein AR (2007) Gap junction adhesion is necessary for radial migration in the neocortex. Nature 448:901-907.

Emery B (2010) Regulation of Oligodendrocyte Differentiation and Myelination. Science.

Encinas JL, Garcia-Cabezas MA, Barkovich J, Fontecha CG, Peiro JL, Soto GM, Borrell V, Reillo I, Lopez-Santamaria M, Tovar JA, Farmer DL (2011) Maldevelopment of the cerebral cortex in the surgically induced model of myelomeningocele: implications for fetal neurosurgery. J Pediatr Surg 46:713-722.

Engel AK, Muller CM (1989) Postnatal development of vimentin-immunoreactive radial glial cells in the primary visual cortex of the cat. J Neurocytol 18:437-450.

Englund C, Fink A, Lau C, Pham D, Daza RA, Bulfone A, Kowalczyk T, Hevner RF (2005) Pax6, Tbr2, and Tbr1 are expressed sequentially by radial glia, intermediate progenitor cells, and postmitotic neurons in developing neocortex. The Journal of neuroscience : the official journal of the Society for Neuroscience 25:247-251.

Epstein DJ (2012) Regulation of thalamic development by sonic hedgehog. Front Neurosci 6:57.

Estivill-Torrus G, Pearson Hv, Heyningen V, Price D, Rashbass P (2002) Pax6 is required to regulate the cell cycle and the rate of progression from symmetrical to asymmetrical division in mammalian cortical progenitors. Development 129:455-466.

Fang Y, Rowe T, Leon AJ, Banner D, Danesh A, Xu L, Ran L, Bosinger SE, Guan Y, Chen H, Cameron CC, Cameron MJ, Kelvin DJ (2010) Molecular characterization of in vivo adjuvant activity in ferrets vaccinated against influenza virus. J Virol 84:8369-8388.

Fernandez C, Tatard V, Bertrand N, Dahmane N (2010) Differential modulation of Sonic-hedgehog-induced cerebellar granule cell precursor proliferation by the IGF signaling network. Dev Neurosci 32:59-70.

Fietz SA, Huttner WB (2011) Cortical progenitor expansion, self-renewal and neurogenesis-a polarized perspective. Curr Opin Neurobiol 21:23-35.

Fietz SA, Kelava I, Vogt J, Wilsch-Brauninger M, Stenzel D, Fish JL, Corbeil D, Riehn A, Distler W, Nitsch R, Huttner WB (2010) OSVZ progenitors of human and ferret neocortex are epithelial-like and expand by integrin signaling. Nat Neurosci 13:690-699.

Fietz SA, Lachmann R, Brandl H, Kircher M, Samusik N, Schroder R, Lakshmanaperumal N, Henry I, Vogt J, Riehn A, Distler W, Nitsch R, Enard W, Paabo S, Huttner WB (2012) Transcriptomes of germinal zones of human and mouse fetal neocortex suggest a role of extracellular matrix in progenitor self-renewal. Proc Natl Acad Sci U S A.

Finlay BL, Darlington RB (1995) Linked regularities in the development and evolution of mammalian brains. Science 268:1578-1584.

Fish JL, Dehay C, Kennedy H, Huttner WB (2008) Making bigger brains-the evolution of neural-progenitor-cell division. J Cell Sci 121:2783-2793.

Fishell GH, ME. (1991) Astrotactin provides a receptor system for CNS neuronal migration. Development 113:755-765.

Fiszman M, Borodinsky L, Neale J (1999) GABA induces proliferation of immature cerebellar granule cells grown in vitro. Brain Res Dev Brain Res 115:1-8.

Flames N, Long JE, Garratt AN, Fischer TM, Gassmann M, Birchmeier C, Lai C, Rubenstein JL, Marin O (2004) Short- and long-range attraction of cortical GABAergic interneurons by neuregulin-1. Neuron 44:251-261.

Florio M, Huttner WB (2014) Neural progenitors, neurogenesis and the evolution of the neocortex. Development 141:2182-2194.

Folsom TD, Fatemi SH (2013) The involvement of Reelin in neurodevelopmental disorders. Neuropharmacology 68:122-135.

Francis F, Meyer G, Fallet-Bianco C, Moreno S, Kappeler C, Socorro A, Tuy F, Beldjord C, Chelly J (2006) Human disorders of cortical development: from past to present. Eur J Neurosci 23:877-893.

Gal JS, Morozov YM, Ayoub AE, Chatterjee M, Rakic P, Haydar TF (2006) Molecular and morphological heterogeneity of neural precursors in the mouse neocortical proliferative zones. The Journal of neuroscience : the official journal of the Society for Neuroscience 26:1045-1056.

Gallo V, Deneen B (2014) Glial development: the crossroads of regeneration and repair in the CNS. Neuron 83:283-308.

Garcia-Moreno F, Vasistha NA, Trevia N, Bourne JA, Molnar Z (2012) Compartmentalization of cerebral cortical germinal zones in a lissencephalic primate and gyrencephalic rodent. Cereb Cortex 22:482-492.

Garey LJ (2006) Brodmann´s localization in the cerebral cortex. London: Springer Third Ed. Edition.

Gertz CC, Lui JH, LaMonica BE, Wang X, Kriegstein AR (2014) Diverse behaviors of outer radial glia in developing ferret and human cortex. The Journal of neuroscience : the official journal of the Society for Neuroscience 34:2559-2570.

Geyer MA, Swerdlow NR, Lehmann-Masten V, Teschendorf HJ, Traut M, Gross G (1999) Effects of LU-111995 in three models of disrupted prepulse

inhibition in rats. . J Pharmacol Exp 290:716-724.

Gilmore EC, Ohshima T, Goffinet AM, Kulkarni AB, Herrup K (1998) Cyclin-dependent kinase 5-deficient mice demonstrate novel developmental arrest in cerebral cortex. The Journal of neuroscience : the official journal of the Society for Neuroscience 18:6370-6377.

Gotz M, Hartfuss E, Malatesta P (2002) Radial glial cells as neuronal precursors: a new perspective on the correlation of morphology and lineage restriction in the developing cerebral cortex of mice. Brain Res Bull 57:777-788.

Gotz M, Huttner WB (2005) The cell biology of neurogenesis. Nature Rev Mol Cell Biol 6:777-788.

Gotz M, Stoykova A, Gruss P (1998) Pax6 controls radial glia differentiation in the cerebral cortex. Neuron 21:1031-1044.

Gupta A, Sanada K, Miyamoto DT, Rovelstad S, Nadarajah B, Pearlman AL, Brunstrom J, Tsai LH (2003) Layering defect in p35 deficiency is linked to improper neuronal-glial interaction in radial migration. Nat Neurosci 6:1284-1291.

Haberly LP, JL. (1978) Association and commissural fiber systems of the olfactory cortex of the rat. J Comp Neurol 178:711-740.

Hansen DV, Lui JH, Parker PR, Kriegstein AR (2010) Neurogenic radial glia in the outer subventricular zone of human neocortex. Nature 464:554-561.

Hartfuss E, Forster E, Bock HH, Hack MA, Leprince P, Luque JM, Herz J, Frotscher M, Gotz M (2003) Reelin signaling directly affects radial glia morphology and biochemical maturation. Development 130:4597-4609.

Hatanaka Y, Hisanaga S, Heizmann CW, Murakami F (2004) Distinct migratory behavior of early- and late-born neurons derived from the cortical ventricular zone. J Comp Neurol 479:1-14.

Haubensak W, Attardo A, Denk W, Huttner WB (2004) Neurons arise in the basal neuroepithelium of the early mammalian telencephalon: a major site of neurogenesis. Proc Natl Acad Sci U S A 101:3196-3201.

Haydar TF, Kuan CY, Flavell RA, Rakic P (1999) The role of cell death in regulating the size and shape of the mammalian forebrain. Cereb Cortex 9:621-626.

Haydar TF, Nowakowski RS, Yarowsky PJ, Krueger BK (2000a) Role of founder cell deficit and delayed neuronogenesis in microencephaly of the trisomy 16 mouse.

The Journal of neuroscience : the official journal of the Society for Neuroscience 20:4156-4164.

Haydar TF, Wang F, Schwartz ML, Rakic P (2000b) Differential modulation of proliferation in the neocortical ventricular and subventricular zones. The Journal of neuroscience : the official journal of the Society for Neuroscience 20:5764-5774.

Herculano-Houzel S (2009) The human brain in numbers: a linearly scaled-up primate brain. Front Hum Neurosci 3:31.

Herculano-Houzel S (2012) Neuronal scaling rules for primate brains: the primate advantage. Prog Brain Res 195:325-340.

Herculano-Houzel S, Mota B, Lent R (2006) Cellular scaling rules for rodent brains. Proc Natl Acad Sci U S A Aug 8:12138-12143.

Hilgetag C, Barbas H (2006a) Role of mechanical factors in the morphology of the primate cerebral cortex. PLoS Comput Biol 3:2.

Hilgetag CC, Barbas H (2006b) Role of mechanical factors in the morphology of the primate cerebral cortex. PLoS Comput Biol 2:e22.

Hirota Y, Ohshima T, Kaneko N, Ikeda M, Iwasato T, Kulkarni AB, Mikoshiba K, Okano H, Sawamoto K (2007) Cyclin-dependent kinase 5 is required for control of neuroblast migration in the postnatal subventricular zone. The Journal of neuroscience : the official journal of the Society for Neuroscience 27:12829-12838.

Howard B, Chen Y, Zecevic N (2006) Cortical progenitor cells in the developing human telencephalon. Glia 53:57-66.

Humphrey (1939) Studies of the Vertebrate Telencephlaon. Journal of Comparative Neurobiology 71:121-213.

Huttner W, Brand M (1997) Asymmetric division and polarity of neuroepithelial cells. Curr Opin Neurobiol 7:29-39.

Huttner WB, Kosodo Y (2005) Symmetric versus asymmetric cell division during neurogenesis in the developing vertebrate central nervous system. Curr Opin Cell Biol 17:648-657.

Insausti (1993) Comparative anatomy of the entorhinal cortex and hippocampus in mammals. Hippocampus 3:19-26.

Itoh Y, Moriyama Y, Hasegawa T, Endo TA, Toyoda T, Gotoh Y (2013) Scratch regulates neuronal migration onset via an epithelial-mesenchymal transition-like mechanism. Nat Neurosci 16:416-425.

Iwata T, Hevner RF (2009) Fibroblast growth factor signaling in development of the cerebral cortex. Dev Growth Differ 51:299-323.

Jackson CA, Peduzzi JD, Hickey TL (1989) Visual cortex development in the ferret. I. Genesis and migration of visual cortical neurons. J Neurosci 9:1242-1253.

Jacobshagen M, Niquille M, Chaumont-Dubel S, Marin P, Dayer A (2014) The serotonin 6 receptor controls neuronal migration during corticogenesis via a ligand-independent Cdk5-dependent mechanism. Development 141:3370-3377.

Jakovcevski I, Mayer N, Zecevic N (2011) Multiple origins of human neocortical interneurons are supported by distinct expression of transcription factors. Cereb Cortex 21:1771-1782.

Jarvis E, Güntürkün O, Bruce L, Csillag A, Karten H, Kuenzel W, Medina L, Paxinos G, Perkel D, Shimizu T, Striedter G, Wild J, Ball G, Dugas-Ford J, Durand S, Hough G, Husband S, Kubikova L, Lee D, Mello C, Powers A, Siang C, Smulders T, Wada K, White S, Yamamoto K, Yu J, Reiner A, Butler A (2005)

Avian brains and a new understanding of vertebrate brain evolution. Nat Rev Neurosci 2005 6:151-159.

Javaherian A, Kriegstein A (2009) A stem cell niche for intermediate progenitor cells of the embryonic cortex. Cereb Cortex 19 Suppl 1:i70-77.

Jellinger KR, A. (1976) Agyria-pachygyria (lissencephaly syndrome). Neuropadiatrie 7:66-91.

Johansson P, Almqvist E, Johansson J, Mattsson N, Andreasson U, Hansson O, Wallin A, Blennow K, Zetterberg H, Svensson J (2013) Cerebrospinal fluid (CSF) 25-hydroxyvitamin D concentration and CSF acetylcholinesterase activity are reduced in patients with Alzheimer's disease. PLoS One 8.

Johansson P, Dziegielewska K, Liddelow S, Saunders N (2008) The blood-CSF barrier explained: when development is not immaturity. Bioessays 30:237-248.

Kappeler C, Saillour Y, Baudoin JP, Tuy FP, Alvarez C, Houbron C, Gaspar P, Hamard G, Chelly J, Metin C, Francis F (2006) Branching and nucleokinesis defects in migrating interneurons derived from doublecortin knockout mice. Hum Mol Genet 15:1387-1400.

Kawasaki H, Toda T, Tanno K (2013) In vivo genetic manipulation of cortical progenitors in gyrencephalic carnivores using in utero electroporation. Biol Open 2:95-100.

Kelava I, Lewitus E, Huttner W (2013) The secondary loss of gyrencephaly as an example of evolutionary phenotypical reversal. Front Neuroanat 2013 26:7:16.

Kelava I, Reillo I, Murayama AY, Kalinka AT, Stenzel D, Tomancak P, Matsuzaki F, Lebrand C, Sasaki E, Schwamborn JC, Okano H, Huttner WB, Borrell V (2012) Abundant Occurrence of Basal Radial Glia in the Subventricular Zone of Embryonic Neocortex of a Lissencephalic Primate, the Common Marmoset Callithrix jacchus. Cereb Cortex 22:469-481.

Kepecs A, Fishell G (2014) Interneuron cell types are fit to function. Nature 505:318-326.

Kettenmann H, Kirchhoff F, Verkhratsky A (2013) Microglia: new roles for the synaptic stripper. Neuron 77:10-18.

Kielar M, Tuy FP, Bizzotto S, Lebrand C, de Juan Romero C, Poirier K, Oegema R, Mancini GM, Bahi-Buisson N, Olaso R, Le Moing AG, Boutourlinsky K, Boucher D, Carpentier W, Berquin P, Deleuze JF, Belvindrah R, Borrell V, Welker E, Chelly J, Croquelois A, Francis F (2014) Mutations in Eml1 lead to ectopic progenitors and neuronal heterotopia in mouse and human. Nat Neurosci.

Kim S, Lehtinen M, Sessa A, Zappaterra M, Cho S, Gonzalez D, Boggan B, Austin C, Wijnholds J, Gambello M, Malicki J, LaMantia A, Broccoli V, Walsh C (2010) The apical complex couples cell fate and cell survival to cerebral cortical development. Neuron 66:69-84.

Knoblich JA (2008) Mechanisms of asymmetric stem cell division. Cell 132:583-597.

Konno D, Shioi G, Shitamukai A, Mori A, Kiyonari H, Miyata T, Matsuzaki F (2008) Neuroepithelial progenitors undergo LGN-dependent planar divisions to maintain self-renewability during mammalian neurogenesis. Nat Cell Biol 10:93-101.

Kornack DR, Rakic P (1998) Changes in cell-cycle kinetics during the development and evolution of primate neocortex. Proc Natl Acad Sci U S A 95:1242-1246.

Kosodo Y, Suetsugu T, Suda M, Mimori-Kiyosue Y, Toida K, Baba S, Kimura A, Matsuzaki F (2011) Regulation of interkinetic nuclear migration by cell cycle-

coupled active and passive mechanisms in the developing brain. EMBO J 30:1690-1704.

Kostovic I, Rakic P (1990) Developmental history of the transient subplate zone in the visual and somatosensory cortex of the macaque monkey and human brain. J Comp Neurol 297:441-470.

Kostovic L, Jovanov-Milosevic N (2006) The development of cerebral connections during the first 20-45' weeks gestation Semin Fetal Neonatal Med 6:415-422.

Kostovic L, Judas M (2010) The development of the subplate and thalamocortical connections in the human foetal brain. Acta Paediatr 8:1119-1127.

Kowalczyk T, Pontious A, Englund C, Daza RA, Bedogni F, Hodge R, Attardo A, Bell C, Huttner WB, Hevner RF (2009) Intermediate neuronal progenitors (basal progenitors) produce pyramidal-projection neurons for all layers of cerebral cortex. Cereb Cortex 19:2439-2450.

Kriegstein A A-BA (2009) The glial nature of embryonic and adult neural stem cells. Annu Rev Neurosci 32:149-184.

Kriegstein A, Noctor S, Martinez-Cerdeno V (2006) Patterns of neural stem and progenitor cell division may underlie evolutionary cortical expansion. Nat Rev Neurosci 7:883-890.

Kriegstein AR, Noctor SC (2004) Patterns of neuronal migration in the embryonic cortex. Trends Neurosci 27:392-399.

LaMonica BE, Lui JH, Hansen DV, Kriegstein AR (2013) Mitotic spindle orientation predicts outer radial glial cell generation in human neocortex. Nat Commun 4:1665.

Lancaster MA, Knoblich JA (2012) Spindle orientation in mammalian cerebral cortical development. Curr Opin Neurobiol 22:737–746.

Lange C, Huttner WB, Calegari F (2009) Cdk4/cyclinD1 overexpression in neural stem cells shortens G1, delays neurogenesis, and promotes the generation and expansion of basal progenitors. Cell Stem Cell 5:320-331.

Lathia J, B. Patton, D. Mark Eckley, T. Magnus, M R. Mughal, T. Sasaki, M A. Caldwell, M S. Rao, M P. Mattson, Chs. ffrench-Constant (2007) Patterns of laminins and integrins in the embryonic ventricular zone of the CNS. J Comp Neurol 505:630-643.

LeBlanc JJ, Fagiolini M (2011) Autism: a "critical period" disorder? Neural Plast 2011:921680.

Lehtinen M, Bjornsson C, Dymecki S, Gilbertson R, Holtzman D, Monuki E (2013) The choroid plexus and cerebrospinal fluid: emerging roles in development, disease, and therapy. J Neurosci 33:17553-17559.

Lehtinen M, Zappaterra M, Chen X, Yang Y, Hill A, Lun M, Maynard T, Gonzalez D, Kim S, Ye P, D'Ercole A, Wong E, LaMantia A, Walsh C (2011) The cerebrospinal fluid provides a proliferative niche for neural progenitor cells. Neuron 69:893-905.

Letinic K, Zoncu R, Rakic P (2002) Origin of GABAergic neurons in the human neocortex. Nature 417:645-649.

Leung L, Klopper A, Grill S, Harris W, Norden C (2011) Apical migration of nuclei during G2 is a prerequisite for all nuclear motion in zebrafish neuroepithelia. . Development 138:5003-5013.

Levelt CN, Hubener M (2012) Critical-period plasticity in the visual cortex. Annu Rev Neurosci 35:309-330.

Levitt P, Rakic P (1980) Immunoperoxidase localization of glial fibrillary acidic protein in radial glial cells and astrocytes of the developing rhesus monkey brain. J Comp Neurol 193:815-840.

Lewitus E, Kelava I, Huttner WB (2013) Conical expansion of the outer subventricular zone and the role of neocortical folding in evolution and development. Front Hum Neurosci 7:424.

Liu X, Hashimoto-Torii K, Torii M, Ding C, Rakic P (2010) Gap junctions/hemichannels modulate interkinetic nuclear migration in the forebrain precursors. J Neurosci 30:4197-4209.

Loo D, Kanner S, Aruffo A (1998) Filamin binds to the cytoplasmic domain of the beta1-integrin. Identification of amino acids responsible for this interaction. J Biol Chem 273:23304-23312.

LoTurco JJ, Owens DF, Heath MJ, Davis MB, Kriegstein AR (1995) GABA and glutamate depolarize cortical progenitor cells and inhibit DNA synthesis. Neuron 15:1287-1298.

Loulier K, Lathia J, Marthiens V, Relucio J, Mughal M, Tang S, Coksaygan T, Hall P, Chigurupati S, Patton B, Colognato H, Rao M, Mattson M, Haydar T, Ffrench-Constant C (2009) beta1 integrin maintains integrity of the embryonic neocortical stem cell niche. PLoS Biol 7:8.

Louvi A, Grove E (2011) Cilia in the CNS: the quiet organelle claims center stage. Neuron 69:1046-1060.

Lui JH, Hansen DV, Kriegstein AR (2011) Development and evolution of the human neocortex. Cell 146:18-36.

Lukaszewicz A, Savatier P, Cortay V, Giroud P, Huissoud C, Berland M, Kennedy H, Dehay C (2005) G1 phase regulation, area-specific cell cycle control, and cytoarchitectonics in the primate cortex. Neuron 47:353-364.

Ma S, Kwon H, Johng H, Zang K, Huang. (2013) Radial glial neural progenitors regulate nascent brain vascular network stabilization via inhibition of Wnt signaling. PLoS Biol 11.

Malatesta P, Hartfuss E, Gotz M (2000) Isolation of radial glial cells by fluorescent-activated cell sorting reveals a neuronal lineage. Development 127:5253-5263.

Manto MU, Jissendi P (2012) Cerebellum: links between development, developmental disorders and motor learning. Front Neuroanat 6:1.

Manzini MC, Walsh CA (2011) What disorders of cortical development tell us about the cortex: one plus one does not always make two. Curr Opin Genet Dev 21:333-339.

Marin-Padilla (1969) Origin of the pericellular baskets of the pyramidal cells of the human motor cortex: a Golgi study. Brain Res 14:633-646.

Marín-Padilla (1999) The development of the human cerebral cortex. A cytoarchitectonic theory. Rev Neurol 29:208-216.

Marín (2013) Cellular and molecular mechanisms controlling the migration of neocortical interneurons. Eur J Neurosci 38:2019-2029.

Marin O, Plump AS, Flames N, Sanchez-Camacho C, Tessier-Lavigne M, Rubenstein JL (2003) Directional guidance of interneuron migration to the cerebral cortex relies on subcortical Slit1/2-independent repulsion and cortical attraction. Development 130:1889-1901.

Marin O, Rubenstein JL (2001) A long, remarkable journey: tangential migration in the telencephalon. Nat Rev Neurosci 2:780-790.

Marin O, Rubenstein JL (2003) Cell Migration in the Forebrain. Annu Rev Neurosci 26:441-483.

Marin O, Valiente M, Ge X, Tsai LH (2010) Guiding neuronal cell migrations. Cold Spring Harb Perspect Biol 2:a001834.

Martinez-Cerdeno V, Cunningham CL, Camacho J, Antczak JL, Prakash AN, Cziep ME, Walker AI, Noctor SC (2012) Comparative analysis of the subventricular zone in rat, ferret and macaque: evidence for an outer subventricular zone in rodents. PLoS One 7:e30178.

Martini FJ, Valiente M, Lopez Bendito G, Szabo G, Moya F, Valdeolmillos M, Marin O (2009) Biased selection of leading process branches mediates chemotaxis during tangential neuronal migration. Development 136:41-50.

McAlonan GM, Daly E, Kumari, V., Critchley HD, Van Amelsvoort T, Suckling J, Simmons A, Sigmundsson T, Greenwood K, Russel A, Schmitz N, Happe F, Howlin P, Murphy DG (2002) Brain anatomy and sensorimotor gating in Asperger's syndrome. . Brain 125:1594-1606.

Milosevic J, Schwarz S, Krohn Kea (2005) Low atmospheric oxygen avoids maturation, senescence and cell death of murine mesencephalic neural precursors. J Neurochem 92:718–729.

Miyata T, Kawaguchi A, Okano H, Ogawa M (2001) Asymmetric inheritance of radial glial fibers by cortical neurons. Neuron 31:727-741.

Miyata T, Kawaguchi A, Saito K, Kawano M, Muto T, Ogawa M (2004) Asymmetric production of surface-dividing and non-surface-dividing cortical progenitor cells. Development 131:3133-3145.

Mo Z, Moore AR, Filipovic R, Ogawa Y, Kazuhiro I, Antic SD, Zecevic N (2007) Human cortical neurons originate from radial glia and neuron-restricted progenitors. The Journal of neuroscience : the official journal of the Society for Neuroscience 27:4132-4145.

Mo Z, Zecevic N (2008) Is Pax6 critical for neurogenesis in the human fetal brain? Cereb Cortex 18:1455-1465.

Mo Z, Zecevic N (2009) Human fetal radial glia cells generate oligodendrocytes in vitro. Glia 57:490-498.

Molnár Z, Blakemore C (1995) ow do thalamic axons find their way to the cortex? Trends Neurosci 18:389-397.

Molyneaux BJ, Arlotta P, Menezes JR, Macklis JD (2007) Neuronal subtype specification in the cerebral cortex. Nat Rev Neurosci 8:427-437.

Morest D (1970) A study of neurogenesis in the forebrain of opossum pouch young. Z Anat Entwickl-Gesch 130:265-305.

Morrison S, Csete M, Groves Aea (2000) Culture in reduced levels of oxygen promotes clonogenic sympathoadrenal differentiation by isolated neural crest stem cells. . The Journal of neuroscience : the official journal of the Society for Neuroscience 20:7370–7376.

Mota B, Herculano-Houzel S (2012) How the cortex gets its folds: an inside-out, connectivity-driven model for the scaling of Mammalian cortical folding. Front Neuroanat 2013 2:6-3.

Mountcastle VB (1957) Modality and topographic properties of single neurons of cat's somatic sensory cortex. J Neurophysiol 20:408-434.

Nadarajah B, Brunstrom JE, Grutzendler J, Wong RO, Pearlman AL (2001) Two modes of radial migration in early development of the cerebral cortex. Nat Neurosci 4:143-150.

Nakajima K (2007) Control of tangential/non-radial migration of neurons in the developing cerebral cortex. Neurochemistry international 51:121-131.

Nakamura K, Oga T, Takahashi M, Kuribayashi T, Kanamori Y, Matsumiya T, Maeno Y, Yamamoto M (2012) Symmetrical hemispheric priming in spatial neglect: a hyperactive left-hemisphere phenomenon? Cortex 48:421-428.

Nasrallah IM GJ (2006) Brain malformations associated with cell migration. Pediatr Dev Pathol 9:89-97.

Neil J, Shiran S, McKinstry R, Schefft G, Snyder A, Almli C, Akbudak E, Aronovitz J, Miller J, Lee B, Conturo T (1998) Normal brain in human newborns: apparent diffusion coefficient and diffusion anisotropy measured by using diffusion tensor MR imaging. Radiology 1:57-66.

Neugebauer J, Amack J, Peterson A, Bisgrove B, Yost H (2009) FGF signalling during embryo development regulates cilia length in diverse epithelia. Nature 458:651-654.

Nicholas AK, Khurshid M, Desir J, Carvalho OP, Cox JJ, Thornton G, Kausar R, Ansar M, Ahmad W, Verloes A, Passemard S, Misson JP, Lindsay S, Gergely F, Dobyns WB, Roberts E, Abramowicz M, Woods CG (2010) WDR62 is associated with the spindle pole and is mutated in human microcephaly. Nat Genet.

Nimmerjahn A, Kirchhoff F, Helmchen F (2005) Resting microglial cells are highly dynamic surveillants of brain parenchyma in vivo. Science 308:1314-1318.

Noctor SC, Flint AC, Weissman TA, Dammerman RS, Kriegstein AR (2001) Neurons derived from radial glial cells establish radial units in neocortex. Nature 409:714-720.

Noctor SC, Martinez-Cerdeno V, Ivic L, Kriegstein AR (2004) Cortical neurons arise in symmetric and asymmetric division zones and migrate through specific phases. Nat Neurosci 7:136-144.

Noctor SC, Martinez-Cerdeno V, Kriegstein AR (2008) Distinct behaviors of neural stem and progenitor cells underlie cortical neurogenesis. J Comp Neurol 508:28-44.

Noles SR, Chenn A (2007) Cadherin inhibition of beta-catenin signaling regulates the proliferation and differentiation of neural precursor cells. Mol Cell Neurosci 35:549-558.

Nonaka-Kinoshita M, Reillo I, Artegiani B, Martinez-Martinez MA, Nelson M, Borrell V, Calegari F (2013) Regulation of cerebral cortex size and folding by expansion of basal progenitors. EMBO J 32:1817-1828.

O'Leary DD, Borngasser D (2006) Cortical ventricular zone progenitors and their progeny maintain spatial relationships and radial patterning during preplate development indicating an early protomap. Cereb Cortex 16 Suppl 1:i46-56.

O'Leary DN, Y. (2002) Patterning centers, regulatory genes and extrinsic mechanisms controlling arealization of the neocortex. Curr Opin Neurobiol 12:14-25.

O'Rourke NA, Dailey ME, Smith SJ, McConnell SK (1992) Diverse migratory pathways in the developing cerebral cortex. Science 258:299-302.

O'Rourke NA, Sullivan DP, Kaznowski CE, Jacobs AA, McConnell SK (1995) Tangential migration of neurons in the developing cerebral cortex. Development 121:2165-2176.

Ohshima T, Gilmore EC, Longenecker G, Jacobowitz DM, Brady RO, Herrup K, Kulkarni AB (1999) Migration defects of cdk5(-/-) neurons in the developing cerebellum is cell autonomous. The Journal of neuroscience : the official journal of the Society for Neuroscience 19:6017-6026.

Ohshima T, Hirasawa M, Tabata H, Mutoh T, Adachi T, Suzuki H, Saruta K, Iwasato T, Itohara S, Hashimoto M, Nakajima K, Ogawa M, Kulkarni AB, Mikoshiba K

(2007) Cdk5 is required for multipolar-to-bipolar transition during radial neuronal migration and proper dendrite development of pyramidal neurons in the cerebral cortex. Development 134:2273-2282.

Ohshima T, Ogawa M, Veeranna, Hirasawa M, Longenecker G, Ishiguro K, Pant HC, Brady RO, Kulkarni AB, Mikoshiba K (2001) Synergistic contributions of cyclin-dependant kinase 5/p35 and Reelin/Dab1 to the positioning of cortical neurons in the developing mouse brain. Proc Natl Acad Sci U S A 98:2764-2769.

Ohshima T, Ward JM, Huh CG, Longenecker G, Veeranna, Pant HC, Brady RO, Martin LJ, Kulkarni AB (1996) Targeted disruption of the cyclin-dependent kinase 5 gene results in abnormal corticogenesis, neuronal pathology and perinatal death. Proc Natl Acad Sci U S A 93:11173-11178.

Okamoto M, Namba T, Shinoda T, Kondo T, Watanabe T, Inoue Y, Takeuchi K, Enomoto Y, Ota K, Oda K, Wada Y, Sagou K, Saito K, Sakakibara A, Kawaguchi A, Nakajima K, Adachi T, Fujimori T, Ueda M, Hayashi S, Kaibuchi K, Miyata T (2013) TAG-1-assisted progenitor elongation streamlines nuclear migration to optimize subapical crowding. Nat Neurosci 16:1556-1566.

Osumi N, Shinohara H, Numayama-Tsuruta K, Maekawa M (2008) Concise review: Pax6 transcription factor contributes to both embryonic and adult neurogenesis as a multifunctional regulator. Stem Cells 26:1663-1672.

Paridaen JT, Huttner WB (2014) Neurogenesis during development of the vertebrate central nervous system. EMBO Rep 15:351-364.

Parnavelas JG, Alifragis P, Nadarajah B (2002) The origin and migration of cortical neurons. Prog Brain Res 136:73-80.

Parnavelas JL, AR. Webster, KE. (1977) Organization of neurons in the visual cortex, area 17, of the rat. J Anat 124:305-322.

Penfield (1924) Oligodendroglia and its relation to classical neuroglia. Brain.

Peyre E, Morin X (2012) An oblique view on the role of spindle orientation in vertebrate neurogenesis. Dev Growth Differ 54:287-305.

Pilaz L, Patti D, Marcy G, Ollier E, Pfister S, Douglas R, Betizeau M, Gautier E, Cortay V, Doerflinger N, Kennedy H, Dehay C (2009) Forced G1-phase reduction alters mode of division, neuron number, and laminar phenotype in the cerebral cortex. Proc Natl Acad Sci U S A 106:21924-21929.

Pilz GA, Shitamukai A, Reillo I, Pacary E, Schwausch J, Stahl R, Ninkovic J, Snippert HJ, Clevers H, Godinho L, Guillemot F, Borrell V, Matsuzaki F, Gotz M (2013) Amplification of progenitors in the mammalian telencephalon includes a new radial glial cell type. Nat Commun 4:2125.

Polleux F, Whitford K, Dijkhuizen P, Vitalis T, Ghosh A (2002) Control of cortical interneuron migration by neurotrophins and PI3-kinase signaling. Development 129: 3147–3160.

Poluch S, Juliano SL (2013) Fine-tuning of Neurogenesis Is Essential for the Evolutionary Expansion of the Cerebral Cortex. Cereb Cortex.

Postiglione M, Jüschke C, Xie Y, Haas G, Charalambous C, Knoblich J (2011) Mouse inscuteable induces apical-basal spindle orientation to facilitate intermediate progenitor generation in the developing neocortex. Neuron 72:269-284.

Puelles L, Martínez Pérez S, Martínez de la Torre M (2008) Neuroanatomía. Editorial Médica Panamericana.

Rakic P (1972) Mode of cell migration to the superficial layers of fetal monkey neocortex. J Comp Neurol 145:61-83.

Rakic P (1974) Neurons in rhesus monkey visual cortex: systematic relation between time of origin and eventual disposition. Science 183:425-427.

Rakic P (1988) Specification of cerebral cortical areas. Science 241:170-176.

Rakic P (1995a) Radial versus tangential migration of neuronal clones in the developing cerebral cortex. Proc Natl Acad Sci U S A 92:11323-11327.

Rakic P (1995b) A small step for the cell, a giant leap for mankind: a hypothesis of neocortical expansion during evolution. Trends Neurosci 18:383-388.

Rakic P (2003) Developmental and evolutionary adaptations of cortical radial glia. Cereb Cortex 13:541-549.

Rakic P (2009) Evolution of the neocortex: a perspective from developmental biology. Nat Rev Neurosci 10:724-735.

Rakic P, Ayoub AE, Breunig JJ, Dominguez MH (2009) Decision by division: making cortical maps. Trends Neurosci 32:291-301.

Ramon y Cajal S (1909-1911) Neuronal theory.

Ramón y Cajal S (1911) Histologie du Système Nerveux de l'Homme et des Vertébrés. Paris: Maloine.

Rao G, Pedone C, Del Valle L, Reiss K, Holland E, Fults D (2004) Sonic hedgehog and insulin-like growth factor signaling synergize to induce medulloblastoma formation from nestin-expressing neural progenitors in mice. Oncogene 23:6156-6162.

Rasin MR, Gazula VR, Breunig JJ, Kwan KY, Johnson MB, Liu-Chen S, Li HS, Jan LY, Jan YN, Rakic P, Sestan N (2007) Numb and Numbl are required for maintenance of cadherin-based adhesion and polarity of neural progenitors. Nat Neurosci 10:819-827.

Reillo I, Borrell V (2012) Germinal zones in the developing cerebral cortex of ferret: ontogeny, cell cycle kinetics, and diversity of progenitors. Cereb Cortex 22:2039-2054.

Reillo I, de Juan Romero C, Garcia-Cabezas MA, Borrell V (2011) A role for intermediate radial glia in the tangential expansion of the Mammalian cerebral cortex. Cereb Cortex 21:1674-1694.

Rice DS, Curran T (2001) Role of the reelin signaling pathway in central nervous system development. Annu Rev Neurosci 24:1005-1039.

Río-Hortega (1921) Estudios sobre la neuroglia. La glía de escasas radiaciones (oligodendroglía) Real Sociedad Española de Historia Natural.

Rivas RJ, Hatten ME (1995) Motility and cytoskeletal organization of migrating cerebellar granule neurons. The Journal of neuroscience : the official journal of the Society for Neuroscience 15:981-989.

Roessmann U, Velasco M, Sindely SD GP (1980) Glial fibrillary acidic protein (GFAP) in ependymal cells during development. An immunocytochemical study. Brain Res 1980 Oct 27;200(1):13-21 200:13-21.

Rowitch D, Kriegstein A (2010) Developmental genetics of vertebrate glial–cell specification. Nature 468:214-222.

Saeed AI, Sharov V, White J, Li J, Liang W, Bhagabati N, Braisted J, Klapa M, Currier T, Thiagarajan M, Sturn A, Snuffin M, Rezantsev A, Popov D, Ryltsov A, Kostukovich E, Borisovsky I, Liu Z, Vinsavich A, Trush V, Quackenbush J (2003) TM4: a free, open-source system for microarray data management and analysis. Biotechniques 34:374-378.

Sarkisian MR, Bartley CM, Rakic P (2008) Trouble making the first move: interpreting arrested neuronal migration in the cerebral cortex. Trends Neurosci 31:54-61.

Schaar BT, Kinoshita K, McConnell SK (2004) Doublecortin microtubule affinity is regulated by a balance of kinase and phosphatase activity at the leading edge of migrating neurons. Neuron 41:203-213.

Schafer D, Lehrman E, Stevens B (2013) The "quad-partite" synapse: microglia-synapse interactions in the developing and mature CNS. Glia 61:24-36.

Schmechel DE, Rakic P (1979a) Arrested proliferation of radial glial cells during midgestation in rhesus monkey. Nature 277:303-305.

Schmechel DE, Rakic P (1979b) A Golgi study of radial glial cells in developing monkey telencephalon: morphogenesis and transformation into astrocytes. Anat Embryol (Berl) 156:115-152.

Shitamukai A, Konno D, Matsuzaki F (2011) Oblique radial glial divisions in the developing mouse neocortex induce self-renewing progenitors outside the germinal zone that resemble primate outer subventricular zone progenitors. The Journal of neuroscience : the official journal of the Society for Neuroscience 31:3683-3695.

Sidman RL, Rakic P (1973) Neuronal migration, with special reference to developing human brain: a review. Brain Res 62:1-35.

Siegenthaler JA, Ashique AM, Zarbalis K, Patterson KP, Hecht JH, Kane MA, Folias AE, Choe Y, May SR, Kume T, Napoli JL, Peterson AS, Pleasure SJ (2009) Retinoic acid from the meninges regulates cortical neuron generation. Cell 139:597-609.

Smart (1972a) Proliferative characteristics of the ependymal layer during the early development of the mouse diencephalon, as revealed by recording the number, location, and plane of cleavage of mitotic figures. . J Anat 113:109-129.

Smart (1972b) Proliferative characteristics of the ependymal layer during the early development of the spinal cord in the mouse. J Anat 111:365-380.

Smart IH, Dehay C, Giroud P, Berland M, Kennedy H (2002) Unique morphological features of the proliferative zones and postmitotic compartments of the neural epithelium giving rise to striate and extrastriate cortex in the monkey. Cereb Cortex 12:37-53.

Soriano E, Del Rio JA (2005) The cells of cajal-retzius: still a mystery one century after. Neuron 46:389-394.

Stahl R, Walcher T, De Juan Romero C, Pilz GA, Cappello S, Irmler M, Sanz-Aquela JM, Beckers J, Blum R, Borrell V, Gotz M (2013) Trnp1 regulates expansion and folding of the mammalian cerebral cortex by control of radial glial fate. Cell 153:535-549.

Stancik E, Navarro-Quiroga I, Sellke R, Haydar T (2010) Heterogeneity in ventricular zone neural precursors contributes to neuronal fate diversity in the postnatal neocortex. J Neurosci 30:7028-7036.

Stenzel D, Wilsch-Brauninger M, Wong FK, Heuer H, Huttner WB (2014) Integrin alphavbeta3 and thyroid hormones promote expansion of progenitors in embryonic neocortex. Development 141:795-806.

Stitt TH, ME. (1990) Antibodies that recognize astrotactin block granule neuron binding to astroglia. Neuron 5:639-649.

Stubbs D, DeProto J, Nie K, Englund C, Mahmud I, Hevner R, Molnar Z (2009) Neurovascular congruence during cerebral cortical development. Cereb Cortex 19 Suppl 1:i32-41.

Sutor B, Hagerty T (2005) Involvement of gap junctions in the development of the neocortex. Biochim Biophys Acta 1719:59-68.

Szentágothai J, Arbib M (1974) Conceptual models of neural organization. Neurosci Res Program Bull 12:305-510.

Tabata H, Nakajima K (2003) Multipolar migration: the third mode of radial neuronal migration in the developing cerebral cortex. The Journal of neuroscience : the official journal of the Society for Neuroscience 23:9996-10001.

Takahashi T, Nowakowski RS, Caviness VS, Jr. (1995) The cell cycle of the pseudostratified ventricular epithelium of the embryonic murine cerebral wall. The Journal of neuroscience : the official journal of the Society for Neuroscience 15:6046-6057.

Tanaka T, Serneo FF, Tseng HC, Kulkarni AB, Tsai LH, Gleeson JG (2004) Cdk5 phosphorylation of doublecortin ser297 regulates its effect on neuronal migration. Neuron 41:215-227.

Tashiro A, Zhao C, Gage FH (2006) Retrovirus-mediated single-cell gene knockout technique in adult newborn neurons in vivo. Nat Protoc 1:3049-3055.

Taverna E, Gotz M, Huttner WB (2014) The Cell Biology of Neurogenesis: Toward an Understanding of the Development and Evolution of the Neocortex. Annu Rev Cell Dev Biol.

Teissier A, Waclaw R, Griveau A, Campbell K, Pierani A (2012) Tangentially migrating transient glutamatergic neurons control neurogenesis and maintenance of cerebral cortical progenitor pools. Cereb Cortex 22:403-416.

Toro R, Perron M, Pike B, Richer L, Veillette S, Pausova Z, Paus T (2008) Brain size and folding of the human cerebral cortex. Cereb Cortex 10:2352-2357.

Tremblay M, Stevens B, Sierra A, Wake H, Bessis A, Nimmerjahn A (2011) The role of microglia in the healthy brain. The Journal of neuroscience : the official journal of the Society for Neuroscience 31:16064-16069.

Tsai JW, Chen Y, Kriegstein AR, Vallee RB (2005) LIS1 RNA interference blocks neural stem cell division, morphogenesis, and motility at multiple stages. J Cell Biol 170:935-945.

Turetsky BI, Calkins ME, Light GA, Olincy A, Radant AD, Swerdlow NR (2007) Neurophysiological endophenotypes of schizophrenia: the viability of selected candidate measures. . Schizophr Bull 33:69-94.

Tyler W, Haydar T (2013) Multiplex genetic fate mapping reveals a novel route of neocortical neurogenesis, which is altered in the Ts65Dn mouse model of Down syndrome. J Neurosci 33:5106-5119.

Ueno M, Yamashita T (2014) Bidirectional tuning of microglia in the developing brain: from neurogenesis to neural circuit formation. Curr Opin Neurobiol 27:8-15.

Valiente M, Ciceri G, Rico B, Marin O (2011) Focal adhesion kinase modulates radial glia-dependent neuronal migration through connexin-26. The Journal of neuroscience : the official journal of the Society for Neuroscience 31:11678-11691.

Valiente M, Marin O (2010) Neuronal migration mechanisms in development and disease. Curr Opin Neurobiol 20:68-78.

Van Essen DC (1997) A tension-based theory of morphogenesis and compact wiring in the central nervous system. Nature 385:313-318.

Wake H, Moorhouse A, Miyamoto A, Nabekura J (2013) Microglia: actively surveying and shaping neuronal circuit structure and function. Trends Neurosci 36:209-217.

Walsh CC, CL. (1988) Clonally related cortical cells show several migration patterns. Science 241:1342-1345.

Wang WZ, Oeschger FM, Montiel JF, Garcia-Moreno F, Hoerder-Suabedissen A, Krubitzer L, Ek CJ, Saunders NR, Reim K, Villalon A, Molnar Z (2011a) Comparative Aspects of Subplate Zone Studied with Gene Expression in Sauropsids and Mammals. Cereb Cortex.

Wang X, Tsai JW, Lamonica B, Kriegstein AR (2011b) A new subtype of progenitor cell in the mouse embryonic neocortex. Nat Neurosci 14:555-561.

Ward MR, Y. (2005) Investigations of neuronal migration in the central nervous system. Methods Mol Biol 294:137-156.

Warren N, Caric D, Pratt T, Clausen J, Asavaritikrai P, Mason J, Hill R, DJ. P (1999) The transcription factor, Pax6, is required for cell proliferation and differentiation in the developing cerebral cortex. Cereb Cortex 9:627-635.

Watanabe HM, F. (2009) Real time analysis of pontine neurons during initial stages of nucleogenesis. Neurosci Res 64:20-29.

Weissman T, Noctor SC, Clinton BK, Honig LS, Kriegstein AR (2003) Neurogenic radial glial cells in reptile, rodent and human: from mitosis to migration. Cereb Cortex 13:550-559.

Welker W (1990) Why does cerebral cortex fissure and fold? A review of determinants of gyri and sulci. In: Cerebral Cortex, vol. 8B (Peters, A. and Jones, E. G., eds), pp 3-136 New York and London: Plenum Press.

Xie SB, Tsai LH. (2006) Cyclin-dependent kinase 5 permits efficient cytoskeletal remodeling--a hypothesis on neuronal migration. Cereb Cortex 16:64-68.

Xie Y, Juschke C, Esk C, Hirotsune S, Knoblich JA (2013) The phosphatase PP4c controls spindle orientation to maintain proliferative symmetric divisions in the developing neocortex. Neuron 79:254-265.

Xie Z, Sanada K, Samuels BA, Shih H, Tsai LH (2003) Serine 732 phosphorylation of FAK by Cdk5 is important for microtubule organization, nuclear movement, and neuronal migration. Cell 114:469-482.

Xu G, Knutsen AK, Dikranian K, Kroenke CD, Bayly PV, Taber LA (2010) Axons pull on the brain, but tension does not drive cortical folding. J Biomech Eng 132:071013.

Yamashita (2013) From neuroepithelial cells to neurons: changes in the physiological properties of neuroepithelial stem cells. Arch Biochem Biophys 534:64-70.

Yamashita N, Morita A, Uchida Y, Nakamura F, Usui H, Ohshima T, Taniguchi M, Honnorat J, Thomasset N, Takei K, Takahashi T, Kolattukudy P, Goshima Y (2007) Regulation of spine development by semaphorin3A through cyclin-dependent kinase 5 phosphorylation of collapsin response mediator protein 1. The Journal of neuroscience : the official journal of the Society for Neuroscience 27:12546-12554.

Yee KT, Simon HH, Tessier-Lavigne M, O'Leary DM (1999) Extension of long leading processes and neuronal migration in the mammalian brain directed by the chemoattractant netrin-1. Neuron 24:607-622.

Yokota Y, Gashghaei, H.T., Han, C., Watson, H., Campbell, K.J. & Anton, E.S. (2007) Radial glial dependent and independent dynamics of interneuronal migration in the developing cerebral cortex. PLoS One 2:794.

Yoon KJ, Koo BK, Im SK, Jeong HW, Ghim J, Kwon MC, Moon JS, Miyata T, Kong YY (2008) Mind bomb 1-expressing intermediate progenitors generate notch signaling to maintain radial glial cells. Neuron 58:519-531.

Yoshikawa S, McKinnon RD, Kokel M, Thomas JB (2003) Wnt-mediated axon guidance via the Drosophila Derailed receptor. Nature 422:583-588.

Yu TW, Mochida GH, Tischfield DJ, Sgaier SK, Flores-Sarnat L, Sergi CM, Topcu M, McDonald MT, Barry BJ, Felie JM, Sunu C, Dobyns WB, Folkerth RD, Barkovich AJ, Walsh CA (2010) Mutations in WDR62, encoding a centrosome-associated protein, cause microcephaly with simplified gyri and abnormal cortical architecture. Nat Genet.

Zecevic N (2004) Specific characteristic of radial glia in the human fetal telencephalon. Glia 48:27-35.

Zecevic N, Chen Y, Filipovic R (2005) Contributions of cortical subventricular zone to the development of the human cerebral cortex. J Comp Neurol 491:109-122.

Zecevic N, Hu F, Jakovcevski I (2011) Interneurons in the developing human neocortex. Dev Neurobiol 71:18-33.

ANNEX

Table 1. Number of cells and animals analyzed for each survival period in the quantification of cell lineages shown in Figure 24, 27, 28 and 29.

Layer of rv::*Gfp* delivery	Age	P1-P3	P1-P6	P1-P10	P1-P14
VZ	N cells	1,094	5,544	1,499	4,196
	N kits	4	4	5	3
ISVZ	N cells	962	1,063	2,705	3,107
	N kits	2	2	3	2
OSVZ	N cells	420	1,092	3,742	1,663
	N kits	2	3	3	2

Table 2. List of genes differentially-expressed in ferret VZ between E30 and E34 from our ferret-specific microarray analysis, indicating microarray probe identification, value of fold-change (E34 compared to E30) and adjusted *p* value.

Gene Name	Probe ID	Fold-change	Adj. P value
SLC1A3	CUST_17289_PI427051300	**5.50**	**1.32E-02**
SLC1A3	CUST_43030_PI427051300	**4.54**	**3.83E-02**
TNC	CUST_19689_PI427051300	**4.37**	**1.32E-02**
LYPD1	CUST_10832_PI427051300	**4.30**	**1.51E-02**
LYPD1	CUST_10833_PI427051300	**4.29**	**2.15E-02**
SLC1A3	CUST_43029_PI427051300	**4.18**	**1.32E-02**
SLITRK2	CUST_34563_PI427051300	**3.77**	**1.32E-02**
ETV5	CUST_26459_PI427051300	**3.70**	**1.32E-02**
BCAN	CUST_1647_PI427051300	**3.66**	**3.19E-02**
ETV5	CUST_26457_PI427051300	**3.60**	**1.61E-02**
SLITRK2	CUST_43074_PI427051300	**3.53**	**1.32E-02**
SLITRK2	CUST_34561_PI427051300	**3.49**	**2.73E-02**
SLITRK2	CUST_34560_PI427051300	**3.46**	**1.40E-02**
TNC	CUST_19692_PI427051300	**3.19**	**2.41E-02**
PTX3	CUST_15153_PI427051300	**3.12**	**2.41E-02**
PTX3	CUST_15152_PI427051300	**3.01**	**4.09E-02**
C6orf145	CUST_2565_PI427051300	**2.94**	**3.02E-02**
C6orf145	CUST_2564_PI427051300	**2.90**	**1.32E-02**
AIM1	CUST_569_PI427051300	**2.83**	**4.93E-02**
IFIH1	CUST_28153_PI427051300	**2.76**	**1.32E-02**
GSN	CUST_27609_PI427051300	**2.72**	**3.43E-02**
LOC100464061	CUST_39136_PI427051300	**2.71**	**3.60E-02**
ABTB2	CUST_136_PI427051300	**2.69**	**1.32E-02**
FAM84B	CUST_6566_PI427051300	**2.63**	**4.68E-02**
GZMH	CUST_27665_PI427051300	**2.62**	**1.32E-02**
LOC100478008	CUST_40307_PI427051300	**2.56**	**1.32E-02**
LOC100478008	CUST_40308_PI427051300	**2.46**	**2.37E-02**
BCAR3	CUST_1658_PI427051300	**2.40**	**4.09E-02**

Gene Name	Probe ID	Fold-change	Adj. P value
FAM167A	CUST_6407_PI427051300	**2.36**	**1.51E-02**
BCAR3	CUST_1659_PI427051300	**2.25**	**1.32E-02**
ARHGEF26	CUST_22866_PI427051300	**2.25**	**2.23E-02**
SFMBT2	CUST_43004_PI427051300	**2.22**	**2.37E-02**
GSN	CUST_27612_PI427051300	**2.19**	**2.44E-02**
CHST2	CUST_3830_PI427051300	**2.18**	**1.32E-02**
VCAM1	CUST_36846_PI427051300	**2.08**	**1.32E-02**
TMTC2	CUST_19676_PI427051300	**2.06**	**2.45E-02**
SLC24A3	CUST_34316_PI427051300	**2.04**	**3.92E-02**
GPR114	CUST_7764_PI427051300	**2.04**	**1.32E-02**
DIO2	CUST_38341_PI427051300	**2.03**	**2.23E-02**
TRIM47	CUST_19989_PI427051300	**2.03**	**1.93E-02**
GXYLT1	CUST_27664_PI427051300	**-2.01**	**2.87E-02**
LOC100127983	CUST_10110_PI427051300	**-2.05**	**4.85E-02**
CCND1	CUST_3214_PI427051300	**-2.10**	**3.83E-02**
FRZB	CUST_7108_PI427051300	**-2.13**	**4.62E-02**
DCN	CUST_25383_PI427051300	**-2.19**	**2.23E-02**
CADPS	CUST_24023_PI427051300	**-2.23**	**2.37E-02**
MSRB3	CUST_11905_PI427051300	**-2.29**	**1.32E-02**
RNU2-1	CUST_33333_PI427051300	**-2.32**	**1.32E-02**
WLS	CUST_21015_PI427051300	**-2.33**	**1.57E-02**
AHR	CUST_22367_PI427051300	**-2.33**	**1.51E-02**
NEXN	CUST_12510_PI427051300	**-2.41**	**2.41E-02**
ZFPM2	CUST_37486_PI427051300	**-2.43**	**1.51E-02**
MSRB3	CUST_11906_PI427051300	**-2.44**	**2.41E-02**
SUSD1	CUST_18556_PI427051300	**-2.44**	**2.23E-02**
ACTA2	CUST_257_PI427051300	**-2.45**	**2.40E-02**
INA	CUST_8983_PI427051300	**-2.46**	**2.86E-02**
PENK	CUST_13736_PI427051300	**-2.51**	**4.79E-02**
EDN3	CUST_5627_PI427051300	**-2.60**	**1.32E-02**
LOC100474220	CUST_39978_PI427051300	**-2.66**	**2.47E-02**

Gene Name	Probe ID	Fold-change	Adj. P value
ST18	CUST_18296_PI427051300	**-2.74**	**2.94E-02**
SLIT1	CUST_17682_PI427051300	**-2.79**	**2.49E-02**
TESC	CUST_18970_PI427051300	**-2.81**	**3.57E-02**
EFNA5	CUST_26045_PI427051300	**-2.95**	**1.77E-02**
ST18	CUST_18293_PI427051300	**-2.95**	**3.18E-02**
EBF2	CUST_5585_PI427051300	**-2.99**	**4.93E-02**
ZFPM2	CUST_37485_PI427051300	**-3.08**	**1.40E-02**
NOL4	CUST_12696_PI427051300	**-3.12**	**1.46E-02**
LOC100451412	CUST_39068_PI427051300	**-3.14**	**1.61E-02**
NEXN	CUST_12509_PI427051300	**-3.17**	**1.32E-02**
NOL4	CUST_12697_PI427051300	**-3.18**	**1.32E-02**
ZFPM2	CUST_37487_PI427051300	**-3.30**	**1.32E-02**
PTPRE	CUST_32592_PI427051300	**-3.62**	**5.86E-03**
ST18	CUST_18295_PI427051300	**-3.64**	**1.32E-02**
SV2B	CUST_35314_PI427051300	**-3.65**	**1.32E-02**
LOC100442421	CUST_39057_PI427051300	**-3.69**	**1.32E-02**
COL21A1	CUST_4155_PI427051300	**-3.74**	**2.41E-02**
PAPPA2	CUST_42739_PI427051300	**-3.90**	**1.51E-02**
EYA2	CUST_6205_PI427051300	**-4.87**	**1.48E-02**
NHLH2	CUST_12556_PI427051300	**-5.49**	**5.86E-03**

Table 3 - List of genes differentially-expressed in ferret VZ between E34 and P1 indicating microarray probe identification number, value of fold-change (P1 compared to E34) and adjusted *p* value. Only the top 30 probes with highest positive fold-change, 30 with highest negative, plus TRNP1, are included.

Gene Name	Probe ID	Fold-change	Adj. P value
NTRK2	CUST_31058_PI427051300	**19.16**	**4.57E-04**
NTRK2	CUST_31057_PI427051300	**18.87**	**4.97E-04**
APOE	CUST_989_PI427051300	**17.85**	**2.78E-06**
APOE	CUST_988_PI427051300	**16.05**	**1.42E-06**
CTSW	CUST_4601_PI427051300	**15.08**	**3.07E-03**
RFTN2	CUST_33104_PI427051300	**13.40**	**9.11E-05**
GJB6	CUST_7477_PI427051300	**13.08**	**1.69E-06**
SLC7A11	CUST_17633_PI427051300	**12.02**	**2.98E-04**
ZCCHC24	CUST_21239_PI427051300	**11.42**	**1.80E-04**
ZCCHC24	CUST_21240_PI427051300	**11.06**	**5.21E-05**
RFTN2	CUST_33107_PI427051300	**10.46**	**9.54E-05**
LOC480072	CUST_41591_PI427051300	**9.73**	**9.11E-05**
ACE	CUST_22166_PI427051300	**9.72**	**5.32E-07**
TRIL	CUST_19952_PI427051300	**9.51**	**2.79E-05**
KLF9	CUST_28985_PI427051300	**9.48**	**4.82E-05**
BATF2	CUST_1620_PI427051300	**9.43**	**8.91E-05**
BBOX1	CUST_1626_PI427051300	**9.31**	**5.17E-04**
PID1	CUST_13954_PI427051300	**9.26**	**1.80E-04**
TRIL	CUST_19950_PI427051300	**9.07**	**6.56E-05**
MGLL	CUST_11413_PI427051300	**8.86**	**4.82E-05**
ITGA7	CUST_9149_PI427051300	**8.79**	**1.39E-04**
OLIG1	CUST_13076_PI427051300	**8.79**	**6.39E-04**
AQP4	CUST_22747_PI427051300	**8.74**	**2.63E-03**
GJB6	CUST_7478_PI427051300	**8.61**	**1.42E-06**
LTBP1	CUST_29561_PI427051300	**8.48**	**6.78E-03**
TIMP3	CUST_19212_PI427051300	**8.46**	**3.68E-05**
CNKSR3	CUST_4045_PI427051300	**8.46**	**3.66E-05**

Gene Name	Probe ID	Fold-change	Adj. P value
HEPACAM	CUST_8294_PI427051300	**8.28**	**5.63E-03**
ZDHHC17	CUST_37412_PI427051300	**8.15**	**5.56E-03**
RFTN2	CUST_33105_PI427051300	**7.99**	**1.65E-03**
GHRL	CUST_7445_PI427051300	**7.92**	**2.10E-03**
C21orf63	CUST_2380_PI427051300	**7.71**	**7.82E-05**
MIER1	CUST_30123_PI427051300	**7.65**	**3.10E-03**
SCRG1	CUST_16613_PI427051300	**7.61**	**5.24E-05**
SMOX	CUST_34688_PI427051300	**7.39**	**5.43E-03**
ITGA7	CUST_9152_PI427051300	**7.33**	**5.24E-05**
LTBP1	CUST_29560_PI427051300	**7.27**	**1.56E-03**
LTBP1	CUST_29563_PI427051300	**7.24**	**2.00E-03**
HSD11B1	CUST_8615_PI427051300	**7.21**	**1.57E-04**
TRNP1	**CUST_20041_PI427051300**	**2.86**	**2.44E-04**
SEMA4F	CUST_16756_PI427051300	**-5.12**	**4.65E-02**
CCDC41	CUST_24208_PI427051300	**-5.16**	**7.92E-03**
OBFC2A	CUST_31173_PI427051300	**-5.18**	**7.49E-04**
GTPBP8	CUST_8086_PI427051300	**-5.25**	**1.68E-03**
CSRP2	CUST_4506_PI427051300	**-5.27**	**8.98E-04**
CSRP2	CUST_4509_PI427051300	**-5.27**	**2.40E-03**
LOC283174	CUST_10479_PI427051300	**-5.29**	**1.63E-04**
ATP11A	CUST_23113_PI427051300	**-5.32**	**1.44E-02**
HIF1AN	CUST_8349_PI427051300	**-5.36**	**1.55E-02**
HBD	CUST_27715_PI427051300	**-5.37**	**7.60E-03**
HIF1AN	CUST_8350_PI427051300	**-5.38**	**1.78E-02**
LRTOMT	CUST_10747_PI427051300	**-5.40**	**1.40E-02**
PRR13	CUST_14866_PI427051300	**-5.41**	**9.19E-03**
RBM10	CUST_32930_PI427051300	**-5.41**	**1.76E-03**
KCTD21	CUST_9436_PI427051300	**-5.48**	**4.52E-03**
B3GNT4	CUST_1540_PI427051300	**-5.50**	**1.58E-04**
DCC	CUST_4889_PI427051300	**-5.56**	**3.26E-04**
CXCR7	CUST_4677_PI427051300	**-5.58**	**1.58E-03**

Gene Name	Probe ID	Fold-change	Adj. P value
HBM	CUST_8197_PI427051300	**-5.58**	**5.64E-03**
C14orf101	CUST_23694_PI427051300	**-5.65**	**3.08E-03**
FKBP4	CUST_6948_PI427051300	**-5.68**	**3.92E-03**
ST18	CUST_18295_PI427051300	**-5.73**	**6.37E-05**
GRB10	CUST_7910_PI427051300	**-5.86**	**1.36E-03**
MTCH2	CUST_30311_PI427051300	**-5.90**	**3.09E-03**
SHMT1	CUST_17079_PI427051300	**-5.98**	**1.08E-03**
NARS2	CUST_12260_PI427051300	**-5.99**	**2.29E-03**
JPH3	CUST_9259_PI427051300	**-6.39**	**5.91E-03**
CCND1	CUST_3214_PI427051300	**-6.56**	**3.74E-05**
HBA1	CUST_8191_PI427051300	**-6.63**	**4.64E-04**
MTCH2	CUST_30310_PI427051300	**-6.69**	**3.94E-03**
MTCH2	CUST_30309_PI427051300	**-6.76**	**5.06E-03**
NEUROD6	CUST_12506_PI427051300	**-7.34**	**3.67E-04**
HBA1	CUST_8192_PI427051300	**-7.42**	**1.04E-03**
HBM	CUST_8196_PI427051300	**-7.45**	**1.55E-03**
OBFC2A	CUST_31172_PI427051300	**-8.20**	**5.59E-04**
C3orf63	CUST_23857_PI427051300	**-8.32**	**8.88E-04**
NDNF	CUST_12338_PI427051300	**-9.73**	**1.69E-06**
EYA2	CUST_6205_PI427051300	**-11.20**	**1.17E-04**
CXCR7	CUST_4678_PI427051300	**-16.11**	**1.11E-05**